Casein Kinase 2 Determines the Voltage Dependence of the Kv3.1 Channel in Auditory Neurons and Transfected Cells

Carolyn M. Macica and Leonard K. Kaczmarek

Department of Pharmacology, Yale University School of Medicine, New Haven, Connecticut 06520-8066

The Kv3.1 potassium channel can be distinguished from most other delayed rectifier channels by its very high threshold of activation and lack of use-dependent inactivation. This allows neurons that express this channel to fire at very high frequencies. We have now found that this feature of the Kv3.1 channel is strongly influenced by its constitutive phosphorylation by the enzyme casein kinase II. Using stably transfected Chinese hamster ovary cells expressing Kv3.1, we show that Kv3.1 is highly phosphorylated under basal conditions. Whole-cell patch clamp recordings were used to characterize the electrophysiological consequence of dephosphorylation using alkaline phosphatase. This enzyme produced an increase in whole-cell conductance and shifted the voltage dependence of activation to more negative potentials by >20 mV. In addition, a similar shift in the voltage dependence of inactivation was observed. These findings were also confirmed in native Kv3.1 channels expressed in medial nucleus of the trapezoid body (MNTB) neurons. Furthermore, inhibitors of casein kinase 2 mimicked the effect of phosphatase treatment on voltage-dependent activation and inactivation, whereas inhibitors of protein kinase C failed to alter these parameters. The combination of biochemical and electrophysiological evidence suggests that the biophysical characteristics of Kv3.1 that are important to its role in MNTB neurons, allowing them to follow high-frequency stimuli with fidelity, are largely determined by phosphorylation of the channel.

Key words: Kv3.1; potassium channel; constitutive phosphorylation; casein kinase; MNTB neuron; voltage dependence of activation; voltage dependence of inactivation

Kv3.1 is a voltage-dependent, delayed rectifier potassium channel that is expressed in neurons that are capable of firing trains of action potentials at very high rates and is expressed at high levels in the auditory brainstem, including the medial nucleus of the trapezoid body (MNTB) (Perney et al., 1992; Weiser et al., 1995; Wang et al., 1998a,b). The Kv3.1 channel has several unique biophysical properties that distinguish it from most other members of the *Shaker* potassium channel family (Luneau et al., 1991; Vega-Saenz de Miera et al., 1992; Kanemasa et al., 1995). These include a high threshold for activation, rapid time constants, and the lack of use-dependent inactivation. All of these characteristics contribute significantly to its physiological role in MNTB neurons, where its presence is required for neurons to follow very high-frequency stimuli (Brew and Forsythe, 1995; Wang et al., 1998a). The presence of a Kv3.1-like current in MNTB neurons allows action potentials to repolarize at high frequencies without affecting the height of the action potential and confers on these cells the ability to phase-lock to high-frequency synaptic and electrical stimuli. This high-threshold K^+ current in MNTB is, like Kv3.1, selectively blocked by low concentrations of TEA, and has been identified with the Kv3.1 channel based on its localization, pharmacological, biophysical characteristics, and by genetic knock-out approaches (Perney et al., 1992; Brew and Forsythe, 1995; Perney and Kaczmarek, 1997; Wang et al., 1998a,b; Macica et al., 2000). Moreover, changing the amplitude of this current in MNTB neurons by pharmacological manipulation, or in computer-based models of MNTB neurons, reveals that altering the levels of Kv3.1 strongly influences the fidelity of the transmission of high-frequency synaptic inputs and the ability of the MNTB synapse to transmit information during repetitive stimulation (Brew and Forsythe, 1995; Kanemasa et al., 1995; Wang and Kaczmarek, 1998; Wang et al., 1998a).

The presence of multiple putative phosphorylation sites in the Kv3.1 amino acid sequence suggests that modulation of Kv3.1 may occur in MNTB neurons. We have now examined the modulation of Kv3.1 by protein kinases using both biochemical and electrophysiological techniques in Kv3.1 transfected cells and in neurons. We have found that the Kv3.1 channel protein exists as a constitutively phosphorylated protein and that the key biophysical parameters that allow Kv3.1 to function as a high-threshold current in rapidly firing neurons depend on this basal phosphorylation. Although previous work has shown that the amplitude of Kv3.1 may be modulated by protein kinase C (PKC) (Critz et al., 1993; Kanemasa et al., 1995), our present findings indicate that the basal characteristics of the current, including its voltage dependence of activation and inactivation are influenced by basal phosphorylation by casein kinase 2 (CK2).

MATERIALS AND METHODS

Electrophysiological recordings from Chinese hamster ovary cells. The stable transfection of Kv3.1 into Chinese hamster ovary (CHO) cells has been previously described (Wang et al., 1998a). CHO cells with DHFR deficiency (CHO/DHFR(−)) were maintained in Iscove's modified Aulbecco's medium (Life Technologies, Gaithersburg, MD) supplemented with 10% fetal bovine serum, 0.1 mM hypoxanthine, and 0.05 mg/ml geneticin (Life Technologies) and maintained in a 5% CO_2 incubator at 37°C. CHO cells were grown on coverslips 24–48 hr preceding recordings and transferred to extracellular solution (in mM: 140 NaCl, 1.3 $CaCl_2$, 5.4

Received March 13, 2000; revised Dec. 5, 2000; accepted Dec. 7, 2000.

This research was supported by National Institutes of Health Grant DC-01919 (L.K.K.) and National Research Service Award Fellowship MH12257-02 (C.M.M.). We thank Drs. Lu Yang-Wang, Neil Magoski, and Jennifer Ledwell for helpful discussion and technical advice.

Correspondence should be addressed to Leonard K. Kaczmarek, Department of Pharmacology, Yale University School of Medicine, 333 Cedar Street, New Haven, CT 06520. E-mail: leonard.kaczmarek@yale.edu.

KCl, 25 HEPES, and 10 glucose, pH 7.4) 1 hr before recording. Voltage-clamp recordings were made in the whole-cell configuration, using an Axopatch 2D amplifier (Axon Instruments, Foster City, CA). The patch electrodes were pulled from thin-walled, borosilicate glass capillaries with filament (World Precision Instruments, Sarasota, FL) using a Narishige P-83 two-stage puller and had a resistance of 3 MΩ when filled with intracellular solution (in mM: 32.5 KCl, 97.5 K-Gluconate, 5 EGTA, and 10 HEPES, pH 7.2) supplemented with 2 mM ATP and 0.2 mM GTP, unless otherwise noted. For phosphatase experiments, 5 U of calf intestinal alkaline phosphatase (Boehringer Mannheim, Indianapolis, IN) was included in the intracellular solution and allowed to dialyze into the cell over a period of 30 min. All data were low-pass filtered at 2 kHz, digitized using a Digidata 2000 analog-to-digital converter (Axon Instruments), and were stored on hard disk. The compensation for series resistance was set at 85% with a lag of 10 μsec. Unless noted, currents were leak-subtracted by the P/4 protocol, and data were analyzed using pClamp6.0 software. Conductance values were obtained by dividing the current by the electrochemical driving force ($I_K/(V_m - E_k)$). Normalized conductance–voltage plots were obtained by normalizing conductance (G) to maximal conductance (G_{max}) and fit using the nonlinear least-squares fit of a Boltzmann isoform $G = G_{max}/[1 + \exp(V - V_{1/2}/k)]$, where $V_{1/2}$ is the voltage at half-maximal activation, and k is the slope factor. Although recordings were partially corrected for series resistance (~85%), no compensation for additional errors was performed. We estimate that residual uncorrected errors in the estimates of the shift in voltage dependence of activation should be minimal. In particular, this value is most affected by current detectable near the threshold of activation, where the calculated maximal error is <1 mV. Conductances were normalized to those measured at a membrane potential of +60 mV, which was designated as V_{max}. Because Kv3.1 current is relatively nonsaturating even at very positive potentials, and the current density in our expression system is high, only those experiments in which the currents did not exceed the output of the amplifier at +60 mV were used in this analysis (Kanemasa et al., 1995).

Inactivation curves for Kv3.1-transfected CHO cells were obtained by a 200 msec test pulse to 40 mV, preceded by 30 sec prepulses ranging from −80 to +20 mV in 20 mV increments. The holding potential was kept at −80 mV. Data were fit using the Boltzmann isotherm. To ensure full recovery of inactivated currents between trials, the cells were given a 1 min recovery period at −80 mV. Average data are expressed as means ± SE. It should, however, be noted that because a 2 min prepulse potential at −40 mV was used to exclusively study the native high-threshold component of outward K current in MNTB neurons, we also conducted preliminary experiments in CHO cells after phosphatase treatment using a 2 min prepulse at −40 mV. After a prepulse potential to −40 mV for 2 min, channels were inactivated in excess of 50 when current was evoked at a test potential of +20 mV.

Phorbol 12-myristate 13-acetate (PMA), 1-[5-isoquinolinesulfonyl]-2-methyl piperazine (H-7), *N*-(2-aminoethyl)-5-chloronaphthalene-1-sulfonamide-HCl (A3), and 5,6-dichloro-1-β-D-ribofuranosylbenzimidazole (DRB) were obtained from Calbiochem (San Diego, CA).

Preparation of brainstem slices. Brains were rapidly removed from postnatal 9- to 14-d-old rats, after decapitation and placed into ice-cold bicarbonate-buffered artificial CSF (ACSF) (in mM: 125 NaCl, 2.5 KCl, 26 $NaHCO_3$, 1.25 NaH_2PO_4, 2 Na pyruvate, 3 myo-inositol, 10 glucose, 2 $CaCl_2$, and 1 $MgCl_2$, pH 7.4) solution gassed with 95% O_2 and 5% CO_2. The area of the brainstem containing MNTB nuclei was cut into four to six transverse slices using a vibrotome. The slices were incubated at 37°C for 1 hr and thereafter kept at room temperature (22–25°C).

Electrophysiological recordings from MNTB. One slice was transferred to a recording chamber mounted on an Olympus microscope fitted with Nomarski optics and a 60× water immersion objective. The chamber was continually perfused (1 ml/min) with gassed ACSF. Whole-cell voltage clamp recordings were made from visually identified MNTB neurons as described in CHO cells. Current-clamp experiments were conducted using an Axopatch 2D amplifier. Intracellular solution contained 32.5 mM KCl, 97.5 K-gluconate, 5 mM EGTA, 10 mM HEPES, and 1 mM $MgCl_2$, pH 7.2. The extracellular calcium concentration was lowered to 0.5 mM to minimize the contribution of calcium-activated K channels, and TTX (0.5 μM) was included in the ACSF to block sodium currents. The mean cell capacitance was 12.0 ± 0.4 pF with a mean series resistance of 5.3 ± 0.4 MΩ. Total current was compared before and after addition of activators of PKC in the presence and absence of PKC inhibitors. Averaged data are expressed as means ± SE. Conductance and normalized conductance values were obtained as described above.

Metabolic labeling and immunoprecipitation. Stably transfected CHO cells expressing Kv3.1 or untransfected cells were grown to 80% confluence. Cells were preincubated with methionine-deficient DMEM (Life Technologies) plus 25 mM HEPES for 30 min, which was replaced with fresh media supplemented with 100 μCi/ml of [^{35}S]methionine (Amersham, Arlington Heights, IL). Medium was removed, and cells were washed three times with ice-cold PBS. Cells were lysed with RIPA buffer (150 mM NaCl, 1.0% Nonidet P-40, 0.5% deoxycholate, 0.1% SDS, and 50 mM Tris, pH 8.0) containing a protease inhibitor cocktail (Boehringer Mannheim) and phosphatase inhibitors (100 μM NaF and 0.2 mM $NaVO_3$), and allowed to incubate on a rocking platform for 30 min at 4°C. Lysates were spun in a microfuge for 15 min, and the supernatant was transferred to a new tube. Lysates were precleared with a 50% slurry aliquot of protein A Sepharose beads (Pharmacia Biotech, Piscataway, NJ), followed by incubation with a specific anti-Kv3.1 antibody at 1:1000 dilution, 4°C, overnight (Perney and Kaczmarek, 1997). Lysates were immunoprecipitated with protein A Sepharose beads for 2 hr at 4°C, spun, and washed three times in Triton X-100 buffer (0.1% Triton X-100, 0.1% SDS, 300 mM NaCl, and 50 mM Tris, pH 7.5). For those samples treated with alkaline phosphatase, beads were resuspended in 50 μl of phosphatase buffer (50 mM Tris-HCl, pH 8.0, 5 mM $MgCl_2$, 100 mM NaCl, and 5% glycerol), and the reaction was initiated by the addition of 5 U/μl phosphatase. Samples were incubated for 1 hr at 37°C, followed by three washes with Triton X-100 buffer. All samples were eluted by boiling in 1× SDS-PAGE sample buffer (62.5 mM Tris, pH 6.8, 4% SDS, 10% glycerol, 0.02% bromophenol blue, and 4% β-mercaptoethanol) for 5 min. Samples were subjected to SDS-PAGE on a 7.5% gel. The gel was fixed with 10% acetic acid and 50% methanol for 1 hr, washed, and soaked in Amplify (Amersham). The gel was dried, and labeled peptides were visualized by fluorography.

For ^{32}P metabolic labeling, stably transfected CHO cells expressing Kv3.1 were labeled metabolically with [^{32}P]orthophosphate. Stably transfected CHO cells were grown to 70–80% confluence in Iscove's media. Cells were preincubated with phosphate-deficient DMEM (Life Technologies) plus 25 mM HEPES for 30 min, which was replaced with fresh media supplemented with 500 μCi/ml of carrier-free [^{32}P]orthophosphate (Amersham) and allowed to incubate to equilibrium. Cells were then subjected to agonist stimulation for 15 min, medium was removed, and cells were washed three times with ice-cold PBS. Cells were lysed, immunoprecipitated, and subjected to SDS-PAGE as described above. Immunoprecipitates treated with alkaline phosphatase were performed as described above. The gel was fixed as above, dried, and bands were visualized by autoradiography.

Phosphoamino analysis. Stably transfected CHO cells expressing Kv3.1 were labeled metabolically with [^{32}P]orthophosphate. Lysates were prepared, immunoprecipitated, and electrophoresed as above. The gel was transferred to a polyvinylidene difluoride (PVDF) membrane, and the Kv3.1 protein band was visualized by autoradiography. The bands corresponding to Kv3.1 were excised, rehydrated with methanol, and hydrolyzed with 6N HCl for 1 hr at 110°C. The samples were spun in a microfuge, decanted, and lyophilized. The lyophilized sample was resuspended in 10 μl of pH 1.9 buffer (2.5% formic acid and 7.8% acetic acid) containing 5 mM each of phosphoamino acid standards. The sample was spotted 1.5 cm from the edge of a 10 × 10 cm cellulose TLC plate (Macalaster Bicknell, New Haven, CT) and analyzed by two-dimensional high-voltage electrophoresis. The sample was run in the first dimension for 45 min at 1000 V. The plate was dried and re-wet with pH 3.5 buffer (0.5% pyridine and 5.0% acetic acid) and run in the second dimension for 15 min at 1000 V. The plate was dried, and standards were visualized by ninhydrin (0.2% solution in acetone) for 5 min in an 80°C oven. The sample phosphoamino acids were visualized by autoradiography.

RESULTS

Kv3.1 is constitutively phosphorylated

Kv3.1 has 11 putative PKC phosphorylation sites and 10 putative CK2 sites. The direct incorporation of phosphate into the Kv3.1 channel protein has not been demonstrated, although the amplitude of Kv3.1 current has been shown to decrease in response to activators of PKC in several heterologous expression systems (Critz et al., 1993; Kanemasa et al., 1995). We therefore examined phosphorylation of Kv3.1 expressed in

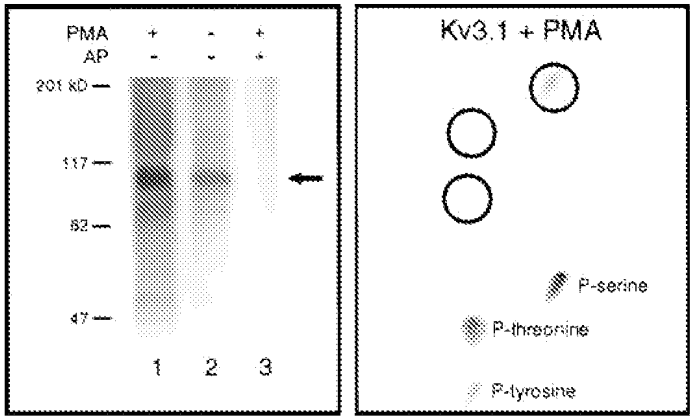

Figure 1. *In vivo* phosphorylation of Kv3.1 in CHO cells. CHO cells expressing Kv3.1 were radiolabeled with [^{32}P]orthophosphate to equilibrium, stimulated with or without 100 nM PMA for 15 min, and lysed. Lysates were immunoprecipitated with anti-Kv3.1 antibody (*lanes 1, 2*). An additional ^{32}P-labeled Kv3.1 sample was subjected treatment of the immunoprecipitated phosphoprotein with calf intestinal alkaline phosphatase (*AP*) for 1 hr at 37°C (*lane 3*). Samples were run on a 7% SDS-PAGE gel, and samples were visualized by autoradiography (*right panel*). Mobility of molecular weight markers is shown on *left*. Phosphoamino acid analysis of the Kv3.1 channel protein. Lysates were prepared, immunoprecipitated, and electrophoresed as above. The gel was transferred to a PVDF membrane, and the Kv3.1 protein band was visualized by autoradiography. The bands corresponding to Kv3.1 were excised, rehydrated with methanol, and hydrolyzed with 6N HCl for 1 hr at 110°C. Labeled phosphoamino acids were resolved by two-dimensional thin layer, the plate was dried, and standards were visualized by ninhydrin staining and sample phosphoamino acids were visualized by autoradiography.

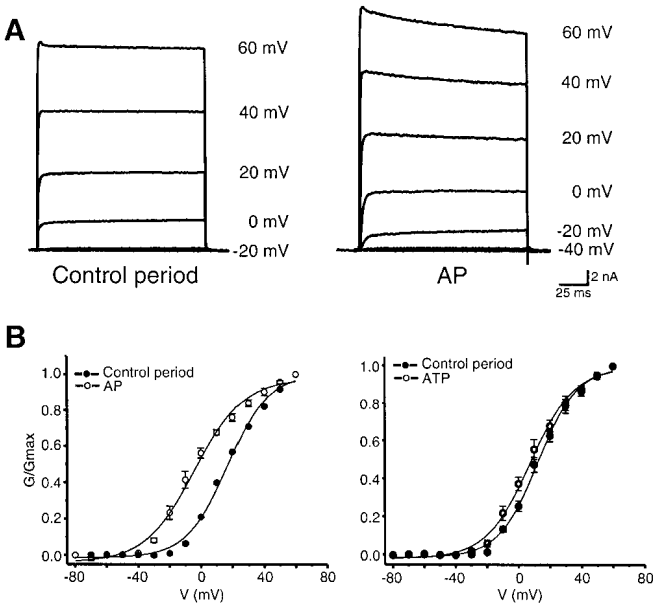

Figure 2. *A,* Current–voltage relationship for Kv3.1 currents recorded from CHO cells in the whole-cell configuration during the control period of AP treatment (5 U/ml) and 30 min after dialysis in the intracellular solution. Currents were evoked by depolarizing the membrane from a holding potential of −80 mV to test potentials from −80 to +60 mV in 10 mV increments, with 20 mV increments shown for raw currents. *B,* Conductance values were obtained by dividing current by the electrochemical driving force ($I_K/(V_m - E_k)$). Normalized conductance–voltage plots were obtained by normalizing conductance (G) to maximal conductance (G_{max}) and fit using the nonlinear least-squares fit of a Boltzmann isoform. Summary of normalized conductance–voltage relationship for Kv3.1 comparing the control period at $t = 0$ min to 30 min phosphatase treatment (*left*) or ATP (*right*).

CHO cells in both the presence and absence of the phorbol ester activator of PKC, PMA. Cells stably expressing the channel protein were radiolabeled to equilibrium with [^{32}P]orthophosphate and then stimulated for 15 min with 100 nM PMA or vehicle alone. Immunoprecipitation of Kv3.1 revealed incorporation of ^{32}P into the Kv3.1 protein, which has a molecular mass of ~110 kDa in both stimulated and unstimulated cells (Fig. 1, *left panel, lanes 1* and *2*, respectively). Immunoprecipitation also yielded an additional band corresponding to the predicted molecular weight of the unglycosylated form of the channel protein (80 kDa), which is the size of Kv3.1 when it is translated *in vitro* in the absence of membranes (data not shown). Incorporation of ^{32}P into the Kv3.1 channel protein could be completely reversed by treatment of the immunoprecipitated phosphoprotein with calf intestinal alkaline phosphatase (Fig. 1, *left panel, lane 3*).

Of the 21 consensus phosphorylation sites for CK2 and PKC in Kv3.1, 9 are serine, and 12 are threonine. We determined the incorporation of phosphate into specific amino acids by immunoprecipitating Kv3.1 from PMA-stimulated CHO cells radiolabeled with [^{32}P]orthophosphate. Immunoprecipitates were then subjected to phosphoamino acid analysis. Radioactivity comigrating with unlabeled phosphoserine, but not phosphothreonine or phosphotyrosine, was detected after acid hydrolysis of ^{32}P-labeled Kv3.1 (Fig. 1, *right panel*). Similar results were obtained in CHO cells that were not stimulated with PMA (data not shown). These results indicate that, of the putative consensus sites for PKC- and CK2-mediated phosphorylation, only those containing serine residues are phosphorylated.

Dephosphorylation shifts the voltage dependence of activation of Kv3.1 in transfected cells

To determine the role of basal phosphorylation of the Kv3.1 protein on its electrical properties, we performed whole-cell patch clamp recording in which phosphatase was included in the intracellular solution over a 30 min recording period. A time-dependent increase in macroscopic current was observed in response to alkaline phosphatase ($n = 8$; Fig. 2*A*). In control recordings (+ATP) without phosphatase, very little change in current amplitude occurred over the same time period (see below). The increase in whole-cell conductance was significantly greater at negative potentials, and the threshold of activation was shifted to more negative potentials (−40 mV) in all experiments conducted. Thus, currents could be evoked at potentials in which no current is detectable in control recordings. When the normalized conductance was plotted as a function of membrane potential, the voltage dependence of activation was found to be shifted to negative potentials after dialysis with phosphatase. Curves were well fit by a single Boltzmann isotherm (Fig. 2*B, left*). The half-activation potential ($V_{1/2}$ max) for the control period was 16.9 ± 1.3 mV ($k = 13.1 \pm 1.1$) versus −3.92 ± 1.63 mV ($k = 15.4 \pm 1.6$) after 30 min dialysis with phosphatase, resulting in a total leftward shift of over 20 mV in the voltage dependence of activation ($n = 4$).

To eliminate the possibility that the shift in voltage dependence was attributable to washout of intracellular anions, as has been reported for other channels when recorded in the whole-cell configuration (Fenwick et al., 1982; Oliva et al., 1988), we dia-

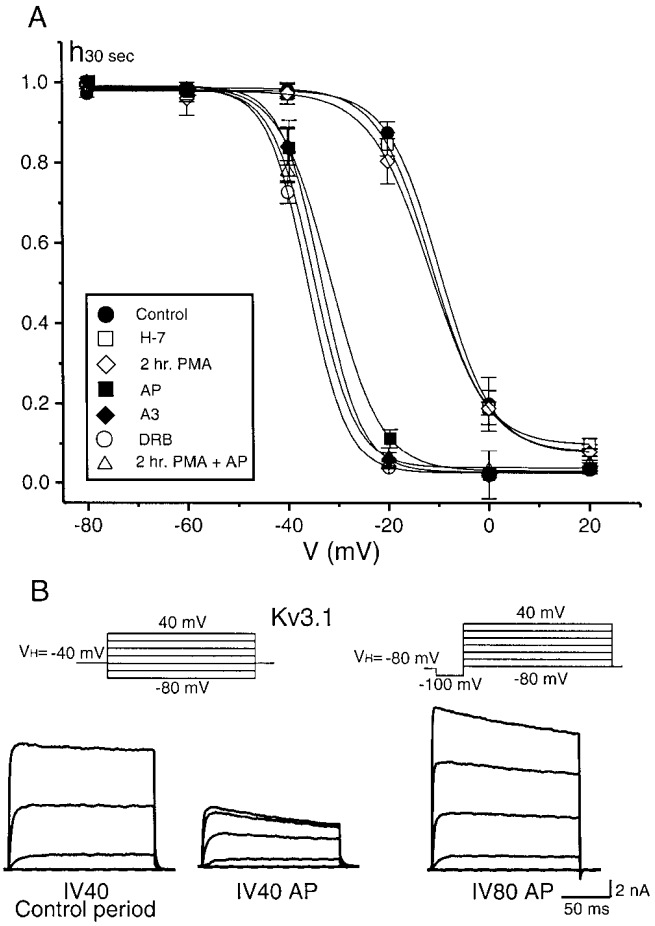

Figure 3. Steady-state inactivation ($h_{30\ sec}$) of Kv3.1. *A*, Steady-state inactivation of Kv3.1 was determined by holding the membrane potential from a prepulse potential ranging from −80 to 20 mV for 30 sec to a test pulse of 40 mV for 150 msec, with a 1 min period between each prepulse. Current amplitude was normalized to the maximum current, and the inactivation curve was fit using the nonlinear least-squares fit of a Boltzmann isoform. Treatment and absolute $V_{1/2}$ values are summarized in Table 1. *B, Left*, Evoked current from a holding potential of −40 mV for 2 min to test potentials from −80 mV to +40 mV in 20 mV increments during control period and after AP treatment; *right*, recovery of current from inactivation by stepping from a holding potential of −80 mV in 20 mV increments from −80 mV to +40 mV.

lyzed Kv3.1-transfected CHO cells with intracellular solution without alkaline phosphatase (AP), but containing 1 mM ATP to minimize shifts in voltage dependence associated with dephosphorylation. Only a small change in whole-cell conductance and shift in voltage dependence of activation was observed under these conditions (Fig. 2*B, right; n* = 6). The potential at which Kv3.1 is half activated during the control period was 12.5 ± 0.98 mV (k = 12.6 ± 0.87 mV) and was 7.7 ± 1.10 mV (k = 14.0 ± 1.09 mV) after 30 min dialysis.

Dephosphorylation shifts the voltage dependence of inactivation of Kv3.1 in transfected cells

To determine whether the inactivation characteristics of Kv3.1 were also affected by dephosphorylation, we used a two-pulse protocol to measure voltage dependence of inactivation. A 30 sec prepulse to potentials between −80 and 20 mV allowed inactivation to develop, and this was followed by a test pulse to 40 mV. In the absence of exogenous phosphatase (ATP alone), the potential at which Kv3.1 is half inactivated ($V_{1/2}$) is −9.65 mV (Fig. 3, *filled circles*). Alkaline phosphatase produced a 20 mV leftward shift in the inactivation curve to a midpoint potential of inactivation of −31.8 mV (Fig. 3, *filled squares*). These data are summarized in Table 1. Dialysis of CHO cells for 30 min in the presence of ATP did not produce the significant shifts in voltage dependence of inactivation that were observed with AP treatment, producing only modest shifts of $V_{1/2}$ to −16.7 ± 2.1 mV (n = 10).

Table 1. Effect of inhibitors on voltage dependence of inactivation

Sample	$V_{1/2}$ (mV)	k (mV)	n
Control (ATP)	−9.7 ± 0.3	5.1 ± 0.2	5
H-7[a]	−11.2 ± 0.7	5.3 ± 0.3	5
2 hr/PMA[a]	−11.5 ± 0.8	5.9 ± 0.5	6
AP	−31.8 ± 0.1	5.0 ± 0.3	5
A3[b]	−33.3 ± 0.8	4.0 ± 0.4	3
DRB[b]	−36.1 ± 1.1	3.9 ± 1.0	5
2 hr. PMA + AP	−34.8 ± 1.0	4.1 ± 0.7	3

[a]PKC inhibitor.
[b]CKII inhibitor.

Because the voltage dependence of inactivation was shifted to more negative potentials, we determined the effect on Kv3.1 current by holding the membrane at −40 mV for 2 min, in anticipation of experiments conducted in native MNTB neurons (see below). Based on our findings in Figure 3*A*, we predicted that we would see a loss of evoked currents caused by an increase in the number of channels in the inactivated state. Indeed, from a holding potential of −40 mV in CHO cells expressing Kv3.1, an apparent saturation of current was observed after alkaline phosphatase treatment (Fig. 3*B, left panel*). The onset of steady-state inactivation was slow; stepping from a holding potential of −40 mV for a period ranging from 0 to 2 min resulted in an incremental decrease in outward current in response to subsequent depolarizations (data not shown). Full recovery from the inactivated state resulted when current was again evoked from a holding potential of −80 mV (Fig. 3*B, right panel*).

Dephosphorylation of native Kv3.1 current in MNTB neurons affects its voltage dependence

To determine whether the effect of alkaline phosphatase on Kv3.1 in transfected CHO cells is preserved in MNTB neurons, we next tested the effect of phosphatase using the whole-cell configuration in brainstem slices. In MNTB neurons, the high-threshold Kv3.1 current can be discriminated from a smaller, low-threshold outward current by holding the membrane potential at −40 mV for 2 min, a potential at which the low-threshold, TEA-insensitive component of the outward current is fully inactivated. The high-threshold component, corresponding to Kv3.1, accounts for >80% of total outward current in MNTB neurons (Wang et al., 1998a). As previously reported in MNTB neurons, stepping from a holding potential of −40 mV to test potentials of −80 to +40 mV in 20 mV steps, revealed large, outward, noninactivating currents, with a threshold of activation of −20 mV (Brew and Forsythe, 1995; Wang et al., 1998a). Alkaline phosphatase produced an increase in holding current at −40 mV (Fig. 4*A,B*). The increase in holding current is consistent with a shift in the activation of Kv3.1 to more negative potentials in response to phosphatase. This current at −40 mV after phosphatase treatment was significantly blocked by 1 mM TEA (Fig. 4*A,C*), a concentration that blocks only the Kv3.1 current but does not affect the low-threshold outward currents in MNTB neurons

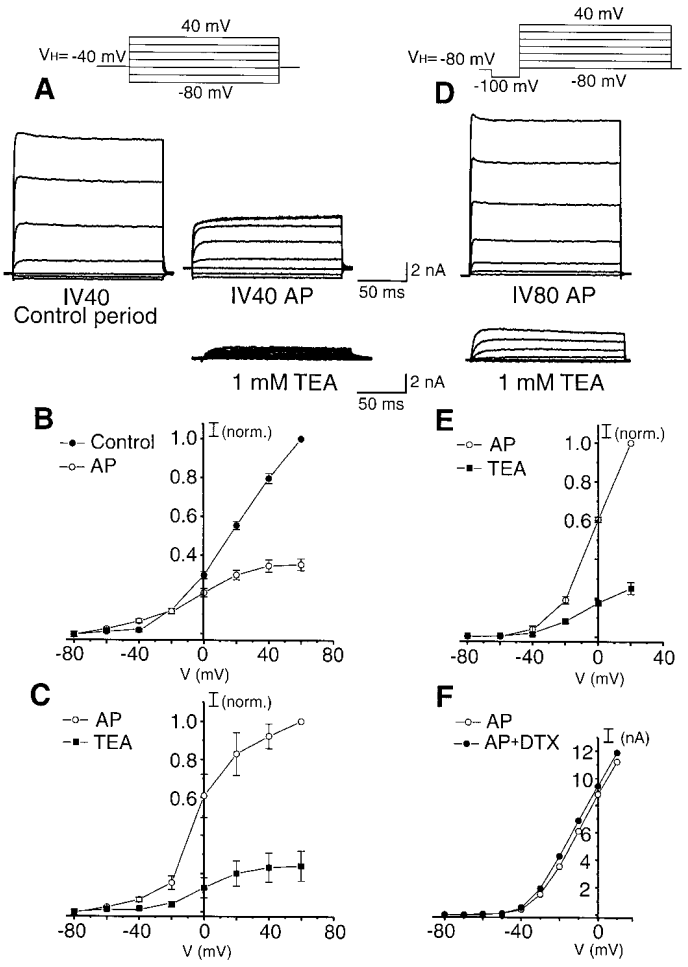

Figure 4. AP shifts the voltage dependence of activation and inactivation in MNTB neurons. To discriminate the high-threshold TEA-sensitive current from total outward current, the membrane potential was held at −40 mV for 2 min; currents were evoked by stepping from a holding potential of −40 to +40 mV in 20 mV increments taken at the beginning of dialysis of phosphatase (t = 0) and at t = 15 min. *A, Top*, Reduction of current amplitude after AP treatment, leak subtraction was disabled to discriminate any changes in the current that may occur at more negative potentials; *bottom*, inhibition of current by 1 mM TEA. *B*, Summary of normalized high-threshold current during control period and 15 min after phosphatase treatment (n = 8). All values are mean ± SEM. *C*, Summary of normalized data of the effect of 1 mM TEA on current after AP treatment (n = 8). *D*, Recording from same neuron in *A* showing recovery of outward current when current was evoked by stepping from a holding potential of −80 to +40 mV in 20 mV increments during the control period and after phosphatase treatment. *E*, Summary of normalized data of TEA-sensitive component of outward current after phosphatase treatment, normalized to current after AP treatment (n = 7). All data are normalized to +20 mV so data from all experiments could be included, i.e., those experiments in which current exceeded the output of the amplifier at +40 to +60 mV. *F*, Current–voltage relationship of total outward current after phosphatase treatment and after 7 min perfusion of 100 nM DTX into the bath from a holding potential of −80 mV.

(Wang et al., 1998a). Treatment with alkaline phosphatase also produced a rapid reduction in the high-threshold current that was maximal by 15–20 min of dialysis with the phosphatase (Fig. 4*A*, *right trace*). A reduction of current from a holding potential of −40 mV was expected because of the shift in the voltage dependence of inactivation to more negative potentials in response to alkaline phosphatase, consistent with the findings in Figure 3.

As seen in CHO cells expressing Kv3.1 (Fig. 3*B*), total outward current evoked by stepping from a holding potential of −80 mV resulted in full recovery from inactivation. Figure 4*D* shows a recording resulting from the same cell as shown in the Figure 4*A*. Under these recording conditions, most of the outward current evoked by stepping from −80 mV could be blocked by 1 mM TEA, indicating that it is likely to correspond to the native Kv3.1 channel (Fig. 4*D,E*). In addition, current evoked by stepping to −40 mV from a holding potential of −80 mV was blocked by 1 mM TEA, suggesting that most of the low-threshold current that is normally evoked by stepping from a holding potential of −80 mV in MNTB neurons runs down in response to phosphatase treatment (or to lack of ATP). To test this possibility, 100 nM dendrodotoxin (DTX) was perfused into the bath after treatment with phosphatase (n = 3), a concentration that blocks the low-threshold component of outward current in MNTB neurons (Brew and Forsythe, 1995; Wang et al., 1998a) but has no effect on Kv3.1 channels (Grissmer et al., 1994; Brew and Forsythe, 1995). DTX had little or no effect on the amplitude of total outward current (Fig. 4*F*). This suggests that most of the remaining current after phosphatase treatment (including current at −40 mV; Fig. 4*B,E*) is almost entirely Kv3.1-like current and that the TEA-resistant low-threshold component of total outward current runs down after phosphatase treatment. Finally, treatment with boiled alkaline phosphatase to destroy enzymatic activity had no effect on the high-threshold current evoked from a holding potential of −40 mV (data not shown).

Protein kinase C is not responsible for the basal phosphorylation of Kv3.1

As stated above, Kv3.1 has 4 putative serine PKC phosphorylation sites and 5 putative serine CK2 sites. We next attempted to identify the kinase responsible for the effect of basal phosphorylation of Kv3.1 by studying the impact of inhibitors of these two kinases on the voltage dependence of activation of Kv3.1 in CHO cells. To test the effect of PKC, cells were preincubated with the cell-permeable PKC inhibitor H-7 (100 μM) for 30 min to 1 hr, and currents were measured. Inhibition of PKC using H-7 had no effect on the voltage dependence of activation, as compared with control cells (control, $V_{1/2}$ = 15.6 ± 1.3, k = 12.7 ± 0.2 mV, n = 14; H-7, $V_{1/2}$ = 17.3 ± 1.3 mV, k = 12.7 ± 0.2 mV, n = 6, respectively). In addition, preincubation with H-7, followed by 30 min intracellular dialysis in the continued presence of H-7, produced changes in current that were similar to those observed in control dialyzed cells (Fig. 5*A, left panel*, representative trace). Finally, when the holding potential was held at −40 mV, H-7 had little effect on total outward current (Fig. 5*B, left panel*).

Inhibition of PKC was also achieved by incubating CHO cells in the presence of 100 nM PMA for 2 hr. We first measured membrane-associated PKC activity biochemically in response to 2 hr PMA treatment using histone IIIS as a substrate (data not shown). This assay revealed that PMA-mediated translocation in CHO cells was maximal by 15 min, followed by a rapid down-regulation of PKC activity. Under these conditions, we again found no shift in the voltage dependence of activation, and the midpoint of activation in the cells was 14.9 ± 1.3 mV, k = 13.1 ± 0.3 mV, n = 7.

We also tested the effect of PKC inhibitors on inactivation of Kv3.1 using the two-pulse protocol. In the presence of 100 μM H-7, the midpoint potential of inactivation was similar to that of untreated control cells (Fig. 3, *open squares*; Table 1). After 2 hr incubation with PMA, the $V_{1/2}$ of inactivation was also unaltered (Fig. 3, *open diamonds*; Table 1). In addition, in cells pretreated

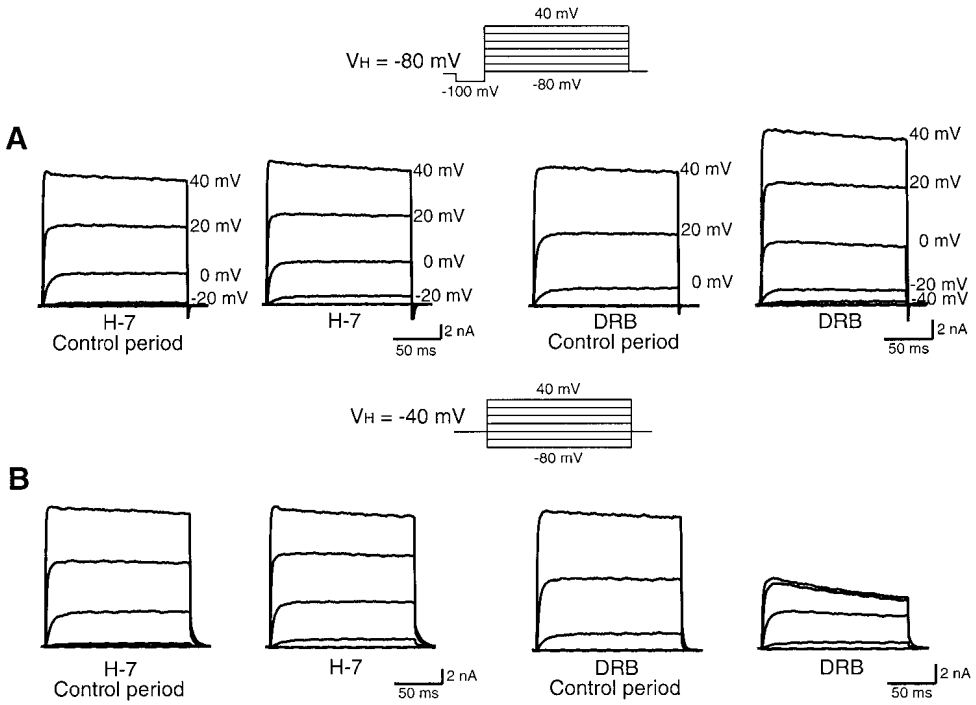

Figure 5. Effect of kinase inhibitors on Kv3.1 current in transected cells. *A,* Outward currents were evoked by stepping from a holding potential of −80 to +40 mV in 20 mV increments during the control period and after treatment with either 100 μM H-7 or 20 μM DRB. *B,* Outward currents evoked by holding from a membrane potential of −40 mV for 2 min to test potentials from −80 to +40 mV in 20 mV increments during the control period and after treatment with either 100 μM H-7 or 20 μM DRB.

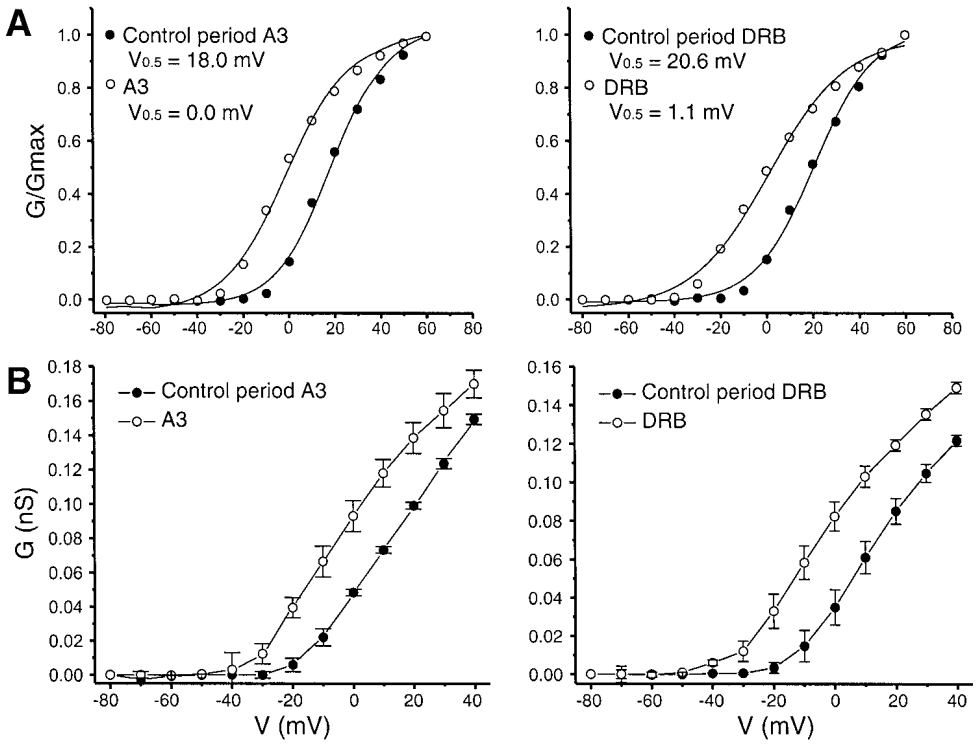

Figure 6. Steady-state activation of Kv3.1 after treatment with CK2 inhibitors. *A,* Normalized conductance–voltage relationship for Kv3.1 during control period and after treatment with either 20 μM A3 or DRB. Conductance values were obtained by dividing current by the electrochemical driving force ($I_K/(V_m - E_k)$). Normalized conductance–voltage plots were obtained by normalizing conductance (G) to maximal conductance (G_{max}) and fit using the nonlinear least-squares fit of a Boltzmann isoform. *B,* Summary of conductance–voltage relationship of all experiments conducted with A3 or DRB.

with 2 hr PMA to downregulate PKC, dialysis of the cells with alkaline phosphatase resulted in a leftward shift in the voltage dependence of inactivation, confirming that a kinase other than PKC was responsible for the basal phosphorylation of Kv3.1 (Fig. 3, *open triangles*; Table 1).

Casein kinase 2 inhibitors mimic the effect of phosphatase on voltage dependence

To test the involvement of CK2, cells were treated with either A3, a kinase inhibitor with inhibitory characteristics similar to H-7, with the exception of being additionally able to inhibit CK2, or with the selective CK2 inhibitor DRB (Zandomeni, 1989). Both of these agents produced changes similar to those observed in phosphatase-treated cells. Dialysis of CHO cells with intracellular solution containing 20 μM A3 for 30 min resulted in current detectable at potentials more negative than −20 mV in all experiments conducted, consistent with a change in the voltage dependence of activation (Fig. 6*A,B, left panel*). In addition, a similar shift in voltage dependence of activation was observed when CHO cells expressing Kv3.1 were dialyzed with the selective CK2

inhibitor DRB (20 μM). Figure 5, *A* and *B* (*right panel*), shows the typical effect of DRB on Kv3.1 current from holding potentials of −80 and −40 mV, respectively. A normalized conductance–voltage curve is shown in Figure 6*A* (*right panel*). A summary of the total data showing the effect of DRB on whole-cell conductance as a function of voltage is shown in Figure 6*B* (*right panel*).

We also found that inhibitors of CK2 could mimic the effect of alkaline phosphatase on the voltage dependence. After 30 min A3 treatment, the midpoint potential of inactivation was comparable with that of phosphatase-treated cells, determined using the two-pulse protocol described earlier (Fig. 3, *closed triangles*; Table 1). Similarly, after 30 min treatment with DRB, there was also a similar shift in the $V_{1/2}$ of inactivation (Fig. 3, *open circles*; Table 1).

In addition, we tested the capacity of GTP to serve as a phosphate donor because CK2 has the unique ability to use both ATP and GTP (Blanquet, 2000). As observed with ATP, dialysis of transfected cells with GTP as the phosphate donor resulted in only small shifts in the voltage dependence of inactivation from −11.2 ± 1.2 mV (k = 3.93) during the control period to −19.6 ± 2.4 mV (k = 4.27) after 30 min dialysis.

We next tested the effect of DRB on native currents of MNTB neurons. Like AP, DRB produced an increase in holding current at −40 mV (Fig. 7*A,B*; n = 8) again, consistent with a shift in the activation of Kv3.1 to more negative potentials in response to phosphatase. This current at −40 mV after DRB treatment was significantly blocked by 1 mM TEA (Fig. 7*A,C*). Like AP treatment, DRB also produced a rapid reduction in the high-threshold current (Fig. 7*A, right trace*). In addition, subsequently resetting the holding potential to −80 mV resulted in full recovery from inactivation (Fig. 7*D*). A majority of the outward current evoked by stepping from −80 mV could be blocked by 1 mM TEA, as expected for the native Kv3.1 channel (Fig. 4*D,E*).

Finally, to determine the effect of DRB on the firing properties of MNTB neurons, principal neurons were stimulated with brief current pulses at high frequencies ranging from 100 to 300 Hz. During the control period of DRB dialysis, neurons were able to fire accurately at frequencies up to 300 Hz (Fig. 8*A*). After dialysis with DRB, neurons were able to fire at frequencies of 100 and 200 Hz. However, at 300 Hz, neurons failed to fire full action potentials after the first action potential (Fig. 8*B*). The effect of AP on these neurons was similar (a failure to fire at high frequencies). Because the effect of AP on the high-threshold current was very rapid, we were however, unable to obtain consistent control recordings from these neurons.

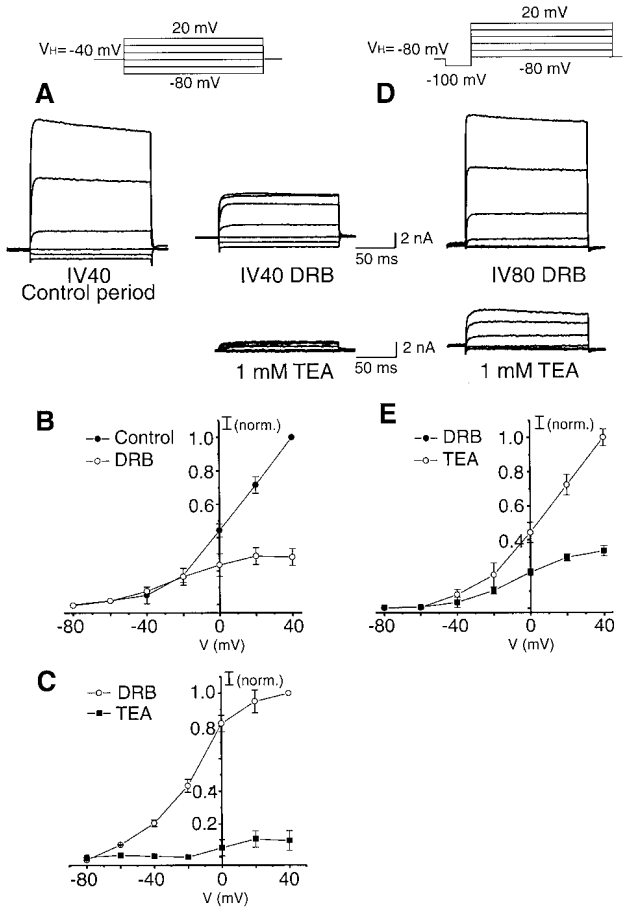

Figure 7. DRB shifts the voltage dependence of activation and inactivation in MNTB neurons, using the same protocol as in Figure 4. *A, Top*, Reduction of current amplitude after DRB treatment, leak subtraction was disabled to discriminate any changes in the current that may occur at more negative potentials; *bottom*, inhibition of current by 1 mM TEA. *B*, Summary of normalized high-threshold current during control period and 30 min after DRB treatment (n = 8). All values are mean ± SEM. *C*, Summary of normalized data of the effect of 1 mM TEA on current after AP treatment (n = 8). *D*, Recording from same neuron in *A* showing recovery of outward current when current was evoked by stepping from a holding potential of −80 to +20 mV in 20 mV during the control period and after phosphatase treatment. *E*, Summary of normalized data of TEA-sensitive component of outward current after phosphatase treatment, normalized to current after AP treatment (n = 7).

DISCUSSION

CK2 inhibitors alter voltage dependence of Kv3.1

CK2 is a ubiquitous second messenger-independent serine–threonine protein kinase consisting of two α catalytic and two regulatory β subunits and is believed to be constitutively active. The regulatory β subunit is also involved in targeting and plays a role in substrate specificity (Allende and Allende, 1995, 1998; Dobrowolska et al., 1999). CK2 has a wide variety of substrates, many of which are involved in cell cycle progression. Other substrates include those involved in protein synthesis, structural proteins, and signal transduction proteins (Allende and Allende, 1995). In addition, CK2 is emerging as an enzyme that plays a key role in neuronal tissue. The highest level of CK2 activity is in the brain and substrates have been identified in both synaptic and nuclear compartments (Blanquet, 2000). Moreover, CK2 has been shown to modulate NMDA channels in hippocampal neurons (Lieberman and Mody, 1999).

The role of constitutive CK2-mediated phosphorylation of voltage-dependent ion channels has however, not been explored previously. Our findings indicate that a high level of constitutive phosphorylation of the Kv3.1 channel, consistent with CK2-mediated phosphorylation, may profoundly influence the biophysical characteristics of the channel when expressed in CHO cells or in MNTB neurons. Inhibitors of CK2 mimic the effect of dephosphorylation by AP, although the effect of AP is more rapid than the effect of the kinase inhibitors. The slower effect of CK2 inhibitors likely reflects the rate of turnover of phosphorylation of the channel protein. DRB is thought to be a specific inhibitor of CK2, whereas A3 inhibits the same kinases as H-7 but additionally inhibits CK2. Because H-7 has little effect in comparison to A3, it is probable that the effect of A3 is attributable to inhibition of CK2. In addition to the use of inhibitors of CK2, we have shown that GTP, like ATP, may serve as a phosphate donor for the kinase responsible for constitutive phosphorylation of this

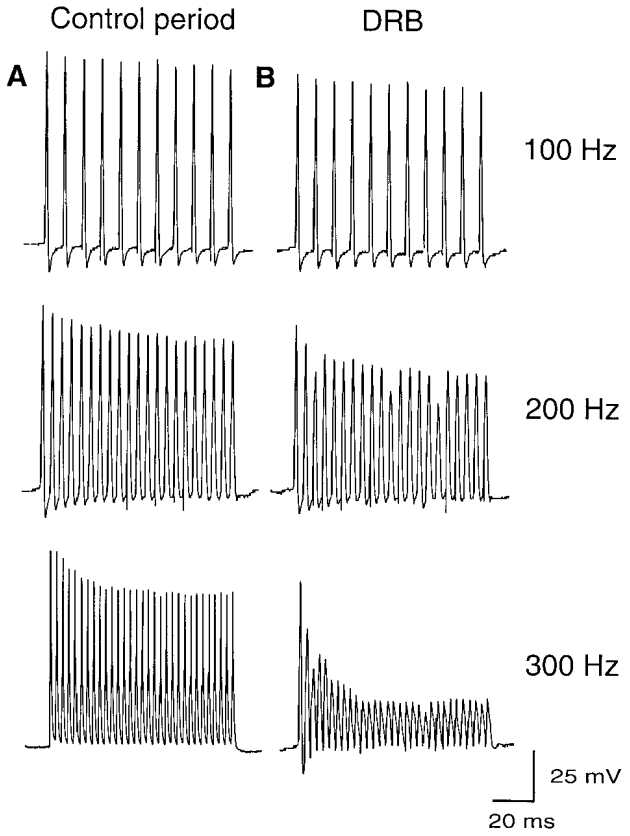

Figure 8. *A,* Representative recording from an MNTB neuron in response to brief current injections (2 nA, 0.3 msec) at three different test frequencies (100–300 Hz) during the control period of DRB dialysis in the intracellular recording solution. *B,* Recording from same neuron after 30 min dialysis with DRB.

channel. The large shifts in the voltage dependence associated with dephosphorylation of the channel were not observed in the presence of either ATP or GTP, being ~6 and 9 mV, respectively.

The properties of Kv3.1 that are sensitive to CK2, such as the their high-threshold of activation and inactivation, have been shown to be critical for the transmission of high-frequency signaling within the MNTB and are likely therefore to play a role in preserving auditory information (Brew and Forsythe, 1995; Wang et al., 1998a). In particular, the unique property of activation and inactivation at relatively positive potentials ensures that Kv3.1 has a minimal effect on the height of the action potential and is available to rapidly repolarize the membrane during high-frequency firing, as compared to other classic delayed rectifiers (Kanemasa et al., 1995; Wang et al., 1998a). Our finding that the ability of these neurons to fire at 300 Hz is impaired after DRB treatment and that the height of the action potential is significantly attenuated is consistent with a shift in the voltage dependence of the channel.

In contrast, our data indicate that PKC-mediated phosphorylation does not influence voltage dependence or kinetics of Kv3.1. However, PKC-mediated phosphorylation can acutely modulate Kv3.1 current amplitude, as has been previously demonstrated (Critz et al., 1993; Kanemasa et al., 1995).

Possible mechanisms for effects of casein kinase 2-mediated phosphorylation

Alkaline phosphatase and CK2 inhibitors produce effects on the voltage dependence of both activation and inactivation of Kv3.1, suggesting that phosphorylation contributes to both parameters. If inactivation occurs only from the open state, the shift in the voltage dependence of inactivation may occur simply as a result of the shift in the voltage dependence of activation. We attribute the saturation of current from a holding potential of −40 mV after phosphatase treatment to a cumulative inactivation. An accumulation of channels in the inactivated state from a holding potential of −40 mV would be predicted to occur as a result of the shift in the voltage dependence of inactivation to more negative potentials and to the short recovery period between pulses. It is however, also possible that the effects on the voltage dependence of activation and inactivation occur independently of each other. Although we cannot rule out the possibility that the effect of phosphatase treatment results from the dephosphorylation of an associated protein, our biochemical evidence that alkaline phosphatase eliminates phosphorylation of the immunoprecipitated Kv3.1 protein supports the hypothesis that the observed changes are attributable to direct dephosphorylation of the channel. Incorporation of a phosphate group into a channel protein may cause a conformational change in the protein or may alter its voltage sensitivity by an electrostatic interaction of the phosphate group with its voltage sensor (Perozo et al., 1989). The addition of the negative charge of the phosphate group at an internal site would be expected to shift the voltage dependence of the channel to more positive potentials, requiring additional depolarization to activate or inactivate the channel. It has been suggested that the incorporation of phosphate groups into the delayed-rectifier potassium channels of both the giant squid axon and of the constitutively phosphorylated neuronal potassium channel Kv2.1 modifies their sensitivity to depolarization by this electrostatic mechanism (Perozo and Bezanilla, 1990; Murakoshi et al., 1997). Phosphorylation of Kv2.1 has been shown to occur early in its biosynthesis, and dephosphorylation resulted in a shift in voltage dependence of activation of >20 mV.

Putative casein kinase 2 phosphorylation sites of Kv3.1

From our data, we are unable to discriminate between individual CK2 phosphorylation sites, although it is conceivable that the effects of CK2 on activation and inactivation may involve more than one site. Potential CK2 phosphorylation sites in the Kv3.1 channel protein are found in both the C and N terminus, with the C terminus containing one serine site, and the N terminus containing two sites. A role for cytoplasmic domains in the modulation of activation and inactivation has been previously demonstrated in Kv2.1 (VanDonger et al., 1990). In addition, Kv3.1 has one putative CK2 site in the S5–S6 linker (the pore region) near the outer region of the pore, which is unlikely to be phosphorylated by a cytoplasmic kinase. Finally, Kv3.1 has a single putative CK2 phosphorylation site present in the intracellular S4/S5 linker, which is conserved in most voltage-dependent potassium currents, including the mammalian *Shaw*-like channels. A role for the S4–S5 linker in both the voltage dependence of activation and inactivation has been previously demonstrated in members of the *Shaker* and *Shaw* potassium channel subfamilies (Isakoff et al., 1991; McCormack et al., 1991; Rettig et al., 1992), and the putative CK2 site in the S4–S5 linker is conserved in most voltage-dependent K channels. Phosphorylation of this residue may influence the apparent voltage-transducing properties of the S4–S5 linker, leading to the observed alterations in voltage dependence of activation and/or inactivation in Kv3.1. Future studies aimed at identifying the sites responsible for the impact of dephosphorylation on the biophysical properties of Kv3.1 will

provide further insight into the potential contribution of CK2 on ion channels properties.

Can constitutively phosphorylated Kv3.1 be modulated by phosphatases?

Although CK2 appears to be a constitutively active enzyme, it is possible that the level of CK2-dependent phosphorylation of substrates may be regulated by phosphatases. Based on electrophysiological, pharmacological, and immunohistochemical evidence, Kv3.1 is present presynaptically at the MNTB synapse (Perney et al., 1992; Wang and Kaczmarek, 1998; Wang et al., 1998b). However, presynaptic potassium current recordings at this synapse, from a holding potential of −40 mV result in little sustained outward current, whereas depolarization from more negative holding potentials results in an outward current that is sensitive to 1 mM TEA (L. Y. Wang, I. D. Forsythe, and L. K. Kaczmarek, unpublished observation). This result would be expected if there were less phosphorylation of Kv3.1 CK2 sites in the presynaptic terminal. Differences between the native Kv3.1 current and those recorded in heterologously expressed cells may be attributed to coassembly with other members of the *Shaw*-like subfamily or interaction with auxiliary subunits. Our findings suggest that differences in native currents found in the presynaptic calyx of Held could also be attributed to differences in the phosphorylation state of the channel.

REFERENCES

Allende JE, Allende CC (1995) Protein kinases 4 Protein kinase CK2: an enzyme with multiple substrates and a puzzling regulation. FASEB J 9:313–323.

Allende CC, Allende JE (1998) Promiscuous subunit interactions: a possible mechanism for the regulation of protein kinase CK2. J Cell Biochem [Suppl] 30–31:129–136.

Blanquet PR (2000) Casein kinase 2 as a potentially important enzyme in the nervous system. Prog Neurobiol 60:211–246.

Brew HM, Forsythe ID (1995) Two voltage-dependent K+ conductances with complementary functions in postsynaptic integration at a central auditory synapse. J Neurosci 15:8011–8022.

Critz SD, Wible BA, Lopez HS, Brown AM (1993) Stable expression and regulation of a rat brain K channel. J Neurochem 60:1175–1178.

Dobrowolska G, Lozeman FJ, Dongxia L, Krebs EG (1999) CK2, a protein kinase of the next millennium. Mol Cell Biochem 191:3–12.

Fenwick EM, Marty A, Neher E (1982) Sodium and calcium channels in bovine chromaffin cells. J Physiol (Lond) 331:599–635.

Grissmer S, Nguyen N, Aiyar J, Hanson DC, Mather RJ, Gutman GA, Karmilowicz J, Auperin DD, Chandy KG (1994) Pharmacological characterization of five cloned voltage-gated K channels, types Kv1.1, 1.2, 1.3, 1.5, and 3.1, stably expressed in mammalian cell lines. Mol Pharmacol 45:1227–1234.

Isakoff EY, Jan YN, Jan LY (1991) Putative receptor for the cytoplasmic inactivation gate in the Shaker K channel. Nature 353:86–90.

Kanemasa T, Gan L, Perney TM, Wang LY, Kaczmarek LK (1995) Electrophysiological and pharmacological characterization of a mammalian Shaw channel expressed in NIH 3T3 fibroblasts. J Neurophysiol 74:207–217.

Lieberman DN, Mody I (1999) Casein kinase-II regulates NMDA channel function in hippocampal neurons. Nat Neurosci 2:125–132.

Luneau CJ, Williams JB, Marshal J, Levitan ES, Oliva C, Smith JS, Antanavage J, Folander K, Stein RB, Swanson R, Kaczmarek L, Buhrow SA (1991) Alternative splicing contributes to K+ channel diversity in the mammalian central nervous system. Pro Natl Acad Sci USA 88:3932–3936.

Macica CM, Wang LY, Joho RH, Ho CS, Kaczmarek LK (2000) Knockout of the Kv3.1 gene impairs high frequency firing in auditory neurons. Soc Neurosci Abstr 26:1705.

McCormack K, Tanouye MA, Iverson LE, Lin J, Ramaswami M, McCormack T, Campanelli JT, Matthew MK, Rudy B (1991) A role for hydrophobic residues in the voltage-dependent gating of Shaker K+ channels. Proc Natl Acad Sci USA 88:2931–2935.

Murakoshi H, Shi G, Scannevin RH, Trimmer JS (1997) Phosphorylation of the Kv21 K+ channel alters voltage-dependent activation. Mol Pharmacol 52:821–828.

Oliva C, Cohen IS, Mathia RT (1988) Calculation of time constants for intracellular diffusion in whole cell patch clamp configuration. Biophys J 54:791–799.

Perney TM, Kaczmarek LK (1997) Localization of a high threshold potassium channel in the rat cochlear nucleus. J Comp Neurol 386:178–202.

Perney TM, Marshall J, Martin KA, Hockfield S, Kaczmarek LK (1992) Expression of the mRNAs for the Kv31 potassium channel gene in the adult and developing brain. J Neurophysiol 68:756–766.

Perozo E, Bezanilla F (1990) Phosphorylation affects voltage gating of the delayed rectifier K+ channel by electrostatic interactions. Neuron 5:685–690.

Perozo E, Bezanilla F, Dipolo R (1989) Modulation of K channels in dialyzed squid axons ATP-mediated phosphorylation J Gen Physiol 93:1195–1218.

Rettig J, Wunder F, Stocker M, Lichtinghagen R, Mastiaux F, Beckh S, Kues W, Pedarzani P, Schroter KH, Ruppersberg JP, Veh R, Pongs O (1992) Characterization of a Shaw-related potassium channel family in rat brain. EMBO J 11:2473–2486.

VanDonger AMJ, Frech GC, Drewe JA, Joho RH, Brown AM (1990) Alteration and restoration of K channel function by deletions at the N- and C-terminal. Neuron 5:433–443.

Vega-Saenz de Miera E, Morena H, Fruhling D, Kentros C, Rudy B (1992) Cloning of ShIII (Shaw-like) cDNAs encoding a novel high-voltage-activating, TEA sensitive, type-A K channel. Proc R Soc Lond B Biol Sci 248:9–18.

Wang LY, Kaczmarek LK (1998) High-frequency firing helps replenish the readily releasable pool of synaptic vesicles. Nature 394:384–388.

Wang LY, Gan L, Forsythe ID, Kaczmarek LK (1998a) Contribution of the Kv3.1 potassium channel to high-frequency firing in mouse auditory neurones. J Physiology 509:183–194.

Wang LY, Gan L, Perney TM, Schwartz I, Kaczmarek LK (1998b) Activation of Kv3.1 channels in neuronal spine-like structures may induce local potassium ion depletion. Proc Natl Acad Sci USA 95:1882–1887.

Weiser M, Bueno E, Sekirnjak C, Martone ME, Baker H, Hillman D, Chen S, Thornhill W, Ellisman M, Rudy B (1995) The potassium channel subunit Kv31b is localized to somatic and axonal membranes of specific populations of CNS neurons. J Neurosci 15:4298–4314.

Zandomeni RO (1989) Kinetics of inhibition by 5,6-dichloro-1-beta-D-ribofuranosylbenzimidazole on calf thymus casein kinase II. Biochem J 262:469–473.

Modulation of the Kv3.1b Potassium Channel Isoform Adjusts the Fidelity of the Firing Pattern of Auditory Neurons

Carolyn M. Macica,[1] Christian A. A. von Hehn,[1] Lu-Yang Wang,[2] Chi-Shun Ho,[3] Shigeru Yokoyama,[4] Rolf H. Joho,[5] and Leonard K. Kaczmarek[1]

[1]Department of Pharmacology, Yale University, New Haven, Connecticut 06520, [2]Division of Neurology, Hospital for Sick Children Research Institute, Toronto, Canada, [3]Department of Physiology, University of Michigan Medical Center, Ann Arbor, Michigan 48109, [4]Department of Biophysical Genetics, Kanazawa University Graduate School of Medicine, Kanazawa, Ishikawa, 920-8640, Japan, and [5]Center for Basic Neuroscience, University of Texas Southwestern Medical Center, Dallas, Texas 75390

Neurons of the medial nucleus of the trapezoid body, which transmit auditory information that is used to compute the location of sounds in space, are capable of firing at high frequencies with great temporal precision. We found that elimination of the *Kv3.1* gene in mice results in the loss of a high-threshold component of potassium current and failure of the neurons to follow high-frequency stimulation. A partial decrease in Kv3.1 current can be produced in wild-type neurons of the medial nucleus of the trapezoid body by activation of protein kinase C. Paradoxically, activation of protein kinase C increases temporal fidelity and the number of action potentials that are evoked by intermediate frequencies of stimulation. Computer simulations confirm that a partial decrease in Kv3.1 current is sufficient to increase the accuracy of response at intermediate frequencies while impairing responses at high frequencies. We further establish that, of the two isoforms of the Kv3.1 potassium channel that are expressed in these neurons, Kv3.1a and Kv3.1b, the decrease in Kv3.1 current is mediated by selective phosphorylation of the Kv3.1b isoform. Using site-directed mutagenesis, we identify a specific C-terminal phosphorylation site responsible for the observed difference in response of the two isoforms to protein kinase C activation. Our results suggest that modulation of Kv3.1 by phosphorylation allows auditory neurons to tune their responses to different patterns of sensory stimulation.

Key words: Kv3.1; potassium channel; MNTB neurons; protein kinase C; phosphorylation; auditory timing; channel isoforms

Introduction

The Kv3.1 potassium channel is expressed at high levels in neurons that characteristically fire rapid trains of action potentials (Perney et al., 1992; Weiser et al., 1995; Rudy, 1999). Particularly high levels of this channel are found in neurons of the auditory brainstem, such as bushy cells of the cochlear nucleus and neurons of the medial nucleus of the trapezoid body (MNTB). These neurons participate in neural circuits that determine the intensity and timing of auditory stimuli and use this information to determine the location of sounds in space (Joris, 1996). To perform their function, these neurons are endowed with a number of cellular specializations that allow them to fire at rates of many hundreds of Hertz both *in vivo* and *in vitro* (Spirou et al., 1990; Banks and Smith, 1992; Wu and Kelly, 1993; Trussell, 1999; Taschenberger and von Gersdorff, 2000). Such cells lock their action potentials precisely to the phase of auditory stimuli at frequencies of up to 2000–4000 Hz or to rapid fluctuations in the amplitude of higher-frequencies sounds (Joris and Yin, 1995; Joris, 1996). At those frequencies at which an action potential cannot be generated to every single stimulus, their firing pattern is characterized by alternating action potentials and failures of action potential generation (Banks and Smith, 1992; Brew and Forsythe, 1995; Wang et al., 1998). For example, in response to a 600 Hz stimulus, an MNTB neuron may fire at 300 Hz, locking its action potentials to every other stimulus (Wang et al., 1998). The synaptic and electrophysiological specializations of bushy cells and MNTB neurons ensure that the delay from a suprathreshold stimulus to the occurrence of an action potential varies by no more than a few tens of microseconds throughout a stimulus train (Borst et al., 1995; Oertel, 1999; Trussel, 1999).

A major component of potassium current in MNTB neurons is a high-threshold voltage-dependent potassium current (I_{HT}) that is selectively blocked by low concentrations of tetraethylammonium (TEA) and whose properties match those of the Kv3.1 potassium channel in heterologous expression systems (Perney and Kaczmarek, 1991; Brew and Forsythe, 1995; Wang et al., 1998; Grigg et al., 2000). Blockade of this current in MNTB neurons significantly impairs their ability to fire high-frequency trains of action potentials (Wang et al., 1998).

The *Kv3.1* gene has retained a high degree of similarity between human and rodents throughout evolution. Alternate splicing at the 3′ end of the *Kv3.1* gene results in two channel isoforms that differ exclusively at their C termini (Luneau et al., 1991). Previous work has shown that these two variants, termed Kv3.1a and Kv3.1b, share a similar expression pattern in the rat brain (Perney et al., 1992; Weiser et al., 1995). Although both variants are present in the same neurons, including MNTB neurons, levels

Received May 13, 2002; revised Nov. 25, 2002; accepted Nov. 26, 2002.

This work was supported by National Institutes of Health Grant DC-01919 (L.K.K.) and National Research Service Award Fellowship MH12257-02 (C.M.M.). We thank Donata Oertel for valuable comments on this manuscript.

Correspondence should be addressed to Leonard K. Kaczmarek, Department of Pharmacology, Yale University School of Medicine, 333 Cedar Street, New Haven, CT 06520. E-mail: leonard.kaczmarek@yale.edu.

 0270-6474/03/231133-09$15.00/0

of the Kv3.1b variant increase markedly at the time of synapse formation, and this isoform predominates in adult neurons (Perney et al., 1992; Liu and Kaczmarek, 1998). The functional significance of such alternately spliced channels that produce similar currents is unknown, although there is evidence that divergent C termini may be involved in targeting channels to different regions of the neuronal membrane (Pounce et al., 1997; Rudy, 1999).

Previous work has shown that, in heterologous expression systems, the Kv3.1 channel can be modulated by activation of protein kinase C, which produces a decrease in current amplitude (Critz at al., 1993; Kanemasa et al., 1995). We now found that regulation by this enzyme is specific to the Kv3.1b isoform and results from phosphorylation of a single site in the C terminus. We also compared the effects of the protein kinase C-induced reduction of Kv3.1 current in MNTB neurons with those of total elimination of the I_{HT} current through homologous recombination, using both native neurons and a computer simulation of their firing patterns. We demonstrate that, whereas total elimination of the Kv3.1 current in MNTB neurons severely impairs high-frequency firing, a partial reduction of current significantly increases both the number of action potentials generated and their temporal fidelity at those intermediate frequencies at which failures to generate action potentials are first detected. Our results suggest that the transition from the Kv3.1a to the Kv3.1b isoform during development allows MNTB neurons to modulate their firing pattern to improve temporal fidelity at intermediate stimulus frequencies.

Materials and Methods

Generation of Kv3.1 mutant mice. The *Kv3.1* gene was mutated by homologous recombination by a replacement vector as previously described in 129/Sv mice (Ho et al., 1997). Briefly, the coding region between *Eco*RI and *Msc*I (35 bp in the S2–S3 linker) was replaced with a neomycin-resistant cassette. Identification of mutant animals was confirmed by PCR using oligonucleotides directed against the 5′ coding region (primer 5′ GAA ATC GAG AAC GTT CGA AAC GG 3′) and the 35 bp recombinant sequence (primer 5′ CTA CTT CCA TTT GTC ACG TCC TG 3′).

Stable expression of Kv3.1a in a Chinese hamster ovary cell line. Chinese hamster ovary (CHO) cells with dihydrofolate reductase thymidylate (DHFR) deficiency [CHO/DHFR(−)] were maintained in Iscove's modified Dulbecco's medium (Invitrogen, San Diego, CA) supplemented with 10% fetal bovine serum, 0.1 mM hypoxanthine, and 0.01 mM thymidine and maintained in a 5% CO_2 incubator at 37°C. Cells were seeded 1 d before transfection at $\sim 5 \times 10^5$ cells/60 mm plate. Kv3.1a expression vector (pcDNA3/Kv3.1a) was added 24 hr later to transfect CHO/DHFR(−) using Lipofectamine (Invitrogen). The cells were then grown in normal medium for 48 hr to develop antibiotic resistance and subsequently exposed to geneticin (0.5 mg/ml; Invitrogen) for another 10–14 d. The geneticin-resistant cells were subjected to single-cell sorting using FACSIV (Becton Dickinson, Mountain View, CA) to generate individual stable cell lines. The stable transfection of Kv3.1b into CHO cells has been described previously (Wang et al., 1998).

Electrophysiological recordings from CHO cells. CHO/DHFR(−) cells were maintained in Iscove's modified Dulbecco's medium (Invitrogen) supplemented with 10% fetal bovine serum, 0.1 mM hypoxanthine, and 0.05 mg/ml geneticin (Invitrogen) and maintained in a 5% CO_2 incubator at 37°C. CHO cells were grown on coverslips 24–48 hr preceding recordings and transferred to extracellular solution (in mM: 140 NaCl, 1.3 $CaCl_2$, 5.4 KCl, 25 HEPES, and 33 glucose, pH 7.4) 1 hr before voltage clamping. Recordings were made as specified either with the perforated-patch technique using nystatin or in the whole-cell configuration using an Axopatch 1D amplifier (Axon Instruments, Foster City, CA). The patch electrodes had a resistance of 3–5 MΩ when filled with intracellular solution (in mM: 32.5 KCl, 97.5 K-gluconate, 5 EGTA, and 10 HEPES, pH 7.2). All data were low-pass filtered at 2 kHz and digitized using a modified digital data recorder (Instrutech, Great Neck, NY). Data were analyzed using pClamp 6.0 software. Average data are expressed as means ± SE. Conductance values were obtained by dividing current by the electrochemical driving force $[I_K/(V_m - E_k)]$. Normalized conductance–voltage plots were obtained by normalizing conductance (G) to maximal conductance (G_{max}) and fit using the Boltzmann isoform $G = G_{max}/[1 + \exp((V - V_{1/2})/k)]$, where $V_{1/2}$ is the voltage at half-maximal activation, and k is the slope factor.

Preparation of brainstem slices. Brains were rapidly removed from postnatal 9–14 d old mice (control 129/Sv or Kv3.1 mutant mice) or rats after decapitation and placed into ice-cold bicarbonate-buffered artificial CSF (ACSF) (in mM: 125 NaCl, 2.5 KCl, 26 $NaHCO_3$, 1.25 NaH_2PO_4, 2 Na pyruvate, 3 myo-inositol, 10 glucose, 2 CaCl2, and 1 $MgCl_2$, pH 7.4) solution gassed with 95% O_2–5% CO_2. The area of the brainstem containing MNTB nuclei were cut into four to six transverse slices using a vibrotome. The slices were incubated at 37°C for 1 hr and thereafter kept at room temperature (22–25°C).

Electrophysiological recordings from MNTB. Recordings were conducted on MNTB neurons as described previously (Macica and Kaczmarek, 2001). Briefly, a slice was transferred to a recording chamber that was continually perfused (1 ml/min) with gassed ACSF. Whole-cell patch-clamp recordings were made from visually identified MNTB neurons using an Axopatch 2D amplifier (Axon Instruments). The patch electrodes had a resistance of 3–5 MΩ when filled with intracellular solution (in mM: 32.5 KCl, 97.5 K-gluconate, 5 EGTA, 10 HEPES, and 1 $MgCl_2$, pH 7.2). For voltage-clamp recordings, the extracellular calcium concentration was lowered to 0.5 mM to minimize the contribution of calcium-activated K channels. TTX (0.5 μM) was also included in ACSF to block sodium currents. The mean cell capacitance was 12.0 ± 0.4 pF, with a mean series resistance of 5.3 ± 0.4 MΩ. The compensation for series resistance was set at least 85%, with a lag of 10 μsec. Data were low-pass filtered at 5 kHz, digitized, and acquired on-line with pClamp 6.0 software (Axon Instruments). Total current was compared before and after addition of activators of PKC in the presence and absence of PKC inhibitors, and averaged data are expressed as means ± SE. Conductance and normalized conductance values were obtained as above.

Immunoprecipitation and chemiluminescence. Stably transfected CHO cells expressing Kv3.1a or Kv3.1b or untransfected cells were grown to 80% confluence. Medium was removed, and cells were washed three times with ice-cold PBS. Cells were lysed with radioimmunoprecipitation assay buffer (150 mM NaCl, 1.0% Nonidet P-40, 0.5% deoxycholate, 0.1% SDS, and 50 mM Tris, pH 8.0) containing a protease inhibitor cocktail (Boehringer Mannheim, Indianapolis, IN) and phosphatase inhibitors (100 μM NaF and 0.2 mM $NaVO_3$) and allowed to incubate on a rocking platform for 30 min at 4°C. Lysates were spun in a microfuge for 15 min, and the supernatant was transferred to a new tube. Rat brain membranes were prepared from whole brain homogenized in 320 mM sucrose–PBS, pH 7.4, containing a protease cocktail inhibitor and centrifuged at 1000 × *g* for 10 min at 4°C. The supernatant was then centrifuged at 15,000 × *g* for 30 min at 4°C, followed by centrifugation of the supernatant at 105,000 × *g* for 1 hr at 4°C. Pellets were reconstituted in sucrose–PBS. Lysates and membranes (brought up to volume with PBS) were precleared with a 50% slurry aliquot of protein A Sepharose beads, followed by incubation with the indicated anti-Kv3.1 antibody (1:1000 dilution) at 4°C overnight. Lysates and membranes were immunoprecipitated with protein A Sepharose beads for 2 hr at 4°C, spun, and washed three times in Triton X-100 buffer (0.1% Triton X-100, 0.1% SDS, 300 mM NaCl, and 50 mM Tris, pH 7.5). Samples were eluted by boiling in 1× SDS-PAGE sample buffer (62.5 mM Tris, pH 6.8, 4% SDS, 10% glycerol, 0.02% bromophenol blue, and 4% β-mercaptoethanol) for 5 min. Samples were subjected to SDS-PAGE on a 7.0% gel and transferred to a polyvinylidene difluoride (PVDF) membrane (Millipore, Bedford, MA). Peptides were visualized by chemiluminescence. Briefly, the membrane was incubated with the Kv3.1 antibody against the C terminus at a 1:4000 dilution in antibody diluent (1% casein and 0.04% Tween 20 in PBS, pH 7.4) for 1 hr, washed three times, incubated with secondary antibody (1:10,000 in diluent buffer), and washed three times. The blot was incubated with substrate (5.5 mg of luminol, 0.28 mg of *p*-coumaric acid, and 1% H_2O_2 –25 ml of PBS) for 1 min and briefly exposed to film.

Metabolic labeling, immunoprecipitation, and phosphoamino acid analysis. Phosphorylation of Kv3.1 was analyzed in stably transfected CHO cells expressing either Kv3.1a or Kv3.1b that was metabolically labeled to equilibrium with [^{32}P]orthophosphate as described previously (Macica and Kaczmarek, 2001). Cells were lysed, immunoprecipitated, and subjected to SDS-PAGE as described above. This gel was fixed as above and dried, and bands were visualized by autoradiography. Phosphoamino acid analysis was also performed on samples prepared as above and analyzed by two-dimensional electrophoresis, as described previously (Macica and Kaczmarek, 2001).

Numerical simulations. Computer modeling was performed using equations that have been used previously to model MNTB neurons (Wang et al., 1998) and other auditory neurons (Perney and Kaczmarek, 1997; Richardson and Kaczmarek, 2000). The model comprised a sodium current I_{Na}, the Kv3.1 current $I_{Kv3.1}$, a low-threshold potassium current I_{LT}, and a leakage conductance I_L. I_{Na} and I_L were given by the equations $I_{Na} = g_{Na}m^3h(50 - V)$ and $I_L = g_L(-63 - V)$, respectively. I_{LT} and $I_{Kv3.1}$ were simulated by the equations $I_{LT} = g_{LT}lr(-80 - V)$ and $I_{Kv3.1} = g_{Kv3.1}n^3(0.8 + 0.2p)(-80 - V)$. Evolution of the variables m, h, l, r, n, and p were determined by Hodgkin-Huxley-like equations as described previously (Perney and Kaczmarek, 1997). Parameters for the sodium current were as follows: $g_{Na} = 0.5$ μS, $k_{\alpha m} = 76.4$ msec^{-1}, $\eta_{\alpha m} = 0.037$ mV^{-1}, $k_{\beta m} = 6.93$ msec^{-1}, $\eta_{\beta m} = -0.043$ mV^{-1}, and $k_{\alpha h} = 0.000533$ msec^{-1}, $\eta_{\alpha h} = -0.0909$ mV^{-1}, $k_{\beta h} = 7.87$ msec^{-1}, and $\eta_{\beta h} = 0.0691$ mV^{-1}. The leakage conductance g_L was 0.002 μS. Parameters for potassium current were obtained from direct fits to traces recorded from MNTB neurons and Kv3.1-transfected CHO cells (Wang et al., 1998). Parameters for the low-threshold potassium current were as follows: $g_{LT} = 0.02$ μS, $k_{\alpha 1} = 1.2$ msec^{-1}, $\eta_{\alpha 1} = 0.03512$ mV^{-1}, $k_{\beta 1} = 0.2248$ msec^{-1}, $\eta_{\beta 1} = -0.0319$ mV^{-1}, $k_{\alpha r} = 0.0438$ msec^{-1}, $\eta_{\alpha r} = -0.0053$ mV^{-1}, $k_{\beta r} = 0.0562$ msec^{-1}, and $\eta_{\beta r} = -0.0047$ mV^{-1}. Parameters for the Kv3.1 channel were as follows: $g_{HT} = 0.15$ μS (control) or 0.10 μS [phorbol 12-myristate 13-acetate (PMA) treated], $k_{\alpha n} = 0.2719$ msec^{-1}, $\eta_{\alpha n} = 0.04$ mV^{-1}, $k_{\beta n} = 0.1974$ msec^{-1}, $\eta_{\beta n} = 0$ mV^{-1}, $k_{\alpha p} = 0.00713$ msec^{-1}, $\eta_{\alpha p} = -0.1942$ mV^{-1}, $k_{\beta p} = 0.0935$ msec^{-1}, and $\eta_{\beta p} = 0.0058$ mV^{-1}. Numerical simulations of the responses of the cells to external stimulation was performed using the equation $C\ dV/dt = I_{Na} + I_{Kv3.1} + I_{LT} + I_{ext(t)}$, where C is the cell capacitance (0.01 nF), and external currents $I_{ext(t)}$ were presented as repeated current steps (1.4 nA, 0.25 msec) applied at frequencies from 100 to 600 Hz.

Results

Contribution of Kv3.1 to the firing pattern of MNTB neurons

We first tested the role of the Kv3.1 channel in MNTB neurons by comparing the properties of MNTB neurons in 9- to 14-d-old brainstem slices from wild-type mice with those in which the *Kv3.1* gene had been deleted by homologous recombination (Ho et al., 1997). As described previously, wild-type mice express a high-threshold potassium current I_{HT} whose properties closely match those of Kv3.1 in transfected cell lines (Wang et al., 1998). This current can be isolated by stepping to positive potentials from a holding potential of −40 mV, at which potential the low-threshold component of total outward current in these neurons is inactivated (Brew and Forsythe, 1995; Wang et al., 1998). This current can be substantially inhibited by extracellular application of 1 mM TEA ions, consistent with the IC_{50} of 250 μM for the Kv3.1 channel (Kanemasa et al., 1995; Wang et al., 1998; Rudy, 1999) (Fig. 1*a*,*b*).

When recordings were made in MNTB neurons from Kv3.1−/− mice, the current evoked by depolarizing commands from −40 mV current was reduced by >90%, indicating that the I_{HT} current had been eliminated (Fig. 1*c*). The remaining ~10% high-threshold current was blocked by 1 mM TEA. In contrast, the low-threshold currents evoked by stepping from a holding potential of −80 mV could still readily be recorded in the Kv3.1−/− mice (data not shown). The low-threshold current, which is TEA insensitive in wild-type mouse, however, displays sensitivity to 1 mM TEA, suggesting a compensatory increase in a TEA-sensitive low-threshold current in these mice (data not shown). It is possible that the afterhyperpolarization in the Kv3.1−/− mice reflects a compensatory increase in low-threshold current in these animals. Combined with previous work demonstrating the loss of Kv3.1 mRNA and protein in the Kv3.1−/− mice (Ho et al., 1997), our findings strongly support the identification of the I_{HT} current recorded at the somata of MNTB neurons with the Kv3.1 channel.

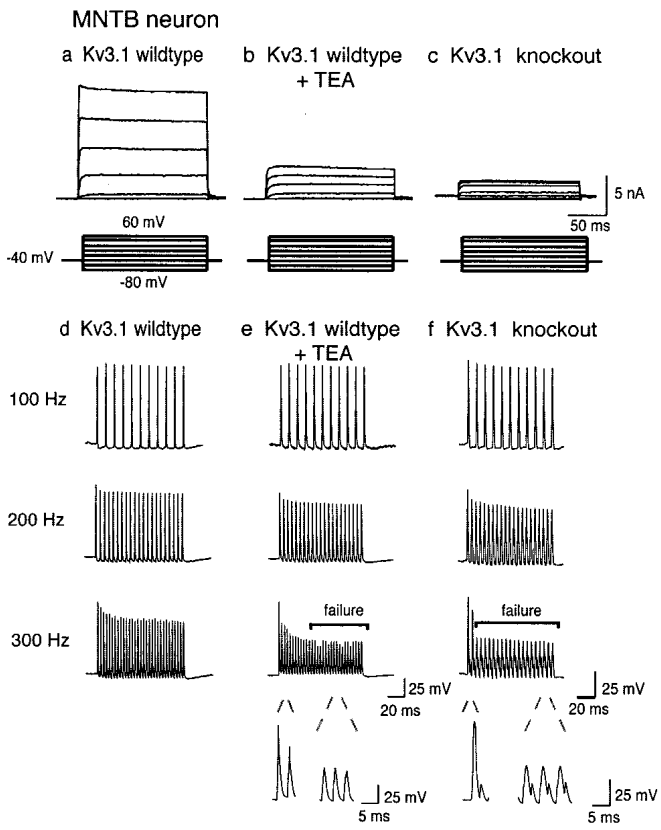

Figure 1. Representative traces comparing native high-threshold current from a 14 d wild-type MNTB neuron with the high-threshold current from a 14 d Kv3.1 mutant MNTB neuron. *a*, *b*, Outward currents evoked by stepping from a holding potential of −40 mV for 2 min (to ensure complete inactivation of low-threshold current) to test potentials from −80 to +40 mV in 20 mV increments in wild-type mice before and after treatment with 1 mM TEA or in Kv3.1 mutant mice (*c*). *d*, *e*, Representative recording from an MNTB neuron in response to brief current injections (2 nA, 0.3 msec) at three different test frequencies (100–300 Hz) in wild-type mice before and after treatment with 1 mM TEA or in Kv3.1 mutant mice (*f*). *Bars* denote failure to evoke an action potential in response to a stimulus. Failure was defined as a membrane depolarization to less than −10 mV in response to a current injection. Expanded *traces* below compare a successful action potential with failures, which showed little regenerative response.

To test the impact of knock-out of the *Kv3.1* gene on the firing properties of MNTB neurons, neurons were stimulated with trains of brief current pulses (0.3 msec, 2 nA) at frequencies ranging from 100 to 300 Hz (Fig. 1*d*). As described previously, wild-type MNTB neurons faithfully follow stimulus frequencies up to 300 Hz (Wang et al., 1998). In the presence of extracellular TEA (1 mM) a normal pattern of action potentials is evoked at the lower frequencies (100–200 Hz), but a progressive loss of full action potentials occurs during a train at 300 Hz and at higher frequencies (Fig. 1*e*). A similar, but more severe, deficit occurs in MNTB neurons from Kv3.1−/− mice. These can follow stimulation at 100 Hz, but attenuation of action potentials is already evident even at 200 Hz. At 300 Hz and at all higher frequencies,

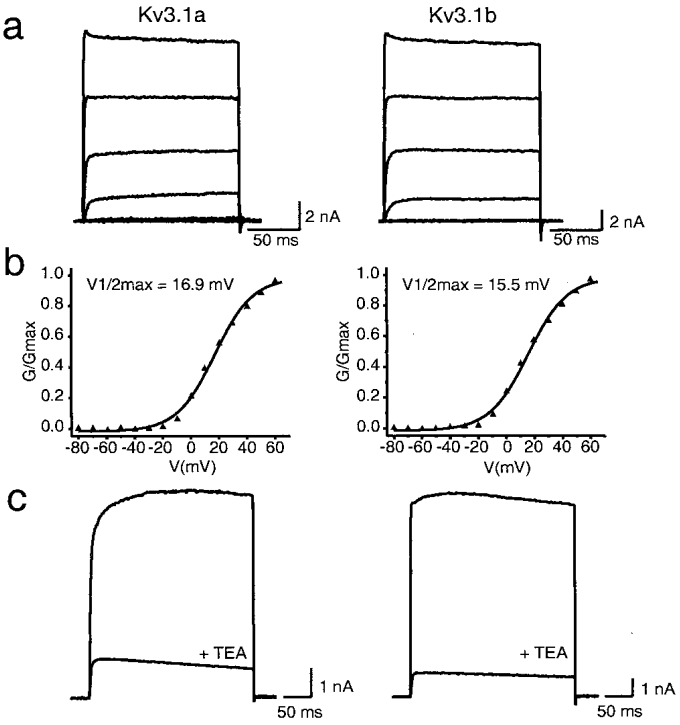

Figure 2. Comparison of Kv3.1 current recorded from CHO cells stably transfected with Kv3.1a or Kv3.1b. *a*, Whole-cell current was evoked by depolarizing the membrane from a holding potential of −80 to +60 mV in 20 mV increments. *b*, Normalized conductance–voltage relationship for Kv3.1a versus Kv3.1b. Conductance values (*G*) were obtained as described in Materials and Methods. *c*, Sensitivity of Kv3.1a or Kv3.1b to 1 mM TEA. Currents were evoked as described in *a*.

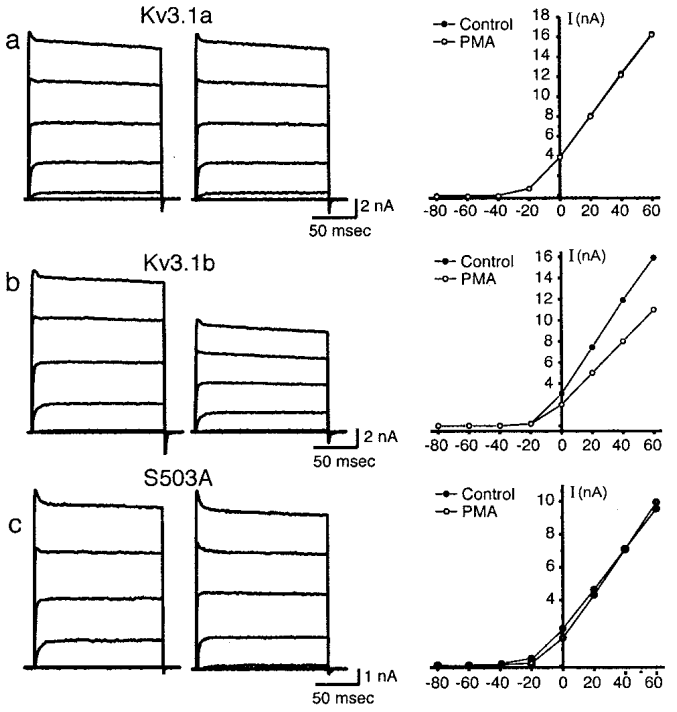

Figure 3. Effect of 100 nM PMA on Kv3.1 current. *a*, Whole-cell currents evoked from CHO cells stably expressing Kv3.1a from a holding potential of −70 mV to test potentials of −80 to +60 mV in 20 mV increments (*left*) and corresponding current–voltage relationship of evoked currents (*right*) before and after PMA treatment. *b*, Whole-cell currents evoked from CHO cells stably expressing Kv3.1b (*left*) and current–voltage relationship of evoked currents. *c*, Whole-cell currents evoked from CHO cells stably expressing Kv3.1b mutant S503A (*left*) and current–voltage relationship of evoked currents.

only a single action potential is evoked at the start of the train (Fig. 1*f*). This complete loss of response at higher frequencies exactly matches that predicted in numerical simulations for elimination of the I_{HT} current (Wang et al., 1998).

The Kv3.1 isoforms differ in their response to activation of protein kinase C

In transfected cells, the amplitude of Kv3.1 current is known to be regulated by activators of protein kinase C, attributed to a decrease in single-channel open probability (Critz et al., 1993; Kanemasa et al., 1995). There exist two isoforms of the Kv3.1 channel, Kv3.1a and Kv3.1b, which arise by alternate splicing of the *Kv3.1* gene. These differ in the number of consensus sites for phosphorylation by protein kinase C. The longer Kv3.1b isoform has two additional consensus sites in the C terminus that are absent in Kv3.1a. Both isoforms are coexpressed in the same neurons, with Kv3.1b predominating in the mature nervous system (Perney et al., 1992; Weiser et al., 1995; Rudy, 1999). To determine the physiological consequences of modulation by protein kinase C, we compared the electrophysiological properties of the two isoforms in transfected cells and of the native I_{HT} current in MNTB neurons.

We first compared the basal electrophysiological properties of the two isoforms. Currents were evoked in CHO cells stably transfected with either Kv3.1a or Kv3.1b by depolarizations to test potentials between −80 and 60 mV (Fig. 2*a*). In some but not all experiments, a transient peak that decreased slightly to a steady-state value was seen at positive potentials at the beginning of the pulse for both Kv3.1a and Kv3.1b, a finding reported previously for Kv3.1b (Rettig et al., 1992; Critz et al., 1993; Kanemasa et al., 1995; Rudy, 1999). The conductance–voltage relationships were fit by Boltzmann isotherms with a midpoint of activation of 17.3 ± 1.26 mV ($n = 9$) versus 20.8 ± 1.60 mV ($n = 9$) for Kv3.1a and Kv3.1b, respectively (Fig. 2*b*). The 10–90% rise times for maximal activation at 60 mV were 1.25 ± 0.16 msec ($n = 9$) versus 1.22 ± 0.09 msec, ($n = 9$) respectively. Deactivation kinetics were obtained from tail currents recorded after a 100 msec depolarizing pulse to +40 mV, followed by membrane potential repolarization to −40mV. These were fit by a single exponential and yielded time constants of 2.38 ± 0.14 msec ($n = 18$) and 2.20 ± 0.12 msec ($n = 10$), respectively. In addition, both Kv3.1a and Kv3.1b were inhibited to a similar degree by 1 mM TEA (87 ± 1.5%, $n = 3$ vs 82 ± 5.1%, $n = 12$) (Fig. 2*c*).

Although the biophysical properties of Kv3.1a and Kv3.1b appear indistinguishable under basal conditions, their response to 100 nM PMA, an activator of protein kinase C, was very different. Kv3.1a or Kv3.1b currents were recorded from nystatin-perforated patches before and after exposure to 100 nM PMA ($n = 9$) (Fig. 3*a*,*b*). PMA produced a significant reduction of Kv3.1b current (32.4 ± 4.3% inhibition), which was maximal by 10–15 min (Fig. 4). 4α-PMA, an analog of PMA that does not activate protein kinase C, did not significantly affect Kv3.1b current (Fig. 4). In contrast, Kv3.1a current amplitude was not significantly affected by PMA (2.26 ± 1.7% inhibition) (Figs. 3*a*, 4). No effect of PMA was detected on the kinetics (data not shown) or the voltage dependence of activation of either isoform (midpoint of activation, 20.3 ± 1.3 mV during control period vs 19.1 ± 1.6 mV after PMA treatment in nystatin-perforated patches).

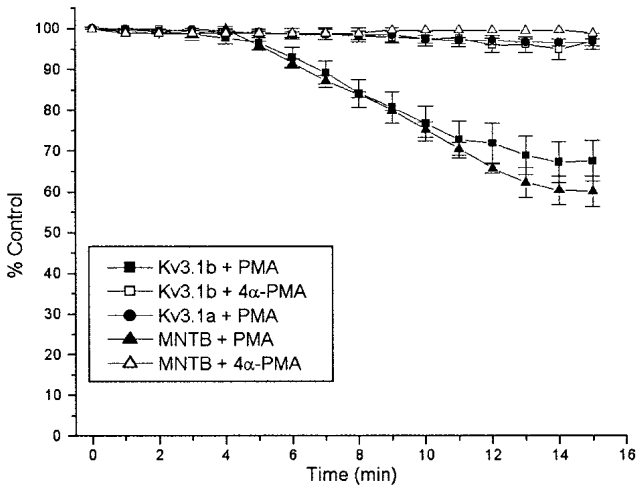

Figure 4. Time course of the effect of 100 nM PMA on Kv3.1 current amplitude. Outward current evoked from a holding potential of −70 mV in Kv3.1-transfected cells or from a holding potential of −40 mV in MNTB neurons to a test potential of +40 mV was monitored in perforated patches every 1 min in response to treatment with exogenous PMA in Kv3.1a-transfected cells (*filled circles*), in Kv3.1b-transfected cells (*filled squares*), or in MNTB neurons (*filled triangles*). The effect of the inactive phorbol ester 4α-PMA was also tested on Kv3.1b-transfected cells (*open squares*) and MNTB neurons (*open triangles*).

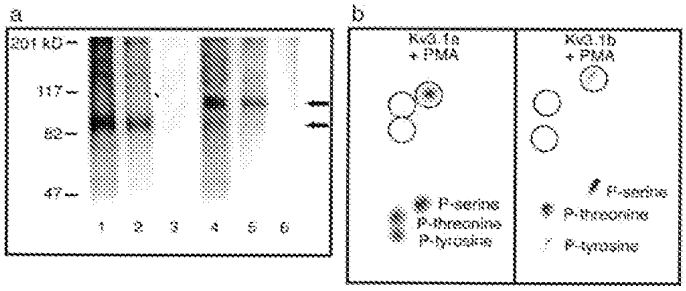

Figure 5. *In vivo* phosphorylation and phosphoamino acid analysis of Kv3.1 in CHO cells. *a*, CHO cells expressing Kv3.1a or Kv3.1b were radiolabeled with [^{32}P]orthophosphate to equilibrium, stimulated with or without 100 nM PMA for 15 min, and lysed. Lysates were immunoprecipitated with Kv3.1 antibody (Kv3.1a, *lanes 1* and *2*, with and without PMA, respectively or Kv3.1b, *lanes 4* and *5*, with and without PMA, respectively) and resolved as outlined in Materials and Methods. An additional ^{32}P-labeled Kv3.1a or Kv3.1b immunoprecipitate was treated with calf intestinal alkaline phosphatase for 1 hr at 37°C (*lanes 3* and *6*, respectively). *b*, Phosphoamino acid analysis of the Kv3.1a or Kv3.1b channel protein obtained from lysates and immunoprecipitated and electrophoresed as above. The gel was transferred to a PVDF membrane, and the Kv3.1 band was visualized by autoradiography. The excised protein was subjected to phosphoamino acid analysis as outlined in Materials and Methods and visualized by ninhydrin staining (*top*), and standard phosphoamino acids were visualized by autoradiography (*bottom*).

Phosphorylation of Kv3.1 channel proteins

To determine whether the actions of activators of protein kinase C on Kv3.1b currents result from the direct phosphorylation of the Kv3.1b protein, CHO cells stably expressing either Kv3.1a or Kv3.1b were radiolabeled to equilibrium with [^{32}P]orthophosphate and were then stimulated for 15 min with 100 nM PMA. Immunoprecipitation revealed substantial basal incorporation of ^{32}P into both channel proteins, as well as stimulated incorporation in the presence of PMA (Fig. 5*a*). Incorporation could be eliminated by treatment of the immunoprecipitated phosphoprotein with alkaline phosphatase. To determine the identity of the amino acids into which ^{32}P was incorporated, the immunoprecipitates were then subjected to phosphoamino acid analysis. Radioactivity comigrating with unlabeled phosphoserine, but not phosphothreonine or phosphotyrosine, was detected after acid hydrolysis of ^{32}P-labeled Kv3.1 (Fig. 5*b*). These results indicate that, of the putative consensus sites for phosphorylation, only those containing serine residues are phosphorylated.

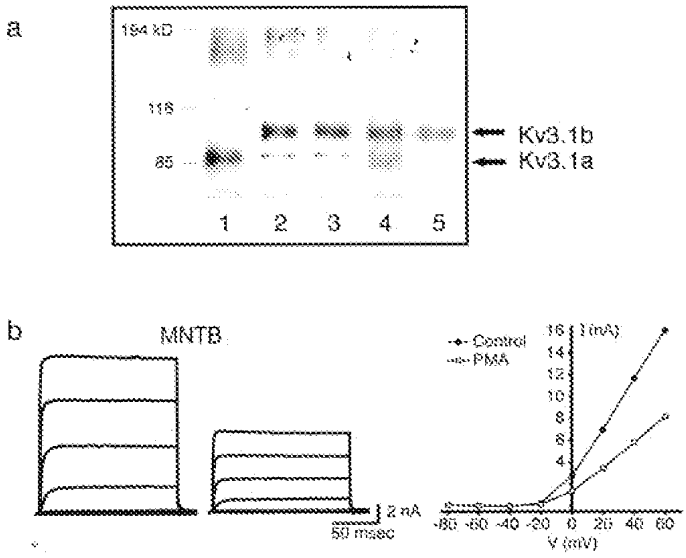

Figure 6. Molecular identity and effect of 100 nM PMA on native Kv3.1 current. *a*, Coimmunoprecipitation of Kv3.1a and Kv3.1b in brain homogenates or in stably transfected CHO cells. *Lane 1*, Kv3.1a/CHO with N-terminal antibody; *lane 2*, Kv3.1b/CHO with N-terminal antibody; *lane 3*, Kv3.1b/CHO with C-terminal antibody; *lane 4*, rat brain membranes with N-terminal antibody; *lane 5*, rat brain membranes with C-terminal antibody. *b*, Whole-cell currents evoked from a 13 d MNTB neuron from a holding potential of −40 mV to test potentials of −80 to +60 mV (*left*) and current–voltage relationship of evoked currents before and after PMA treatment.

Protein kinase C acts at serine 503 of Kv3.1b

Kv3.1b has 11 consensus sites for PKC-mediated phosphorylation, two of which are absent from Kv3.1a as a result of the divergent C terminus. Only one of these (S503), however, is a serine site. The phosphoamino acid analysis suggests, therefore, that this is the only consensus protein kinase C site that differs between the two isoforms. To test the hypothesis that this unique site is responsible for response of Kv3.1b to activation of protein kinase C, a mutant Kv3.1b channel was constructed in which this serine was mutated to alanine. When this mutation (S503A) was stably expressed in CHO cells, the currents appeared identical to those of wild-type Kv3.1 but were completely insensitive to PMA treatment ($n = 6$) (Fig. 3*c*).

The Kv3.1b channel subunit predominates in mature neurons

To identify native Kv3.1 protein isoforms, membranes were prepared from adult rat brain homogenates or from CHO cells stably transfected with either isoform. These were immunoprecipitated with antibodies against either the N terminus, which recognizes both isoforms, or the Kv3.1b C terminus, which recognizes only Kv3.1b (Perney and Kaczmarek, 1991) (Fig. 6*a*). Immunoprecipitated Kv3.1a and Kv3.1b in CHO cells had mobilities corresponding to ~98 and 110 kDa, respectively (Fig. 6*a*, *lanes 1–3*). Immunoprecipitation in both cell lines also yielded additional bands corresponding to the predicted molecular weights of the unglycosylated forms of the channel proteins (85 and 80 kDa, respectively). In support of this interpretation, the size of the *in vitro* translated product of the Kv3.1 channels in the absence of membranes corresponded precisely to the M_r of the lower bands (data not shown). The predominant isoform in brain homoge-

nates is Kv3.1b (Fig. 6*a*, *lane 4*), consistent with the dominant expression pattern of Kv3.1 mRNA transcripts in adult animals (Perney et al., 1992). Although the expression of both isoforms in the same cells (Perney et al., 1992; Weiser et al., 1995) suggests that they could form heteromultimers *in vivo*, Kv3.1a protein could not be detected in immunoprecipitates from rat brain membranes using the C-terminus antibody, which recognizes only the Kv3.1 b channel protein (Fig. 6*a*, *lane 5*).

Effect of phorbol ester treatment on high-threshold current in MNTB neurons

Having confirmed the molecular identity of the native high-threshold current as Kv3.1, we next tested the effect of PMA on potassium currents and the firing pattern of MNTB neurons. In 9 of 12 experiments, the amplitude of the high-threshold component of current evoked from a holding potential of −40 mV was reduced by 44.8 ± 2.17% in response to 100 nM PMA (Fig. 6*b*). The time course of inhibition closely matched that for the inhibition of Kv3.1b by PMA in transfected cells. Moreover, the inactive phorbol ester 4α-PMA had no effect on MNTB current amplitude (Fig. 4). In 3 of the 12 experiments conducted, however, there was very little effect of PMA on I_{HT} current (4.50 ± 0.76%). Finally, PMA had little or no effect on the low-threshold component of current, obtained by subtracting the high-threshold component of current from the total outward current at a test potential of −20 mV, in which a majority of the total outward current is of the low-threshold type (Fig. 7*a*). Consistent with this finding was the observation that the spike threshold is unaltered and that MNTB neurons fire a single action potential in response to a sustained current injection both before and after PMA treatment (Fig. 7*b*). This limited depolarization has been shown to be mediated by the activation of the low-threshold current, which results in the lowering of the input resistance and a shortening of membrane time constants in the depolarizing voltage range, thus preventing repetitive firing in response to a sustained current injection (Wu and Kelly, 1993; Brew and Forsythe, 1995; Wang et al., 1998).

Additional analysis of the action of PMA on the I_{HT} current also showed that its effects closely matched those for Kv3.1 in CHO cells and that PMA produced no change in the activation or deactivation kinetics in any experiment. Native I_{HT} currents had 10–90% rise times for maximal activation at 60 mV of 1.41 ± 0.18 msec (n = 8) during the control period versus 1.12 ± 0.15 msec (n = 8) after 15 min PMA treatment. Deactivation kinetics of macroscopic currents were obtained by tail currents generated by a 100 msec depolarizing pulse to +40 mV, followed by membrane potential repolarization to test potentials between −100 and −20 mV. Deactivation kinetics were fit by a single exponential and yielded time constants of 2.35 ± 0.25 (n = 9) during the control period and 2.24 ± 0.28 (n = 8) at −40 mV after treatment of 15 min PMA. Like the cloned Kv3.1b channel, there was also no effect on the voltage dependence of activation of I_{HT} (midpoint of activation, 16.6 ± 1.5 mV during control period vs 17.8 ± 1.0 mV after PMA).

Other parameters that were measured before and after PMA treatment included the mean slope of the rising phase of action potentials, which remained unchanged (before PMA, 171.8 ± 16.6 mV/msec; after PMA, 189.3 ± 13.8 mV/msec). In addition, the peak voltage reached by action potentials remained unchanged (before PMA, +28.8 ± 0.4 mV; after PMA, +30.6 ± 0.8 mV), and the mean resting potential remained unchanged (before PMA, −64.2 ± 1.12 mV; after PMA, −65.2 ± 0.87 mV). The findings argue that a change in sodium currents is unlikely to contribute to the observed effects.

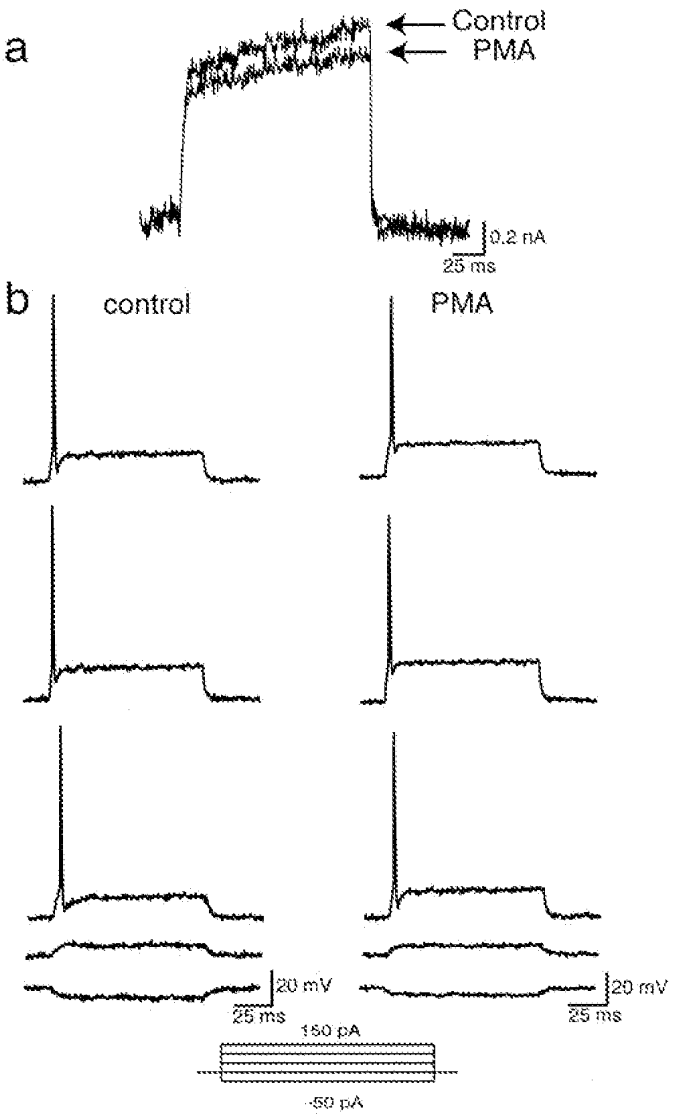

Figure 7. Effect of 100 nM PMA on low-threshold current from an MNTB neuron. *a*, Low-threshold current was obtained by subtracting the high-threshold component of outward current evoked from a holding potential of −40 mV to a test potential of −20 mV from total outward current evoked from a holding potential of −70 mV to a test potential of −20 mV ($I_{LT} = I_{TOT} - I_{HT}$) before and after PMA treatment (n = 8). *b*, Current-clamp recording from an MNTB neuron in response to a series of 100 msec current injections ranging from −50 to 150 pA before and after PMA treatment (n = 4).

Effect of phorbol ester on firing properties of MNTB neurons

In contrast to the complete loss of Kv3.1 current produced by knock-out of the Kv3.1 gene, the partial suppression of Kv3.1b current by protein kinase C might be expected to produce smaller changes in firing characteristics and contribute to the fine-tuning of auditory information processing. We therefore examined the effect of 100 nM PMA on the response of MNTB neurons to different frequencies of stimulation. To avoid the presynaptic effects of PMA at the MNTB synapse (Hori et al., 1999), we used direct current stimulation of MNTB neurons. At frequencies up to 300 Hz, at which MNTB neurons fire action potentials in response to every stimulus pulse, there was no effect of PMA on the ability of the cells to follow stimulation. At slightly higher frequencies, however, action potentials are not generated in re-

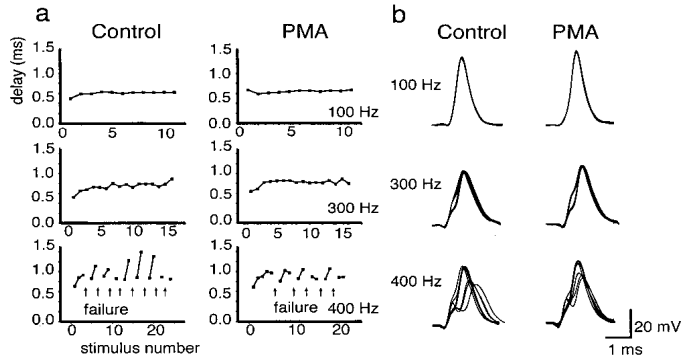

Figure 8. Effect of PMA treatment on firing properties of an MNTB neuron (13 d old) in response to different frequencies of stimulation ($n = 6$). *a*, Plots of the delay from the onset of the stimulus pulse to the peak of the action potential before (*Control*) and 15 min after (*PMA*) treatment with 100 nM PMA. *Arrows* denote failure to evoke an action potential in response to a stimulus. Failure was defined as a membrane depolarization to less than −10 mV in response to a current injection (one that has no detectable regenerative component). *b*, Superimposed action potentials in response to 100, 300, and 400 Hz stimulation. Failures were omitted from the superimposed *traces*.

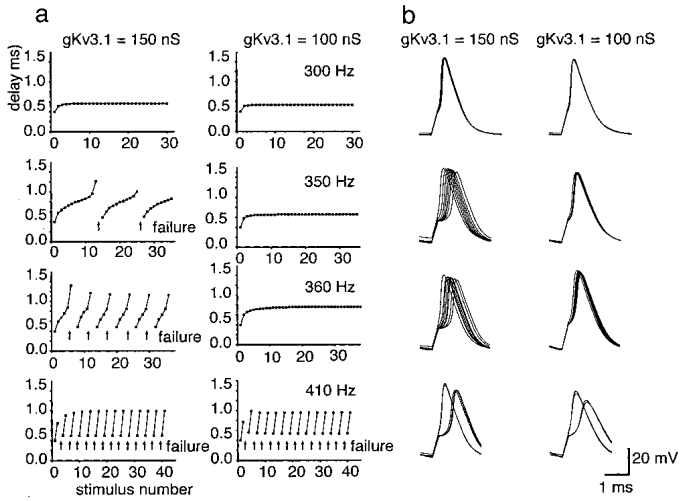

Figure 9. Model of an MNTB neuron in response to different frequencies of stimulation. *a*, Plots of the delay from the onset of the stimulus pulse to the peak of the action potential under control conditions (150 nS Kv3.1 conductance) and under conditions in which the level of Kv3.1 current amplitude is reduced to a similar degree as in PMA-treated neurons (100 nS Kv3.1 conductance). *Arrows* denote failure to evoke an action potential in response to a stimulus. Failure was defined as a membrane depolarization to less than −10 mV in response to a current injection. *b*, Superimposed action potentials in response to 100, 350, 360, or 410 Hz stimulation. Failures were omitted from the superimposed *traces*.

sponse to every stimulus, and the firing pattern is characterized by intermittent failures separated by brief trains of action potentials. For example, in the cell shown in Figure 8*a*, the control response at 400 Hz consists of groups of two or three consecutive action potentials separated by failures to reach threshold for spike initiation. At these intermediate frequencies at which failures are first detected, exposure of MNTB neurons to PMA reduced the number of failures. For example, in the cell shown in Figure 8*a*, PMA produced a small reduction in the number of failures in response to stimulation.

More striking than the effect of PMA on the number of failures was its effect on the timing of action potentials. To examine differences in the timing of the evoked action potentials, we superimposed successive action potentials locked to the stimulus (Fig. 8*b*). In addition, we plotted the change in the delay from the onset of the stimulus to the peak of the action potential during the stimulus trains. At frequencies up to 300 Hz at which all stimuli evoked action potentials, the latency from the onset of the stimulus pulse to the peak of the action potential was invariant, as seen by the superposition of the response to consecutive current pulses. The occurrence of failures, which occurs at higher frequencies, however, substantially disrupts the timing of the action potentials. The latency from onset of the current pulse to the peak of the action potential was found to vary by 500 μsec or more in the burst of action potentials separated by failures. Exposure of MNTB neurons to PMA, however, was found to reduce significantly the variance of the latency at 400 Hz [at 400 Hz, control delay of 0.99 ± 0.17 (SD) msec; after PMA, delay of 0.85 ± 0.11 msec; $p_{(\text{delay})} < 0.0001$; $p_{(\text{variance})} < 0.015$; $n = 46$ action potentials] (Fig. 8*b*).

Because it is certain that, in addition to their effects on Kv3.1 currents, activators of protein kinase C have a variety of other actions on MNTB neurons, we performed numerical simulations to compare the effects of a partial reduction of Kv3.1 current with those of PMA. We used a model that had been used previously to predict the firing pattern of MNTB neurons and that incorporates the amplitudes and kinetics of currents measured directly in these cells (Wang et al., 1998). The response of the model neurons to current pulses at different frequencies were tested with control conditions (150 nS Kv3.1 conductance) and in response to altering the level of Kv3.1 current to a similar degree as in PMA-treated MNTB neurons (100 nS Kv3.1 conductance) (Fig. 9). As with the native neurons, the model neuron was able to respond to each stimulus pulse up to 300 Hz, and the timing of action potentials was uniform throughout a maintained stimulus train, with either level of Kv3.1 current. However, as the stimulus frequency was increased, a critical frequency was reached at which failures began to occur (350 Hz with 150 nS Kv3.1 in Fig. 9*a*). At this point, the timing of the action potentials was also disrupted, with a progressive increase in the latency of the response with consecutive action potentials. At "intermediate" stimulus frequencies above this critical frequency, the latency during a train of action potentials could vary by >1 msec. When the level of Kv3.1 current was reduced by 33% at these frequencies, the failures were reduced or eliminated, and the timing of the action potentials was restored (Fig. 9*b*). As the stimulus frequency was increased, however, the effects of the reduction of Kv3.1 were less apparent (410 Hz in Fig. 9), and, at higher frequencies, the ability of the model neurons to respond was attenuated by the reduction in Kv3.1 current (data not shown). The simulation studies show that a reduction in Kv3.1 current alone is predicted to decrease the number of failures and to significantly reduce the variance of the timing of action potentials at intermediate frequencies of stimulation.

Discussion

Kv3.1 is critical for the preservation of timing information

Within the auditory brainstem, the Kv3.1 channel is expressed at high levels in spherical and globular bushy cells of the cochlear nucleus (Perney and Kaczmarek, 1997) and in principal neurons of the MNTB (Li et al., 2001), which receive a secure synaptic input from the globular bushy cells (Smith et al., 1991). The large calyx of Held synaptic ending from globular bushy cells onto the somata of MNTB neurons is specialized for temporally invariant transmission of excitatory inputs (Morest, 1968; Borst et al., 1995; Joris, 1996; Trussell, 1999), and evidence suggests that MNTB neurons faithfully transmit temporal information from globular bushy cells (Smith et al., 1998). Many globular bushy

cells have spontaneous firing rates of over 100 Hz and, when driven by sounds, attain firing frequencies of 500–600 Hz (Rhode and Smith, 1986; Spirou et al., 1990). Our findings suggest that the Kv3.1 potassium channel is required for the normal ability of these cells to follow such high-frequency stimulation.

MNTB neurons provide an inhibitory input to the lateral superior olive and participate in a pathway that detects interaural intensity differences in high-frequency sounds (Joris and Yin, 1995, 1998; Tollin and Yin, 2002). They also project to other auditory nuclei, including the medial superior olive, which detects interaural timing differences in lower-frequency sounds. The characteristic frequencies of a population of globular bushy cells, which provide the excitatory input to the MNTB, lie within the range at which phase-locking occurs (<4000 Hz), and experiments with cats have shown that these cells have the ability to lock their action potentials very precisely to the phase of auditory stimuli at these frequencies (Smith et al., 1991). Nevertheless, the majority of these neurons, as well as their MNTB targets, have characteristic frequencies >4000 Hz (Guinan et al., 1972; Smith et al., 1991, 1998), and neurons are incapable of phase locking to such higher frequencies. Neurons with high characteristic frequencies, however, also respond to lower sound frequencies, and their ability to phase lock at these lower frequencies is even enhanced over that of cells with lower characteristic frequencies (Joris et al., 1994). Our present results suggest that direct phosphorylation of the Kv3.1 channel by protein kinase C provides a potential mechanism that can adjust the accuracy of timing of the response of MNTB neurons. Such adjustments of timing could occur either at frequencies close to the characteristic frequency or when a neuron is driven at quite different frequencies. Indeed, it has been proposed that the pathway from the globular bushy cells to the lateral superior olive via the MNTB comprises a circuit that can determine timing differences in high-frequency sounds that are amplitude modulated at lower frequencies (Joris and Yin, 1995; Joris, 1996).

Because the effects of PKC activation on the amplitude of Kv3.1 current occur over a period of several minutes, such modulation could reflect a slow adaptation to the auditory environment. Nevertheless, although the pathways that lead to the regulation of protein kinase C in MNTB neurons remains to be defined, it is likely that receptor-mediated activation is more rapid than pharmacological activation and that modulation could occur on a faster time scale.

The Kv3.1b isoform predominates in the principal neurons of the MNTB

The simplest interpretation of the finding that deletion of the Kv3.1 gene results in the near total elimination of the high-threshold I_{HT} current is that the I_{HT} channel represents a homomultimer of Kv3.1 subunits. In addition to Kv3.1, MNTB neurons express mRNA for Kv3.3, another *Shaw* subfamily channel. In contrast to Kv3.1, Kv3.3 produces potassium currents with variable inactivation rates dependent on the heterologous expression system in which the gene is expressed (Rudy, 1999). The I_{HT} current is, however, noninactivating, and its kinetics very closely match those of Kv3.1 (Brew and Forsythe, 1995; Wang et al., 1998). Nevertheless, the small amount of residual high-threshold TEA-sensitive current remaining in Kv3.1−/− mice may also represent Kv3.3 current or some other unidentified potassium channel.

We found that Kv3.1a and Kv3.1b, the two channel subunits that are generated by the Kv3.1 gene, produce indistinguishable basal currents and that both channel proteins are substrates for phosphorylation, but that the two isoforms are differentially modulated by protein kinase C. In particular, phosphorylation of the consensus protein kinase site at serine 503 of Kv3.1b produces a decrease in current for this isoform. This is consistent with previous observations that activators of protein kinase C produce a decrease in channel open probability in Kv3.1b-transfected cells (Kanemasa et al., 1995). Nevertheless, because activation of this enzyme produces little or no change in the voltage dependence or kinetic behavior of the macroscopic currents, we cannot eliminate the possibility that a proportion of channels becomes silent during phosphorylation, as would occur if phosphorylation at serine 503 allowed them to interact with an endogenous inhibitor.

In situ hybridization and RNase protection assays indicate that the regional expression of both Kv3.1 isoforms overlaps in all brain areas (Perney et al., 1992). The Kv3.1a transcript predominates early in development and can be detected as early as embryonic day 17. There is a pronounced increase in the level of the Kv3.1b transcript from postnatal day 8 to postnatal day 14, the major period of synaptogenesis, and Kv3.1b becomes the major isoform in the mature brain, although the Kv3.1a transcript also persist into adulthood (Perney et al., 1992; Liu and Kaczmarek, 1998). In the cerebellum, in which both splice variants are expressed, it has been shown that the levels of the two variants are regulated by distinct mechanisms during development (Weiser et al., 1995; Liu and Kaczmarek, 1998). It has been suggested that the C terminus of Kv3.1a, which diverges from Kv3.1b in the last 10 amino acids, plays a role in targeting heteromultimers of Kv3.1a and Kv3.1b to axons and terminals. Although we did not find evidence of heteromultimerization between Kv3.1a and Kv3.1b by coimmunoprecipitation from whole-brain homogenates, we cannot eliminate the possibility that Kv3.1b heteromultimerizes with Kv3.1a in certain neuronal populations (Rudy, 1999).

PKC-mediated phosphorylation of Kv3.1 improves timing at intermediate frequencies

A high level of basal phosphorylation of Kv3.1 has been demonstrated previously and can be attributed primarily to the actions of casein kinase 2 (Macica and Kaczmarek, 2001). Our present data suggest that the switch from to Kv3.1a to Kv3.1b during development permits the I_{HT} current of MNTB neurons to be modulated by protein kinase C, after synaptic transmission has been established. Activation of this enzyme influences the amplitude of the I_{HT} current with no apparent change in voltage dependence or kinetics. Genetic knock-out, pharmacological, and computer modeling studies all indicate that a decrease in I_{HT} current impairs the ability of the neurons to follow very-high-frequency stimulation. Nevertheless, a partial decrease in I_{HT} current significantly improves the fidelity of firing and the timing of action potentials at those intermediate frequencies at which stimulation produces bursts of two or more action potentials interrupted by failures. Under these conditions, there is a progressive build up of inhibitory potassium conductance (both I_{HT} and I_{LT}) during the burst, resulting in a progressive delay in the occurrence of action potentials. This delay can reach hundreds of microseconds, a condition that would preclude computation of small timing differences by the auditory brainstem circuits. A decrease in I_{HT} current decreases the inhibitory conductance, generating additional action potentials and restoring more uniform spike latencies. At high-stimulus frequencies at which single action potentials are separated by failures, however, a decrease in I_{HT} does not improve responses.

The biophysical characteristics of Kv3.1, particularly its activation only at positive potentials, make it particularly suitable for

modulation of fidelity of propagation through the MNTB. In addition to simulating the effects of small changes in Kv3.1 current, we modeled the actions of decreases in the low-threshold potassium current or of increases in sodium current. Although both of these manipulations can restore one-to-one firing at intermediate frequencies of stimulation, they render the cells more likely to fire spontaneous action potentials and to generate more than one action potential in response to depolarizing currents, changes that would degrade auditory information. Nevertheless, although we did not find any modulation of I_{LT} by PKC, it is probable that channels other than Kv3.1 are also subject to modulation in MNTB neurons.

Each individual auditory nerve fiber, neuron of the cochlear nucleus, or principal neuron of the MNTB can be assigned a characteristic frequency, which represents that frequency of sound for which the neuron has the lowest threshold. Neurons with different characteristic frequencies are organized tonotopically within their nuclei, reflecting their innervation by fibers originating in different regions of the cochlea. At higher sound intensities, however, MNTB neurons respond over a wider range of frequencies (Joris et al., 1994). Modulation of potassium conductances may provide one mechanism for adjusting the firing pattern of a neuron so that it can accurately follow a specific pattern of auditory stimulation. Although the pathways that lead to the regulation of protein kinase C in MNTB neurons remains to be defined, modulation of Kv3.1 by PKC may provide one mechanism for fine-tuning the frequency-dependent responses of MNTB neurons to auditory stimuli.

References

Banks MI, Smith PH (1992) Intracellular recordings from neurobiotin-labeled cells in brain slices of the rat medial nucleus of the trapezoid body. J Neurosci 12:2819–2837.

Borst JG, Helmchen F, Sakmann B (1995) Pre- and postsynaptic whole-cell recordings in medial nucleus of trapezoid body of the rat. J Physiol (Lond) 489:825–840.

Brew HM, Forsythe ID (1995) Two voltage-dependent K^+ conductances with complementary functions in postsynaptic integration at a central auditory synapse. J Neurosci 15:8011–8022.

Critz SD, Wible BA, Lopez HS, Brown AM (1993) Stable expression and regulation of a rat brain K channel. J Neurochem 60:1175–1178.

Grigg JJ, Brew HM, Tempel BL (2000) Differential expression of voltage-gated potassium channel genes in auditory nuclei of the mouse brainstem. Hear Res 140:77–90.

Guinan Jr JJ, Norris BE, Guinan SS (1972) Single auditory units in the superior olivary complex. II. Locations of unit categories and tonotopic organization. Int J Neurosci 4:147–166.

Ho CS, Grange RW, Joho RH (1997) Pleiotropic effects of a disrupted K^+ channel gene: reduced body weight, impaired motor skill and muscle contraction, but no seizures. Proc Natl Acad Sci USA 94:1533–1538.

Hori T, Takai Y, Takahashi T (1999) Presynaptic mechanism for phorbol ester-induced synaptic potentiation. J Neurosci 19:7262–7267.

Joris PX (1996) Envelope coding in the lateral superior olive. II. Characteristic delays and comparison with responses in the medial superior olive. J Neurophysiol 76:2137–2156.

Joris PX, Yin TC (1995) Envelope coding in the lateral superior olive. I. Sensitivity to interaural time differences. J Neurophysiol 73:1043–1062.

Joris PX, Yin TC (1998) Envelope coding in the lateral superior olive. III. Comparison with afferent pathways. J Neurophysiol 79:253–269.

Joris PX, Smith PH, Yin TC (1994) Enhancement of neural synchronization in the anteroventral cochlear nucleus. II. Responses in the tuning curve tail. J Neurophysiol 71(3):1037–1051.

Kanemasa T, Gan L, Perney TM, Wang LY, Kaczmarek LK (1995) Electrophysiological and pharmacological characterization of a mammalian Shaw channel expressed in NIH 3T3 fibroblasts. J Neurophysiol 74:207–217.

Li W, Kaczmarek LK, Perney TM (2001) Localization of two high threshold potassium channel subunits in rat central auditory system. J Comp Neurol 437:196–218.

Liu SJ, Kaczmarek LK (1998) The expression of two splice variants of the Kv3.1 potassium channel gene is regulated by different signaling pathways. J Neurosci 18:2881–2890.

Luneau CJ, Williams JB, Marshal J, Levitan ES, Oliva C, Smith JS, Antanavage J, Folander K, Stein RB, Swanson R, Kaczmarek L, Buhrow SA (1991) Alternative splicing contributes to K^+ channel diversity in the mammalian central nervous system. Pro Natl Acad Sci USA 88:3932–3936.

Macica CM, Kaczmarek LK (2001) Casein kinase 2 determines the voltage dependence of the Kv3.1 channel in auditory neurons and transfected cells. J Neurosci 21:1160–1168.

Morest DK (1968) The collateral system of the medial nucleus of the trapezoid body of the cat, its neuronal architecture and relation to the olivocochlear bundle. Brain Res 9:288–311.

Oertel D (1999) The role of timing in the brainstem auditory nuclei of mammals. Annu Rev Physiol 61:497–519.

Perney TM, Kaczmarek LK (1991) The molecular biology of K^+ channels. Curr Opin Cell Biol 3:663–670.

Perney TM, Kaczmarek LK (1997) Localization of a high threshold potassium channel in the rat cochlear nucleus. J Comp Neurol 386:178–202.

Perney TM, Marshall J, Martin KA, Hockfield S, Kaczmarek LK (1992) Expression of the mRNAs for the Kv3.1 potassium channel gene in the adult and developing brain. J Neurophysiol 68:756–766.

Pounce A, Vega-Saenz de Miera, Kentrol C, Moreno H, Thornbill B, Rudy B (1997) K^+ channel isoforms with divergent carboxy-terminal sequences carry distinct membrane targeting signals. J Membr Biol 159:149–159.

Rettig J, Wunder F, Stocker M, Lichtinghagen R, Mastiaux F, Beckh S, Kues W, Pedarzani P, Schroter KH, Ruppersberg JP, Veh R, Pongs O (1992) Characterization of a Shaw-related potassium channel family in rat brain. EMBO J 11:2473–2486.

Rhode WS, Smith PH (1986) Encoding timing and intensity in the ventral cochlear nucleus of the cat. J Neurophysiol 56:261–286.

Richardson FR, Kaczmarek LK (2000) Modification of delayed rectfier potassium currents by the Kv9.1 potassium channel subunit. Hear Res 147:21–30.

Rudy B (1999) Contributions of Kv3 channels to neuronal excitability. Ann NY Acad Sci 868:304–343.

Smith PH, Joris PX, Carney LH, Yin TC (1991) Projections of physiologically characterized globular bushy cell axons from the cochlear nucleus of the cat. J Comp Neurol 304:387–407.

Smith PH, Joris PX, Yin TC (1998) Anatomy and physiology of principal cells of the medial nucleus of the trapezoid body (MNTB) of the cat. J Neurophysiol 79:3127–3142.

Spirou GA, Brownell WE, Zidanic M (1990) Recordings from cat trapezoid body and HRP labeling of globular bushy cell axons. J Neurophysiol 63:1169–1190.

Taschenberger H, von Gersdorff H (2000) Fine-tuning an auditory synapse for speed and fidelity: developmental changes in presynaptic waveform, EPSC kinetics, and synaptic plasticity. J Neurosci 20:9162–9173.

Tollin DJ, Yin TC (2002) The coding of spatial location by single units in the lateral superior olive of the cat. II. The determinants of spatial receptive fields in azimuth. J Neurosci 22:1468–1479.

Trussell LO (1999) Synaptic mechanisms for coding timing in auditory neurons. Annu Rev Physiol 61:477–496.

Wang LY, Gan L, Forsythe ID, Kaczmarek LK (1998) Contribution of the Kv3.1 potassium channel to high-frequency firing in mouse auditory neurons. J Physiol (Lond) 509:183–194.

Weiser M, Bueno E, Sekirnjak C, Martone ME, Baker H, Hillman D, Chen S, Thornhill W, Ellisman M, Rudy B (1995) The potassium channel subunit Kv3.1b is localized to somatic and axonal membranes of specific populations of CNS neurons. J Neurosci 15:4298–4314.

Wu SH, Kelly JB (1993) Response of neurons in the lateral superior olive and medial nucleus of the trapezoid body to repetitive stimulation: intracellular and extracellular recordings from mouse brain slice. Hear Res 68:189–201.

Contributions of Kv3 Channels to Neuronal Excitability

BERNARDO RUDY,[a,b] ALAN CHOW,[a] DAVID LAU,[a] YIMY AMARILLO,[a] ANDER OZAITA,[a] MICHAEL SAGANICH,[a] HERMAN MORENO,[a] MARCELA S. NADAL,[a] RICARDO HERNANDEZ-PINEDA,[a,c] ARTURO HERNANDEZ-CRUZ,[c] ALEV ERISIR,[d] CHRISTOPHER LEONARD,[d] AND ELEAZAR VEGA-SAENZ DE MIERA[a]

[a]*Department of Physiology and Neuroscience, and Department of Biochemistry, New York University of Medicine, New York, New York 10016, USA*
[c]*Instituto de Fisiología Celular, Universidad Nacional Autónoma de México, México.*
[d]*Department of Physiology, New York Medical College, Valhalla, New York, USA*

ABSTRACT: Four mammalian Kv3 genes have been identified, each of which generates, by alternative splicing, multiple protein products differing in their C-terminal sequence. Products of the Kv3.1 and Kv3.2 genes express similar delayed-rectifier type currents in heterologous expression systems, while Kv3.3 and Kv3.4 proteins express A-type currents. All Kv3 currents activate relatively fast at voltages more positive than −10 mV, and deactivate very fast. The distribution of Kv3 mRNAs in the rodent CNS was studied by *in situ* hybridization, and the localization of Kv3.1 and Kv3.2 proteins has been studied by immunohistochemistry. Most Kv3.2 mRNAs (~90%) are present in thalamic-relay neurons throughout the dorsal thalamus. The protein is expressed mainly in the axons and terminals of these neurons. Kv3.2 channels are thought to be important for thalamocortical signal transmission. Kv3.1 and Kv3.2 proteins are coexpressed in some neuronal populations such as in fast-spiking interneurons of the cortex and hippocampus, and neurons in the globus pallidus. Coprecipitation studies suggest that in these cells the two types of protein form heteromeric channels. Kv3 proteins appear to mediate, in native neurons, similar currents to those seen in heterologous expression systems. The activation voltage and fast deactivation rates are believed to allow these channels to help repolarize action potentials fast without affecting the threshold for action potential generation. The fast deactivating current generates a quickly recovering afterhyperpolarization, thus maximizing the rate of recovery of Na^+ channel inactivation without contributing to an increase in the duration of the refractory period. These properties are believed to contribute to the ability of neurons to fire at high frequencies and to help regulate the fidelity of synaptic transmission. Experimental evidence has now become available showing that Kv3.1-Kv3.2 channels play critical roles in the generation of fast-spiking properties in cortical GABAergic interneurons.

The four known Kv3 genes were identified nearly a decade ago.[1–13] Injection of Kv3 cRNAs into *Xenopus* oocytes induced expression of voltage-gated K^+ channels that had unusual properties, which, as far as we could tell at the time, were unlike any voltage-dependent K^+ currents described in native neurons. In particular, the currents did not activate significantly until the membrane was depolarized to membrane potentials more positive than −10 mV. Yet Northern blot analysis showed that transcripts of at least three of the four genes were abundantly expressed in brain, some of them as abundantly as the most

[b]Address for correspondence: Department of Physiology and Neuroscience, New York University School of Medicine, 550 First Avenue, New York 10016. e-mail: Rudyb01@mcrcr6.med.nyu.edu

abundant K^+ channel transcripts known then.[14,15] We considered three main possibilities to explain the apparent lack of Kv3-like currents in native cells:

1. that native Kv3 channels have different properties from those seen in the oocyte due to posttranslational modifications or interactions of Kv3 subunits with auxiliary proteins;
2. that Kv3 proteins are targeted to neuronal compartments, such as axons and terminals, with restricted accessibility to electrophysiological methods; and
3. that native Kv3 currents have properties such as those in the oocyte but they had not been described in neurons due to the problems of separating components of the total K^+ current.

Moreover, we reasoned that native Kv3 currents may play very specific roles in neurons if their properties are similar to those in the oocyte.

We decided that in either case Kv3 proteins were a good point to start investigating the relationship between cloned channel components and native channels. We also found Kv3 proteins interesting to pursue because the evolution of Kv3 genes appeared to be different from the evolution of Kv genes of other subfamilies. Mammalian products of a given Kv subfamily are more similar to one of four Kv-like genes in *Drosophila* than to a mammalian product of a different subfamily, indicating that precursor genes to each subfamily existed prior to the divergence of chordates and arthropods. Kv3 proteins are more similar to the products of the *Drosophila* Shaw gene than to other *Drosophila* or mammalian Kv proteins.[15] However, the percentage of amino acid identity seen between mammalian Kv3 proteins and Shaw (49–56%) is significantly less than that seen between mammalian and fly homologues in the other Kv subfamilies (70–80%). Even perhaps more significant, while Kv3 proteins are more similar to Shaw in certain regions of the protein, they are more similar to members of other Kv subfamilies in the S4 domain and the sequences near this domain (see TABLE 6 in Ref. 15). Functionally, mammalian Kv3 channels differ considerably from Shaw channels, which lack the unique properties that distinguish Kv3 currents from other voltage-dependent currents (see sections on functional expression and neuronal roles, below). Gene conversion events, or other mechanisms have been suggested to explain the evolution of mammalian Kv3 genes.[15] Whatever the mechanism, mammalian-like Kv3 genes appear to be a recent evolutionary acquisition, specific to species in the evolutionary line leading to mammals, suggesting they might be used in neuronal properties that are specific to mammals and other vertebrates.

A several-year-long effort by our laboratory and others has shown that native Kv3 currents in neurons are similar to those in heterologous expression systems, and is beginning to provide evidence that they indeed play special roles in neuronal excitability.

A review on Kv3 genes was published in 1994.[15] This review discussed in detail several aspects of the work with these genes that will not be considered extensively in this article (such as the patterns of alternative splicing and genomic structure of Kv3 genes, the tissue expression and brain distribution of Kv3 mRNA transcripts, the properties of homomultimeric and heteromultimeric Kv3 channels in *Xenopus* oocytes, and the analysis of structural and functional domains of Kv3 proteins). Instead we will focus here on the work demonstrating that Kv3 channels in neurons have properties similar to those in heterologous expression systems and describe the studies that are particularly relevant to understanding their neuronal roles.

THE Kv3 K^+ CHANNEL GENE SUBFAMILY

The Kv3 or Shaw-related subfamily in mammals is similar to the other Kv subfamilies in that several genes have been formed by gene duplication throughout animal evolution. There are four Kv3 genes known both in rodents and humans,[9,15] and their chromosomal locations have been determined in mouse and human (see chapter by Coetzee et al. in this volume).[16] In the last few years Kv3 genes have been identified in other vertebrate species.[17,18]

All four Kv3 genes known in mammals generate multiple products by alternative splicing. The analysis of cDNAs predicts the existence of twelve different Kv3 proteins in mammals (FIG. 1). The alternatively spliced transcripts of each gene have identical nucleotide sequences from the assumed starting ATG up to a point of divergence near, but prior to, the in-frame stop codon, predicting protein products with different carboxyl ends. The point of divergence conforms to the consensus sequence for donor splice junctions. These sequence relationships suggest that the different transcripts arise by alternative splicing of a primary transcript rather than by transcription from separate but highly homologous genes. Other data supporting this conclusion have been discussed previously (see Ref. 15).

Two sites of alternative splicing have been observed. In some Kv3 genes (such as Kv3.1) the divergence follows the second protein-coding exon, which encodes the transmembrane portion of the protein. In Kv3.2, the point of divergence occurs at the end of the third protein-coding exon. In Kv3.3 and Kv3.4 alternative splicing at both sites has been observed. In all cases, the alternative splicing changes *only* the C-terminal portion of the protein; the point of divergence starts at least 50 residues after the last membrane-spanning domain. In some instances, the alternatively spliced C-termini are very short: 10 amino acids in Kv3.1a. The longest occurs in Kv3.3a, where it is over 200 residues (FIGS. 1 and 3). The variable C-termini do not affect the electrophysiological properties of the currents expressed by the products of a particular Kv3 gene. Possible roles of this alternative splicing are discussed later in this chapter. In addition to the alternative-splicing generating proteins with divergent C-termini, alternative splicing at the 5′ end, generating transcripts with different 5′ UTRs, but not affecting the sequence of the protein, has been observed in some Kv3 genes.[14,15,19] In some genes encoding inward rectifying K^+ channels, alternative splicing of the 5′ UTR results in the expression of transcripts having different tissue expression[20] (see also Coetzee *et al.*, in this volume). Perhaps the alternative splicing of the 5′ UTR of the Kv3.2 gene is associated with the differential developmental expression in the thalamus as compared to other brain areas (see below). The predicted amino acid sequences of the constant region (prior to the point of divergence of the alternative spliced isoforms) of the products of the four Kv3 genes is shown in FIGURE. 2, and the amino acid sequences of the alternatively spliced C-termini in FIGURE 3.

Kv3 CHANNELS IN MAMMALIAN HETEROLOGOUS-EXPRESSION SYSTEMS

The properties of Kv3 currents in *Xenopus* oocytes were previously reviewed.[15,21] Kv3 cDNAs have been transfected in several types of mammalian cells that have negligible intrinsic K^+ currents. Both stable and transient transfection methods have been used. Our laboratory has studied at least one alternatively spliced isoform of each of the four Kv3

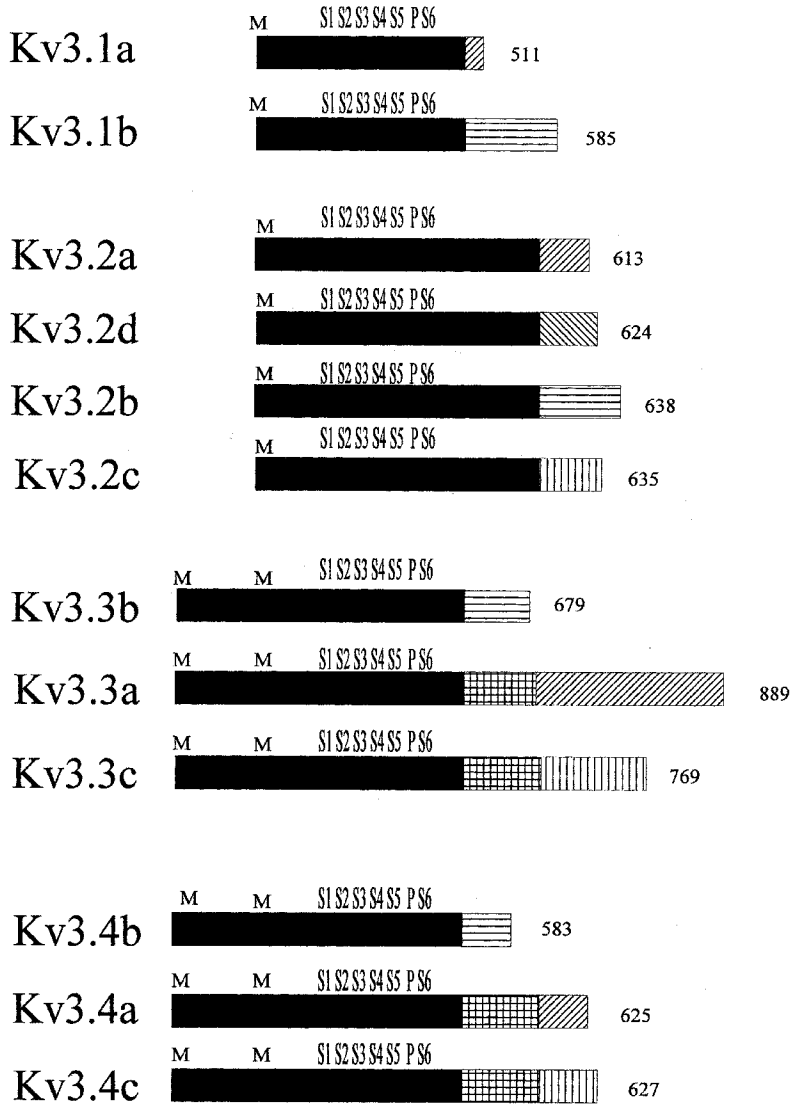

FIGURE 1. Mammalian Kv3 proteins. Four known Kv3 genes encode 12 proteins by alternative splicing. Kv3 isoforms from a given gene differ only in their C-terminal sequence. Proteins expressing inactivating channels (Kv3.3x and Kv3.4x) have an NH-terminal insert preceding the methionine (M) residue, which aligns with the starting methionine of Kv3.1 and Kv3.2 and is responsible for channel inactivation. S1–S6, trasmembrane domains; P, pore domain (also known as H5 domain).

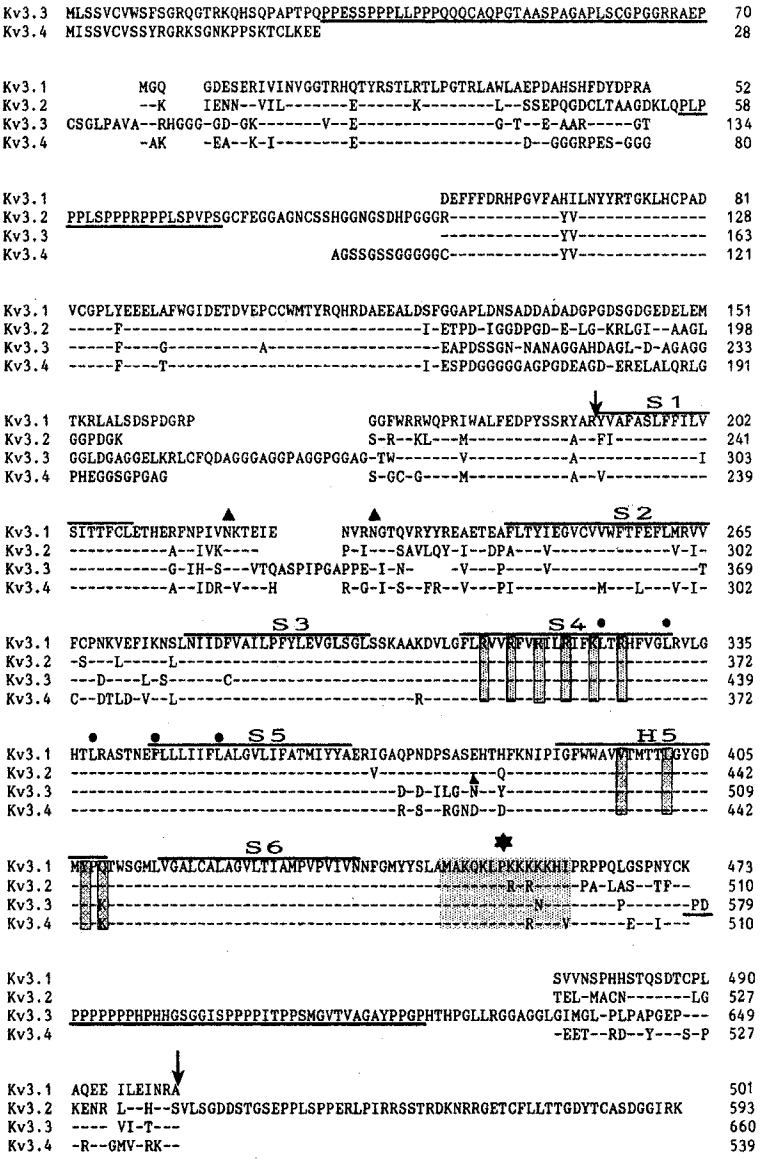
Kv3.3 MLSSVCVWSFSGRQGTRKQHSQPAPTPQPPESSPPPLLPPPQQQCAQPGTAASPAGAPLSCGPGGRRAEP 70
Kv3.4 MISSVCVSSYRGRKSGNKPPSKTCLKEE 28
Kv3.1 MGQ GDESERIVINVGGTRHQTYRSTLRTLPGTRLAWLAEPDAHSHFDYDPRA 52
Kv3.2 --K IENN--VIL-------E------K--------L--SSEPQGDCLTAAGDKLQPLP 58
Kv3.3 CSGLPAVA--RHGGG-GD-GK-------V--E---------G-T--E-AAR-----GT 134
Kv3.4 -AK -EA--K-I--------E----------D--GGGRPES-GGG 80
Kv3.1 DEFFFDRHPGVFAHILNYYRTGKLHCPAD 81
Kv3.2 PPLSPPPRPPPLSPVPSGCFEGGAGNCSSHGGNGSDHPGGGR----------YV---------- 128
Kv3.3 ----------YV---------- 163
Kv3.4 AGSSGSSGGGGGC----------YV---------- 121
Kv3.1 VCGPLYEEELAFWGIDETDVEPCCWMTYRQHRDAEEALDSFGGAPLDNSADDADADGPGDSGDGEDELEM 151
Kv3.2 -----F----------I-ETPD-IGGDPGD-E-LG-KRLGI--AAGL 198
Kv3.3 -----F----G----------A----------EAPDSSGN-NANAGGAHDAGL-D-AGAGG 233
Kv3.4 -----F----T----------I-ESPDGGGGGAGPGDEAGD-ERELALQRLG 191
S1
Kv3.1 TKRLALSDSPDGRP GGFWRRWQPRIWALFEDPYSSRYARYVAFASLFFILV 202
Kv3.2 GGPDGK S-R--KL---M----------A--FI---------- 241
Kv3.3 GGLDGAGGELKRLCFQDAGGGAGGPAGGPGGAG-TW-------V----------A----------I 303
Kv3.4 PHEGGSGPGAG S-GC-G----M----------A--V---------- 239
S2
Kv3.1 SITTFCLETHERFNPIVNKTEIE NVRNGTQVRYYREAETEAFLTYIEGVCVVWFTFEFLMRVV 265
Kv3.2 ----------A--IVK---- P-I---SAVLQY-I--DPA---V----------V-I- 302
Kv3.3 ----------G-IH-S---VTQASPIPGAPPE-I-N- -V---P----V----------T 369
Kv3.4 ----------A--IDR-V---H R-G-I-S--FR--V---PI---------M---L---V-I- 302
S3 S4
Kv3.1 FCPNKVEFIKNSLNIIDFVAILPFYLEVGLSGLSSKAAKDVLGFLRVVRFVRILRIFKLTRHFVGLRVLG 335
Kv3.2 -S---L-----L---------- 372
Kv3.3 ---D----L-S------C---------- 439
Kv3.4 C--DTLD-V--L----------R---------- 372
S5 H5
Kv3.1 HTLRASTNEFLLLIIFLALGVLIFATMIYYAERIGAQPNDPSASEHTHFKNIPIGFWWAVVTMTTVGYGD 405
Kv3.2 ----------V----------Q---------- 442
Kv3.3 ----------D-D-ILG-N--Y---------- 509
Kv3.4 ----------R-S--RGND--D---------- 442
S6
Kv3.1 MEYGTWSGMLVGALCALAGVLTIAMPVPVIVNNFGMYYSLAMAKQKLPKKKKKHIPRPPQLGSPNYCK 473
Kv3.2 ----------R-R----PA-LAS--TF-- 510
Kv3.3 ----------N----------P-------PD 579
Kv3.4 ----------R---V------E--I--- 510
Kv3.1 SVVNSPHHSTQSDTCPL 490
Kv3.2 TEL-MACN-------LG 527
Kv3.3 PPPPPPPPHPHHGSGGISPPPPITPPSMGVTVAGAYPPGPHTHPGLLRGGAGGLGIMGL-PLPAPGEP--- 649
Kv3.4 -EET--RD--Y---S-P 527
Kv3.1 AQEE ILEINRA 501
Kv3.2 KENR L--H--SVLSGDDSTGSEPPLSPPERLPIRRSSTRDKNRRGETCFLLTTGDYTCASDGGIRK 593
Kv3.3 ---- VI-T--- 660
Kv3.4 -R--GMV-RK-- 539

FIGURE 2. Amino acid sequence of the constant region of Kv3 proteins. Amino acids identical to those in Kv3.1 are shown with a *dash*. Gaps required to optimize the alignment are shown as *blanks*. Note that the second methionine of Kv3.3 and Kv3.4 aligns with the starting methionine of Kv3.1 and Kv3.2. The sequences between the first and the second methionine of Kv3.3 and Kv3.4 are required for channel inactivation. Exon boundaries are shown with arrows. The S1–S6 and H5 (or P) domains are *overlined*. Proline-rich sequences in Kv3.2 and Kv3 are *underlined*. Triangles indicate putative N-glycosylation sites. The positively charged residues in S4 have been *boxed*. The leucines in the Shaker leucine heptad repeat adjacent to the S4 domain are indicated with a *solid circle*. In Kv3 proteins the fourth position in the repeat is phenylalanine, but is a leucine in other Kv proteins. Residues in the P domain found by mutagenesis in Kv3.1 to be important in determining pore properties are *boxed*. A cluster of positive charges after the S6 domain is indicated with a *star*. (Modified from Vega-Saenz de Miera *et al.*[15])

genes in Chinese Hamster Ovary (CHO) or HEK293T cells. Studies with mammalian cells have several advantages over the *Xenopus* oocyte expression system. The most important for the purpose of comparison with native neuronal channels is that currents can be recorded with the same methods (patch clamp in the whole cell and various patch configurations) and identical solutions that are used to record the currents in the native cells. Moreover, whole cell clamp of small mammalian cells (as compared to nearly 1-mm-in-diameter frog eggs) allows for better space clamp control and increased resolution. Furthermore, since we are studying mammalian proteins, it is more likely that the protein will be processed correctly in the mammalian cell than in the frog oocyte.

Untransfected CHO and HEK293T cells have negligible outward currents under the pulse protocols used to characterize Kv3 currents (<100 pA for the largest depolarizations). On the other hand, CHO cells transfected with each of the four Kv3 cDNAs (Kv3.1b, Kv3.2a, Kv3.3a, and Kv3.4a) have large voltage-dependent K^+ currents with a similar voltage-dependence, as observed in *Xenopus* oocytes (FIG. 4). The currents become apparent when the membrane is depolarized to potentials more positive than −10 mV. As in oocytes, Kv3.1 and Kv3.2 currents are of the delayed-rectifier type. Upon depolarization, they rise relatively fast, with a similar time course, to a maximum level that is maintained for the duration of pulses lasting a few hundred milliseconds. A slow inactivation becomes evident with pulses of longer duration, which is faster for Kv3.1 than for Kv3.2 channels (data not shown). Kv3.4 currents are of the A-type. They activate and inactivate very fast, as in oocytes. However, Kv3.3 currents, which are also transient when expressed in oocytes, resembled Kv3.1 and Kv3.2 currents when expressed in CHO or HEK-293T cells.

We do not yet understand why Kv3.3 currents are transient in oocytes but sustained in mammalian cells. The differences are not the result of the different methods of expressing the protein in the two expression systems, since CHO cells microinjected with the same Kv3.3a cRNA used in oocytes express identical currents to those seen in Kv3.3a-transfected cells. Inactivation of Kv3.3 and Kv3.4 channels is of the N-type[22] and can be removed by deleting NH-terminal inserts present in Kv3.3 and Kv3.4 proteins, but not in Kv3.1 and Kv3.2 proteins (FIGS. 1 and 2; see also Ref. 15). It is possible that the differences are the result of the different methods used to record whole cell currents in the two preparations: two-microelectrode voltage-clamp of *intact* cells in the case of oocytes and whole cell patch-clamp in the case of mammalian cells. Inactivation may be lost in the mammalian cells because of dialysis into the patch pipette of a cytoplasmic component

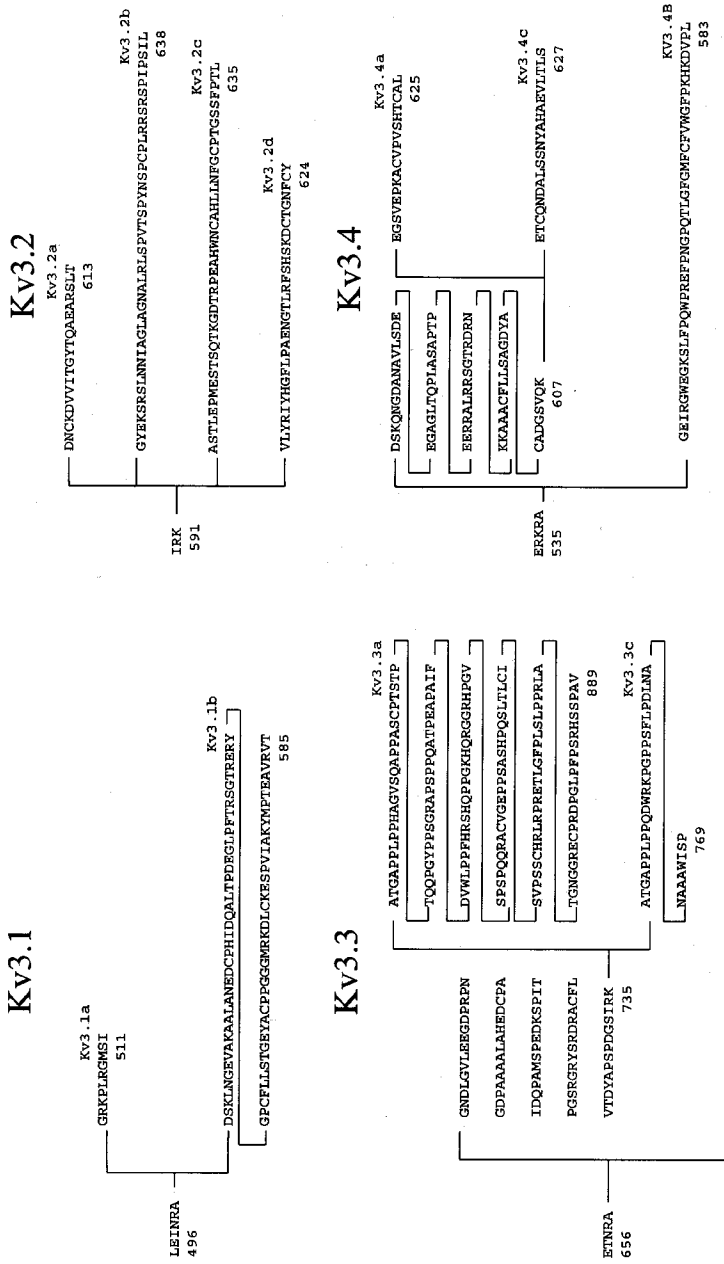

FIGURE 3. Amino acid sequences of the alternatively-spliced C-terminal region of 12 Kv3 proteins.

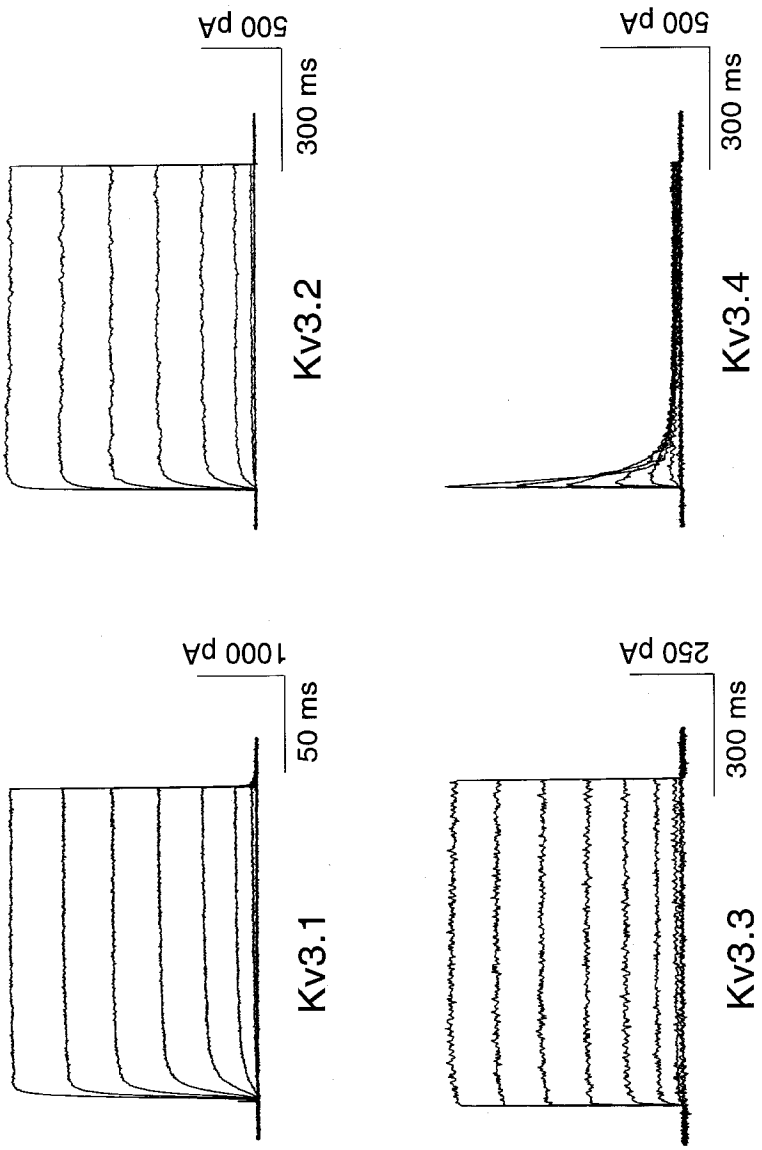

FIGURE 4. Kv3 currents in transfected HEK293 cells. Families of K^+ currents recorded from a holding potential of −80 mV in a Kv3.1, Kv3.2, Kv3.3, or Kv3.4 transfected cell during depolarizing pulses from −40 mV to +40 mV in 10-mV increments.

important for the inactivation process. Inactivation could also be distinct due to differences in the posttranslational processing of the protein in the two expression systems. However, the differences may not be as interesting as these possibilities would suggest. Kv3.3 proteins have a methionine in frame with the predicted starting methionine at the end of the NH2-terminal insert encoding the N-inactivation gate (FIGS. 1 and 2). It is possible that in the mammalian cell, translation of the protein starts at this second methionine. We should point out that if this turns out to be the explanation for the differences of Kv3.3 currents in oocytes and mammalian expression systems, this does not tell us how the protein will be translated in native neurons. The cDNAs that are available lack elements in their 5′ UTR that might be required for the proper selection of translation start site in mammalian cells.

Kv3 currents have several unusual properties that distinguish them from those of other delayed rectifier K^+ channels known (TABLE 1). These include their activation voltage range that is more positive than that of other voltage-gated K^+ channels. The channels with the nearest activation voltage (Kv2.1 and Kv2.2) show significant activation at 10–20 mV more negative potentials. Although Kv3 channel opening becomes significant at high potentials (more positive than −10 mV), the probability of channel opening increases steeply with voltage and >80% of the channels are opened between +30 and +40 mV. As a result of the steep voltage-dependence, the midpoints of the conductance-voltage relationships of Kv3 channels are not that different from those of other voltage-dependent K^+ currents (see Coetzee *et al.* in this volume). This distinguishes mammalian Kv3 currents from the currents expressed by the *Drosophila* Shaw protein, which also start activating at high voltages but have a very weak voltage-dependence, producing a midpoint of activation above +70 mV.[23,24]

The rate of rise of Kv3.1–Kv3.3 currents is relatively fast; faster than many other voltage-gated K^+ channels (e.g., Kv2.x; Kv1.2) but slower than that of other voltage-gated K^+ channels such as several Kv1 channels like Kv1.1, Kv1.4 and Kv1.5 (see Coetzee *et al.* in this volume). Kv3.4 currents rise faster than Kv3.1–Kv3.3 currents. In contrast to other delayed rectifiers, Kv3.1 and Kv3.2 currents are not significantly inactivated by depolarizing prepulses[25] and do not show cumulative inactivation (Ref. 26 and unpublished observations). Records of Kv3.1 and Kv3.2 currents in mammalian cells (but not in oocytes) often show an initial fast transient component. This is usually very small (<5% of the current) and is seen mainly in response to large depolarizing pulses (to >+30 mV). The origin of this component is not clear yet. In our experience its presence and magnitude are very variable; it is more readily seen in HEK293T than in CHO cells; and it is bigger in cells expressing large currents. Critz *et al.*[27] have suggested that it might be associated with K^+ accumulation in the extracellular space. This would be consistent with the variability we have observed. Moreover, other *fast-activating* K^+ channels, lacking a transient component in oocytes, also have a small transient component when expressed in some mammalian cells (see Ref. 26).

Another unusual feature of Kv3 currents is their fast rate of deactivation upon repolarization, first described for Kv3.1 currents expressed in NIH-3T3 and L929 cells by Grissmer *et al.*[26] These authors found that Kv3.1 currents deactivated about 10 times faster than other cloned voltage-gated K^+ channels known at the time. This feature is shared by non-inactivating Kv3.1–Kv3.3 currents (FIG. 5). Kv3.4 channels deactivate slowly because they can not close until inactivation is removed (see below). Inactivating Kv3.3 currents may behave in the same fashion. Since then, many new voltage-gated channels have been identified; however only one of them, Kv1.7, a non-neuronal member of the Kv1 family

TABLE 1. Properties of Kv3 Currents *in Vitro* and *in Vivo* (*abbreviations and notes overleaf*)

A. Electrophysiological Properties

	Activation					Inactivation			
	V_{on} (mV)	$V_{1/2}$ (mV)	k (mV)	t_{on} (mV)	τ_{off} (ms)	$V_{1/2}$ (mV)	k (mV)	τ (ms)	γ (pS)[a]
Kv3.1	−10	14	11	3.4	1.4	—	—	Slow	16 to 27
Kv3.2	−10	12.1	8.4	4	2.9	—	—	Very slow	16 to 20
Kv3.3	−10	12	10 to 14	4.4	1.9[b]	—	—	[c]	14
Kv3.4	−10	14	8.5	4	[d]	−20 to −32	4.8 to 8.3	10–20	12 to 14
$I_{GP\text{-}TEA}$ ("A")	−10	16.9	10.6	5	3.6	—	—	NA	NA
$I_{GP\text{-}TEA}$ ("B")	−10	15.5	14.3	3.42	1.4	—	—	14	NA

B. Pharmacological Properties and Modulation

	Pharmacological Properties (IC_{50})				Protein Kinase Modulation			
	TEA_0 (mM)	4-AP[e] (mM)	DTX (nM)	CTX (nM)	PKA	PKC	PKG	Other Properties
Kv3.1	0.15 to 0.2	0.02 to 0.6	NB	NB	No effect	Inhibits	Inhibits	Blocked by Chromakalin K_D 0.237 mM
Kv3.2	0.15	0.6 to 0.9	NB	NB	Inhibits	Inhibits Kv3.2b but not Kv3.2a	Inhibits	
Kv3.3	0.14	1.2			NA	Stimulates currents and suppresses inactivation	Inhibits	
Kv3.4	0.09 to 0.3	0.5 to 0.6	NB	NB	NA	Suppresses inactivation	Inhibits	Blocked by BDS-I IC_{50} 47nM & BDS-II IC_{50} 56nM

TABLE 1. Properties of Kv3 Currents *in Vitro* and *in Vivo* (*continued*)

ABBREVIATIONS: V_{on}: minimum voltage at which there is significant activation of the current; $V_{1/2;}$ membrane potential at which the conductance is half maximal; k: slope of normalized g–V curve; $t_{on;}$ time for the current to rise from 10 to 90% of its final value for non-inactivating currents and time to peak for inactivating currents, both at +40 mv; τ_{off}: time constant of deactivation at −60 mV; Inactivation τ: time constant of inactivation at +40 mV; NB: not blocked; NA: not available.

[a]Single-channel conductance from *Xenopus* oocytes in physiological potassium concentrations.

[b]Deactivation of the noninactivating Kv3.3 currents obtained in HEK 293 cells.

[c]Currents are noninactivating in CHO and HEK 293 cells, but inactivating in *Xenopus* oocytes; see text.

[d]See discussion on deactivation of Kv3.4 currents and Ruppersberg *et al.*[33]

[e]Block depends on pattern of stimulation.

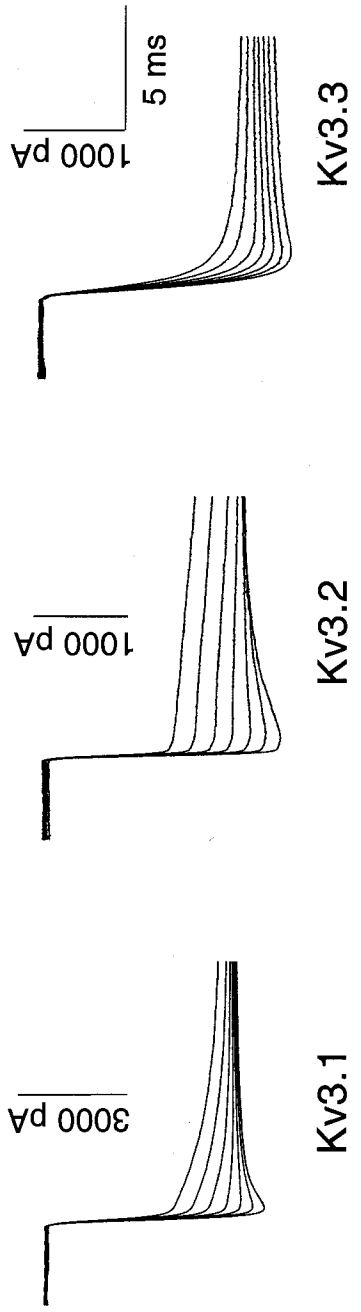

FIGURE 5. Deactivation kinetics of Kv3.1, Kv3.2, and Kv3.3 currents in HEK293 cells. Records of tail currents obtained by repolarizing cells expressing Kv3.1, Kv3.2, or Kv3.3 channels to a series of membrane potentials from −100 mV to −40 mV in 10 mV increments following a 20-ms depolarization to +20 mV.

deactivates fast (closing rates are about 2–3 times the deactivation rates of Kv3 channels.[28] The distinctive properties of Kv3 channels are likely to endow neurons with special electrophysiological properties (see below).

Kv3.1 and Kv3.2 channels (and perhaps also Kv3.3–Kv3.4) are blocked by intracellular Mg^{2+} in a voltage-dependent manner, producing a negative slope conductance in the conductance-voltage curve.[15] Variations in the conductance-voltage relationship between different studies on mammalian cells might be associated with differences in intracellular Mg^{2+} concentrations. Lower Mg^{2+} concentrations will tend to produce apparent shifts in voltage-dependence to the right. It was recently shown that the special sensitivity of Kv3.1 channels (as compared to other Kv channels) to intracellular Mg^{2+} could be transferred to a Shaker channel by transplanting the Kv3.1 P domain.[29]

TABLE 1 also includes the values of the single channel conductance of Kv3 channels, most of which have been derived from measurements in *Xenopus* oocytes. In general, Kv3 channels, particularly Kv3.1 and Kv3.2 have single channel conductances that are larger than most other voltage-gated K^+ channels (see TABLE 4 in Coetzee *et al.* in this volume).

While so far Kv3.3 and Kv3.4 channels have been given less attention than Kv3.1 and Kv3.2 channels, they show very interesting features. The NH-terminal inserts of both Kv3.3 and Kv3.4 responsible for the inactivation of these channels contain a cysteine residue surrounded by a very conserved sequence. A similar sequence is found in Kv1.4, a fast inactivating Shaker-related mammalian channel. The conservation of this sequence is even more notable given that there is otherwise very little amino acid sequence conservation in the amino ends of these proteins.[15] Ruppersberg *et al.*[30] showed that exposure of the cytoplasmic surface of Kv1.4 or Kv3.4 channels to air, presumably to oxygen (in inside-out excised membrane patches), resulted in removal of the inactivation process. In contrast to the effects of amino end deletions and other treatments, this inactivation removal was reversible. Inactivation was restored if the patch was reinserted into the cell or by exposure to reduced glutathione or DTT.[30] The effects of oxidation were not seen in channels expressed from a Kv1.4 protein where the cysteine was replaced with serine.[30] A model by which the redox state of this cysteine may modulate channel inactivation was proposed by these investigators. Similarly, exposure of oocytes expressing Kv1.4, Kv3.3, or Kv3.4 channels to high micromolar concentrations of external H_2O_2 resulted in a reversible removal of inactivation.[31] Concomitant with inactivation removal there was a significant increase in current magnitude, particularly large for Kv3.4 channels. The effects of H_2O_2 were specific to these three channels, and was not observed on channels expressed from a Kv3.3 cDNA in which the cysteine residue was mutated (Vega-Saenz de Miera and Rudy, unpublished observations). Moreover, there was no effect in channels which lack the conserved cysteine-containing sequence, including noninactivating Kv3.2 channels, inactivating *Drosophila* Shaker channels,[31] or inactivating Kv4.1 and Kv4.2 channels.[32] Effects similar to those of H_2O_2 were seen upon exposure to *N*-ethyl maleimide, a reagent which alkylates free sulfhydryls, but in this case the effects were, as expected, irreversible.

Another interesting feature of Kv3.4 channels expressed in heterologous expression systems was described by Ruppersberg *et al.*,[32] who found that inactivated Kv3.4a channels are able to pass current during repolarization. Apparently, these channels are unable to enter the resting closed state, when the membrane is hyperpolarized, until their inactivation is first removed, resulting in a long-lasting current (at voltages much more negative than those required for activation) while they are recovering from inactivation. It remains to be seen whether Kv3.3 channels, which inactivate more slowly, behave in a similar fashion. There is

also no evidence that this behavior is seen in native channels containing Kv3.4 proteins. Such behavior could drastically affect the role played by these channels. If inactivated Kv3.4 channels are indeed able to pass current at negative potentials while they recover from inactivation, they could have subthreshold effects on cell excitability, unlike Kv3 channels lacking this property. Specifically, the first spike in a train could open and then quickly inactivate these channels. Upon repolarization of the membrane, the current through Kv3.4 channels recovering from inactivation could prevent the next spike or delay its onset.

Regulation of Kv3 Currents by Phosphorylation and Dephosphorylation

Several sites that fit the consensus sequence for protein-kinase phosphorylation are found in regions of Kv3 proteins that are thought to be intracellular. Some of these sites are found in products of all of the genes, some are found only in proteins encoded by a single gene, and some are specific to alternatively-spliced isoforms.[15] Three kinase systems, cAMP-dependent protein kinase (PKA), protein kinase C (PKC), and cGMP-dependent protein kinase (PKG) have now been shown to modulate Kv3 channel function in heterologous expression systems (TABLE 1).

PKA

This kinase inhibits Kv3.2a and Kv3.2b channels by phosphorylating the unique PKA-consensus site present in the C-terminal area of the protein, before the point of divergence of the alternatively spliced isoforms. Kv3.1b channels, which lack a consensus site for PKA phosphorylation, are not affected by PKA. Other Kv3 proteins, all of which also lack consensus PKA sites, have not been tested.[34,35]

PKC

This kinase modulates products of several Kv3 genes, but the functional effects vary depending on the subunit. PKC inhibits channels containing some alternatively spliced Kv3.2 isoforms, but not others (see the section entitled Functional Roles of Alternative Splicing below). PKC also inhibits Kv3.1 channels.[27,34,36] It has not yet been demonstrated that these modulations are the result of channel protein phosphorylation. On Kv3.4 channels, PKC slows down N-inactivation by phosphorylating several PKC sites present in the NH-terminal sequence forming the structure responsible for inactivation.[37,38] A similar effect of PKC activation is seen on Kv3.3a and Kv3.3b channels, presumably also due to phosphorylation of the inactivating NH-terminal sequence. However, in addition, PKC produces large (200–400%) increases in Kv3.3 current levels which are independent of the effects on inactivation, and can be induced with lower doses of phorbol esters than those required to slow down inactivation, and are also blocked by PKC inhibitors.[39,40]

PKG

Intracellular increases in cGMP concentrations, produced by the addition of permeable cGMP analogues or by stimulation of guanylyl cyclase with nitric oxide (NO) inhibit

Kv3.1b and Kv3.2a channels in a voltage-dependent manner. These effects are blocked by PKG inhibitors, but appear not to be the result of channel phosphorylation.[41,42] The data suggest that the channel inhibition produced by the activation of PKG is mediated by a specific phosphatase(s). We suggest that these enzymes dephosphorylate the channel proteins at sites that need to be phosphorylated for voltage-dependent activation to proceed normally. This hypothesis is consistent with the observation that exposure of the intracellular side of the membrane to alkaline phosphatase inhibits these channels as well as Kv3.3 and Kv3.4 channels.[40] The effects of PKG activation on Kv3.3 and Kv3.4 currents have not been tested.

Pharmacological Properties

At present there are no specific blockers for Kv3.1–Kv3.3 channels. However, in both *Xenopus* oocytes and in transfected mammalian cells, all Kv3 currents (including Kv3.4) are very sensitive to external tetraethylammonium (TEA) or 4-aminopyridine (4-AP) (TABLE 1). The sensitivity to TEA is particularly important and can be exploited to discriminate between known K^+ channels. Kv3 currents are > 80% blocked by 1 mM TEA. This concentration of TEA produces significant inhibition of only a few other known K^+ channels (see TABLE 4 in Coetzee *et al.* in this volume). These include the large-conductance Ca^{2+} activated K^+ channels containing proteins of the slo family (K_d 80–330 μM), Kv1.1 channels (K_d ~ 0.3 mM), and KCNQ2 (90% blocked by 1 mM). These channel types can be distinguished from Kv3 by other properties (see TABLE 4 in Coetzee *et al.* in this volume). Ca^{2+}-activated K^+ channels can be suppressed by using Ca^{2+} channel blockers in the extracellular solution, and by using BAPTA in the intracellular solution to chelate intracellular Ca^{2+}. There are also many peptide toxins that block these channels (e.g., iberotoxin, IbTx; charybdotoxin, CTX; see Coetzee *et al.* in this volume). Kv1.1 channels are blocked by dendrotoxin (DTX) (K_d ~ 10–20 nM). Kv3 currents are not affected by these or any of the other scorpion- or snake-venom-derived toxins that block other voltage-sensitive channels (TABLE 1). KCNQX are very slowly activating and deactivating K^+ channels (time constants of the order of hundred of ms to sec). In contrast to their high sensitivity to extracellular TEA, Kv3 channels are less sensitive to intracellular TEA than are many other K^+ channels.[43]

Kv3 channels are also very sensitive to 4-AP (TABLE 1). However, the values reported for the IC_{50} for this channel blocker in different studies vary widely (e.g., IC_{50}s ranging from 20 to 600 μM have been reported for Kv3.1). These variations probably reflect, at least in part, the complex kinetics of binding and unbinding of this drug to different states of the channel.[43,44] The degree of channel block by 4-AP depends both on time and on the immediate history of opening and closing of the channel, and therefore on the pattern of stimulation of the cell during the measurements. We therefore believe that TEA is a better blocker than 4-AP to discriminate between Kv3 channels and other K^+ channels. Moreover, many other K^+ channels are as sensitive or more sensitive than Kv3 channels to this drug[45] see also Coetzee *et al.* in this volume), including the ubiquitous "D" current.[46,47]

A new set of peptides obtained from the venom of the sea anemone *Anemonia sulcata,* known as blood-depressing substance I and II (BDS-I and BDS-II) were recently shown to block specifically, reversibly, and at low concentrations (IC_{50} values in the low nanomolar range) Kv3.4 channels in transfected COS cells. The toxins share no sequence similarity

with other K^+ channel toxins derived from sea anemone and did not block other Kv or inward rectifying channels.[48] These toxins are likely to become important tools to investigate the roles of Kv3.4 channels in native tissue.

Properties of Kv3 Heteromeric Channels

Like other members of the Kv family, Kv3 proteins can form heteromultimeric channels with novel properties with other subunits of the same subfamily but not with proteins of other Kv subfamilies.[15,21,49] Heteromultimeric Kv channels have properties that are intermediary between those of the corresponding homomultimers, although some properties might be closer to those of one or the other homomultimer.[15,21,49–53] Since all Kv3 channels have similar voltage dependencies, one would expect that this parameter would not change in heteromultimers and this expectation has been confirmed experimentally. When two different Kv3 cRNAs are injected into *Xenopus* oocytes, the total current has a voltage-dependence similar to that of Kv3 homomultimers. Moreover, and perhaps not surprisingly, the currents recorded in cells co-expressing Kv3.1 and Kv3.2, which produce similar currents in a homomultimeric channel, are similar to Kv3.1 or Kv3.2 currents alone. The most interesting combinations are those of inactivating Kv3.3 or Kv3.4 proteins with those that produce sustained currents (Kv3.1 and Kv3.2). Oocytes injected with such combinations had fast inactivating currents that were several-fold larger than those seen in oocytes injected with the same amount of Kv3.4 or Kv3.3 cRNA alone. This is contrary to what might be expected from the algebraic sum of two independent currents and is consistent with the formation of heteromultimeric channels containing one or more Kv3.3 or Kv3.4 subunits plus several Kv3.1 or Kv3.2 subunits. The rate of inactivation increases with the number of inactivating subunits.[21] There is amplification of the transient current because a single inactivating subunit is sufficient to impart fast inactivating properties to the channel complex.[52]

TISSUE-SPECIFIC EXPRESSION OF Kv3 GENES

It is crucial to know where Kv3 proteins are found in order to identify cells where the properties of native Kv3 channels could be investigated and to be able to generate hypotheses about their physiological roles. We, in our laboratory, and others have therefore dedicated a large effort to determining the distribution of Kv3 products. In rodents, three of the four known Kv3 genes (Kv3.1–Kv3.3) are expressed mainly in brain. Kv3.4 is weakly expressed in brain, but strongly in skeletal muscle. Low levels of Kv3.1 are also seen in skeletal muscle, while low levels of Kv3.3 mRNAs are found in kidney and lung. Kv3.1, Kv3.3, and Kv3.4 products have also been identified in PC12 pheochromocytoma cells.[8,15,21] Kv3 genes are weakly expressed, if at all, in the heart. We and others did not detect any Kv3 transcripts in rat heart by Northern blot analysis.[5,14,15,21] Using the highly sensitive RNAse-protection method, Dixon and McKinnon[54] found extremely low levels for all four Kv3 genes in rat heart (faint signals were observed after very long [7–10-day] exposure as compared to robust signals produced by Kv3 probes in brain or by probes for other Kv subfamily mRNAs in heart after overnight exposure).

The presence of these weak signals might be of functional interest if they are derived from a small subpopulation of cells expressing significant levels of Kv3 transcripts. However, if such a subpopulation of cells exists, it remains to be identified. Kv3 transcripts might be more abundant in cardiac tissue in other species. In a study in enzymatically isolated ferret cardiac myocytes, Brahmajothi *et al.*[55] reported the presence of Kv3 transcripts in several myocytes and Kv3.3 transcripts have been amplified by PCR from mouse heart RNA.

By means of RNAse-protection, Kv3.4 transcripts were found to be abundantly expressed in sympathetic ganglia, at levels 273% higher than in brain. Kv3.3 and Kv3.1 produced very weak signals that could only be detected after 1 week's exposure of the autoradiograms (as compared to robust signals seen after overnight exposure for many other Kv transcripts). Kv3.2 transcripts were not detected.[56] Kv3.1 transcripts are also found in T lymphocytes, where they are thought to encode the principal subunits of the *l*-type K^+ channel[57] (see below). According to one report, Kv3.2 transcripts could be amplified by RT-PCR from transgenically derived betaTC3-neo insulinoma cells, but not from purified pancreatic β cells.[58] Except for this report, and the minimal expression in heart, Kv3.2 transcripts have not been detected outside the CNS. The tissue distribution of Kv3 mRNAs is summarized in TABLE 2.

Quantitative analysis[21] demonstrated that in the adult rat brain, Kv3.1 (Kv3.1b) and Kv3.3 transcripts were the most abundant Kv3 mRNAs. They appeared to be present in amounts similar to Kv1.2 mRNAs, an abundant Shaker-related transcript. Kv3.1 (Kv3.1b) and Kv3.3 mRNAs were ~3 times more abundant than Kv3.2 mRNAs, ~6–8 times more abundant than Kv3.4 transcripts, and about 1/5 as abundant as Na^+ channels α subunit mRNAs.

mRNA Distribution in Brain

In situ hybridization histochemistry has been used to study the distribution of Kv3 mRNAs in the central nervous system (CNS) of adult rats.[14,21,59,60] The work by Perney *et*

TABLE 2. Tissue Expression of Kv3 Transcripts in Rodents

	Kv3.1	Kv3.2	Kv3.3	Kv3.4
Brain	+++	+++	+++	+
Spinal cord	+++	-	+++	+
Sympathetic ganglia	±	-	±	+++
Skeletal muscle	+	-	-	+++
Kidney	-	-	+	-
Lung	-	-	+	-
Heart	±	±	±	±
Lymphocytes	++	NA	NA	NA

SYMBOLS: +++, abundant; ++, moderate; +, low levels; ± barely detectable levels; –, nondetectable; NA, data not available.

al.[59] on Kv3.1 and the work by Weiser *et al.*[21] on Kv3.1–Kv3.4 include, in addition to low-resolution X-ray autoradiography (which provides regional localization), a higher, cellular-resolution microscopic analysis of emulsion-dipped sections. These data have also been extensively reviewed[15] and are summarized in FIGURE 6. More recent studies in mice have largely confirmed the observations in rat. Kv3 genes appear to be expressed in neurons and not in glia.[21,59,61]

In the CNS each Kv3 gene shows a unique pattern of expression; however, transcripts of two or more Kv3 genes overlap in many neuronal populations. Kv3 genes are expressed in many, but not all, and not exclusively, GABAergic and glycinergic neurons in the CNS (FIG. 6). Kv3.1 and Kv3.3 transcripts overlap in many areas, particularly in the posterior part of the brain and in the spinal cord. Kv3.1 and Kv3.2 overlap in some neuronal populations, particularly in the anterior part of the brain, including the cortex, hippocampus, globus pallidus, deep cerebellar nuclei, and certain thalamic nuclei. However, in other areas, Kv3.1 and Kv3.2 transcripts actually show a reciprocal expression pattern. For example, Kv3.2 is strongly expressed in dorsal thalamic nuclei, but extremely weakly in the ventral thalamus (including the reticular thalamic nucleus and the ventral lateral geniculate), while Kv3.1 has the opposite pattern. Similarly, Kv3.2 is strongly expressed in the dorsal cochlear nucleus and the ventral lateral lemniscus nucleus, while Kv3.1 transcripts predominate in the ventral cochlear and dorsal lateral lemniscus nuclei.[21] Kv3.4 transcripts are weakly expressed in brain and only in a few neuronal types, usually in neurons also expressing other Kv3 genes. Kv3.1 and Kv3.3 are coexpressed in many neuronal populations, including most auditory central processing neurons, while Kv3.2 transcripts show the most restricted pattern of expression, with ~90% of Kv3.2 mRNAs being present in thalamic relay neurons *throughout* the dorsal thalamus. In fact, Kv3.2 gene expression is among the most specific of all known K^+ channels.

Protein Localization

Since we last reviewed the patterns of expression of Kv3 mRNAs,[15] specific antibodies against the protein products of two genes (Kv3.1 and Kv3.2) have been raised in our laboratory, allowing localization of the protein product. The antibodies against Kv3.2 are directed to the amino terminal area of the protein and recognize all alternatively spliced isoforms.[34,62,63] In the case of Kv3.1, antibodies have been raised to the C-termini of both the Kv3.1a[64,65] and Kv3.1b[66–68] (see also Refs. 69 and 70) proteins which are specific to each isoform.

Both Kv3.1 and Kv3.2 proteins are present in somas, axons, and terminals. The protein is concentrated in somatic, axonal, and presynaptic-terminal membranes and their underlying cytoplasm. The protein is not detected in dendrites, except in portions of primary dendrites close to the cell body. While most cells expressing Kv3.1 and Kv3.2 have protein in both the somatic and the axonal-terminal compartments (see section entitled Functional Roles of Alternative Splicing for the differential subcellular localization of the Kv3.1a and Kv3.1b isoforms), in thalamic relay neurons, the neuronal population containing the large majority of Kv3.2 transcripts in rodent brain, the protein is localized mainly in axons and terminals.[34] Kv3.2 antibodies stain the barrels in layer IV of somatosensory cortex,[34] and recent immunoelectron microscopy has confirmed the

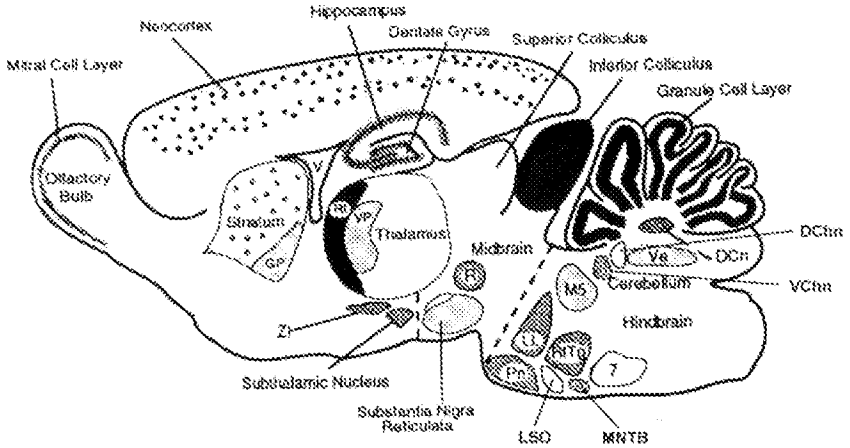

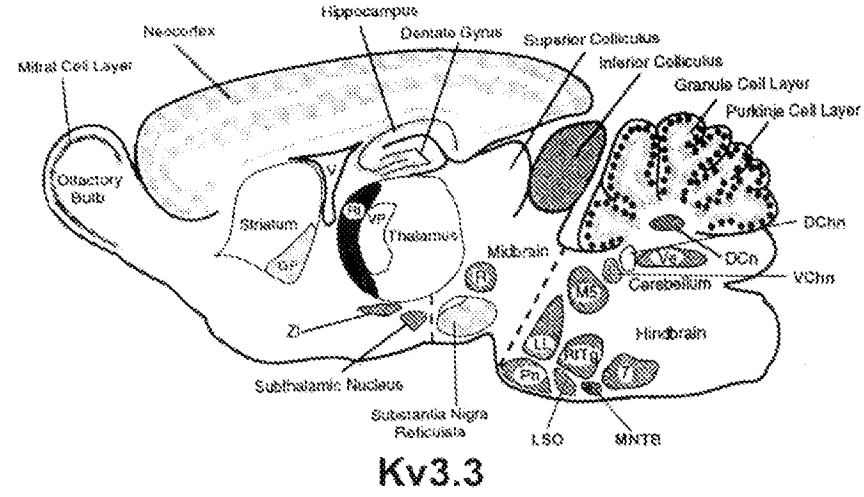

FIGURE 6 *(above and facing page).* Distribution of Kv3 mRNAs in the rat brain (similar patterns have been observed for some Kv3 transcripts in mice). The levels of expression of Kv3 genes based on *in situ* hybridization studies by Weiser *et al.*[21] are represented in these diagrams by different grades of *shading*. The position of some of the structures, particularly in the brain stem, is only approximate, and structures are shown in these diagrams that may not exist in the same sagittal plane. Some important structures expressing one or more Kv3 genes are not illustrated, such as several areas of the basal forebrain.

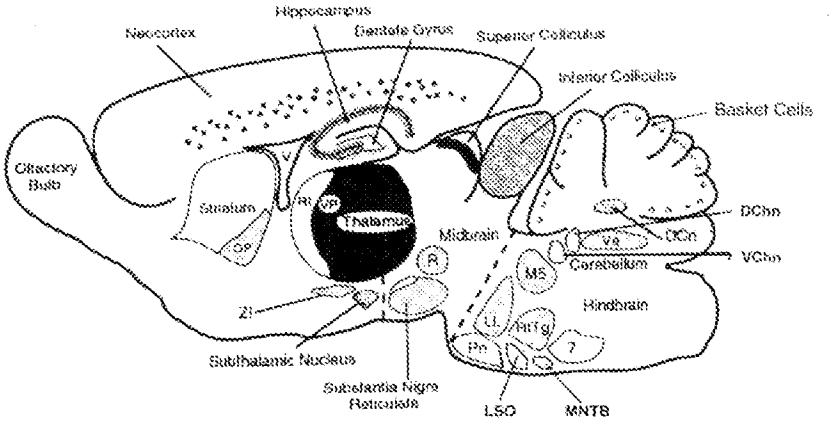

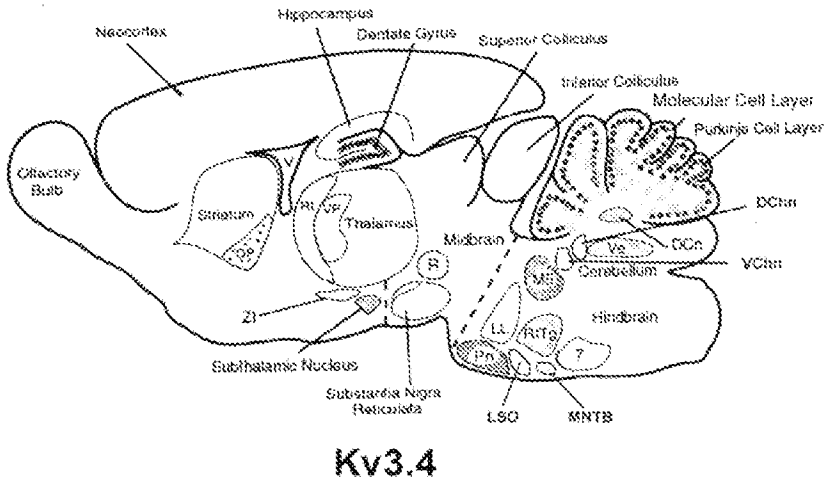

FIGURE 6 *(continued).* Abbreviations: 7, facial nucleus; DChn, dorsal cochlear nucleus; DCn, deep cerebellar nuclei; GP, globus pallidus; LL, lateral lemniscus nuclei; LSO, superior olive; M5, trigeminal motor nucleus; MNTB, medial nucleus of the trapezoid body; Pn, pontine nuclei; R, red nucleus; Rt, reticular thalamic nucleus; RtTg, reticulo tegmental nucleus of the pons; VChn, ventral cochlear nucleus; Ve, vestibular nucleus; VP, ventral-posterior complex of the dorsal thalamus; ZI, zona incerta.

localization of Kv3.2 proteins throughout the axon and terminals of thalamocortical projections in the cortex. Apparently there is Kv3.2 protein in thalamocortical terminals with both spiny stellate neurons and with GABAergic cells.[62,63]

Kv3.1 and Kv3.2 proteins are strongly expressed in a small subpopulation of cortical (FIG. 7) and hippocampal neurons. Double-labeling immunofluorescence was used to identify the neuronal populations containing these proteins. In the cortex, Kv3.1 proteins are present in parvalbumin (PV)-containing GABAergic interneurons in rat and mouse. In fact there is a nearly one to one correlation between the two markers: virtually all cells containing PV express Kv3.1 and vice versa.[62,63,66,67] In the hippocampus, Kv3.1 is also expressed in many PV-containing interneurons but the relationship between the two markers is not as strict as in the neocortex.[66–68] Kv3.1 and parvalbumin are also co-localized in interneurons in the caudate nucleus.[66,69]

Kv3.2 proteins are expressed in cortical and hippocampal GABAergic interneurons as well. In the cortex strongly labeled cells are concentrated in deep layers (V–VI), while very weakly stained cells are seen in superficial layers (I–IV) (FIG. 7), in accordance with the intensity of *in situ* hybridization signals. Double-labeling shows that the weakly stained cells in superficial layers are positive for PV. In deep layers, about 70–80% of the cells expressing Kv3.2 are also positive for PV, and the remaining 20–30% are also GABAergic interneurons which may correspond to the calbindin- and somatostatin-containing Martinotti cells.[62,63] These data show that there are two types of PV-containing interneurons in the cortex with respect to their expression of Kv3 proteins. PV neurons in superficial layers contain mainly Kv3.1 protein, and PV neurons in deep layers contain both, Kv3.1 and Kv3.2.

Since all PV neurons are positive for Kv3.1, and since all PV neurons in deep cortical layers, also express Kv3.2 proteins, it is possible that the two subunits are part of the same heteromeric channels. To test this hypothesis we used co-immunoprecipitation assays from cortical membranes solubilized with nondenaturing detergents (as in Refs. 71 and 72). Antibodies against Kv3.1 immunoprecipitated both Kv3.1 and Kv3.2 proteins, and the antibodies against Kv3.2 also precipitated both subunits.[62,63] It is therefore likely that PV-containing interneurons in the cortex (particularly those in layers V–VI) have heteromeric Kv3.1–Kv3.2 channels. The channels in PV neurons in superficial layers might be Kv3.1 homomultimers or Kv3.1–Kv3.2 heteromultimers in which Kv3.1 proteins dominate. Kv3.1 and Kv3.2 proteins are also co-localized in the globus pallidus, where they are present in the major population of pallidal neurons, the PV-containing projecting cells. Co-immunoprecipitation and functional studies also suggest that in these neurons the channels are heteromeric Kv3.1–Kv3.2 proteins.[25]

In the hippocampus Kv3.2 proteins are expressed in several types of interneurons, including most Kv3.1 containing PV-positive basket cells, as well as interneurons containing somatostatin in the stratum oriens and in the dentate hilus which do not express Kv3.1 (McBain and Rudy, unpublished observations).

We have recently began to characterize the brain distribution of Kv3.3 proteins, which like Kv3.1 and Kv3.2 are expressed in somas and axons. The group of Olaf Pongs has raised antibodies against Kv3.4 proteins. In the CNS Kv3.4 expression was lower than several Kv1 proteins analyzed in the same study, and was seen in areas consistent with the localization of Kv3.4 transcripts.[73,74] In most of these neurons, staining with anti-Kv3.4 antibodies was predominantly seen in axons and terminals.

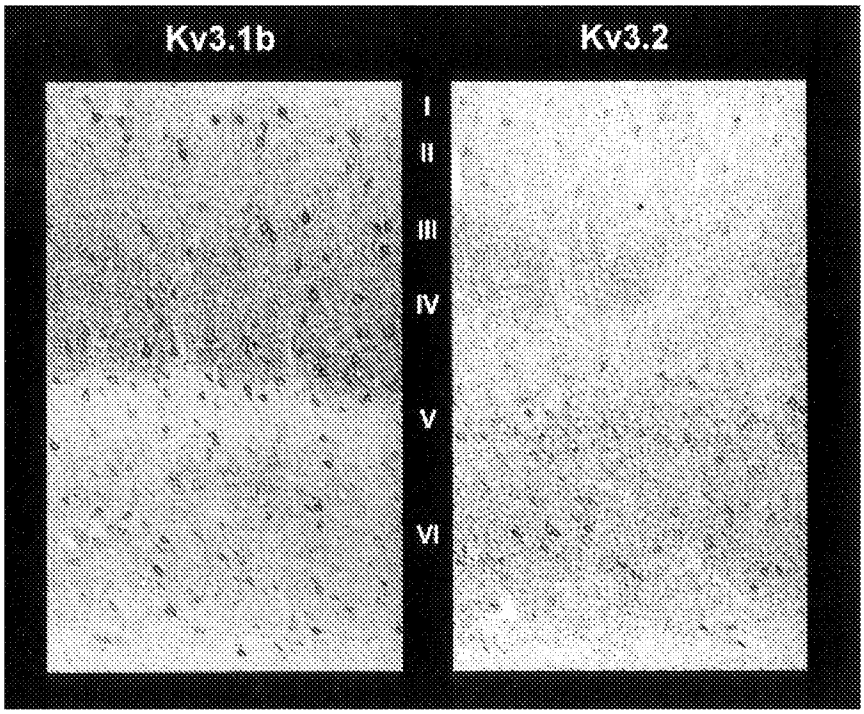

FIGURE 7. Kv3.1 and Kv3.2 proteins in neocortical interneurons. Immunoperoxidase staining of coronal sections of mouse somatosensory cortex for Kv3.1b and Kv3.2 proteins with specific polyclonal antibodies. There is strong somatic staining for Kv3.1b in a population of neurons distributed in layers II–VI. In the section stained with Kv3.2 antibodies there are strong labeled neurons in deep cortical layers (V–VI) and faintly stained cells in upper layers. There is strong staining of the neuropil with both antibodies, most prominent in areas around labeled cells. In addition, there is distinct staining of processes in the cortical barrels with Kv3.2-, but not Kv3.1b-antibodies.

Developmental Expression

Little is known about the expression of Kv3 genes during development. Although Perney *et al.*[59] reported *detectable* levels of expression of Kv3.1 mRNA transcripts in prenatal rats, all available studies agree that most of Kv3.1–Kv3.3 mRNA and protein expression develops after the first postnatal week. Perney *et al.*[59] found a large increase in expression of Kv3.1 transcripts between the 7th and 14th day after birth. By postnatal day 14, rats exhibited a pattern of expression in brain similar to that seen in the adult rat, although adult mRNA levels were somewhat higher than those at p14. In the hippocampus, Du *et al.*[68] could not detect Kv3.1b protein until postnatal day 8. There was a large increase between p8 and p20, but protein levels at p40 were still higher than those at p20. Goldman-Wohl *et al.*[13] studied the developmental expression of Kv3.3c transcripts in cerebellar Purkinje cells. Expression was first seen between postnatal day 8 and 10, and the levels increased as the cerebellum matured. Kv3.2 mRNAs in whole brain are barely detectable

before postnatal day 8–10 (faint transcripts are seen after long exposures), but the levels start increasing rapidly after this age. Interestingly, the developmental expression of the Kv3.2 gene appears to be regulated independently in thalamic relay neurons, where the majority of Kv3.2 mRNAs are found in adult animals, and outside the thalamus. While near adult levels outside the thalamus are achieved by postnatal day 14, in thalamic relay neurons Kv3.2 expression is still low at this age and increases to near adult levels during the third postnatal week.[75,76] In the globus pallidus the levels of both Kv3.1 and Kv3.2 *proteins* were not detectable earlier than postnatal days 5–6, and increased sharply after postnatal day 8. The expression of Kv3.1 developed faster than the expression of Kv3.2: Maximum levels of Kv3.1 protein were seen at p15, while for Kv3.2, maximum levels were not achieved until p20. Once protein levels reached a maximum, they decreased slightly in older animals.[25]

The expression of Kv3.4 transcripts in skeletal muscle is also developmentally regulated.[77] Utilizing semi-quantitative RT-PCR, detectable levels of Kv3.4 mRNAs were found at embryonic day 17, which increased to adult levels during the first 2 weeks after birth. Interestingly, Kv3.4 mRNA expression is muscle fiber type-dependent, with higher levels found in fast muscles. Moreover, the expression levels decreased in myotonic mice or after denervation in wild-type animals, suggesting that excitation of the muscle cell regulates Kv3.4 gene expression.[77]

NATIVE Kv3 CURRENTS RESEMBLE HETEROLOGOUSLY EXPRESSED Kv3 CURRENTS

There is now evidence from several cell types showing that at least for Kv3.1, Kv3.2, and Kv3.4, native channels have properties similar to those in heterologous expression systems. In an initial study combining immunohistochemical and electrophysiological analysis in slice preparations, we found that drugs that block Kv3.1 currents in heterologous expression systems blocked a fraction of the K^+ current from hippocampal interneurons expressing Kv3.1b proteins that resembled Kv3.1 currents in heterologous expression systems.[68] Moreover, concentrations of 4-AP that block Kv3 currents shortened the duration of the action potential of interneurons expressing Kv3.1b proteins, but not in interneurons that did not stain with anti-Kv3.1b antibodies. However, difficulties associated with voltage-clamping neurons in slices limited the extent of the comparisons that could be made between native and heterologously expressed currents in that study.

More recently we have been able to do a more detailed comparison of native and expressed Kv3 currents in freshly dissociated neurons from the globus pallidus. Acutely dissociated and short-term cultured neurons are an excellent system for this kind of study, allowing better conditions for space clamp and pharmacological analysis. Identical recording conditions to those used to study Kv3 currents in CHO cells were used to eliminate differences produced by components of the intracellular or extracellular solutions or other experimental variations. We utilized extracellular Cd^{2+} and intracellular BAPTA, as well as tetrodotoxin (TTX) to suppress Ca^{2+}, Ca^{2+}-activated K^+, and Na^+ currents. 1 mM TEA was used to isolate Kv3-like currents in these cells.

As described earlier, the rat and mouse globus pallidus express both Kv3.1 and Kv3.2 proteins in somatic membrane, probably in heteromeric channels containing both subunits, present in the major neuronal population in this nucleus (the PV-containing projecting

neurons) and at developmental stages in which dissociations were possible.[25] The GP plays key roles in the circuitry involved in movement control, and might also be involved in cognitive functions. There is therefore great interest in the anatomical and physiological characterization of this brain area.[78–80] The studies on Kv3 channels contribute novel information on the classification and cellular properties of pallidal neurons.

We found three morphological subtypes of neurons as a product of the enzymatic dissociation of the GP. The most common were medium to large cells with fusiform or triangular somas resembling the major population of pallidal neurons. When these cells were depolarized from a holding potential of −80 mV, the total current consisted of transient and sustained components. The transient component (which was variable) could be nearly completely inactivated by holding the cell at −40 mV. This holding potential also inactivated a significant portion of the sustained component. We assumed that Kv3.1–Kv3.2 currents contributed little to the suppressed sustained component since a VH of −40 mV has little effects on Kv3.1 and Kv3.2 currents expressed in CHO cells.[25] The currents recorded during depolarizing test pulses from a VH of −40 mV were of the delayed rectifier type. They could be separated into two components, which differed in activation and deactivation kinetics by 1 mM TEA (FIG. 8). The TEA-resistant current activated and deactivated more slowly than the TEA-sensitive component. The differences in kinetics were particularly large for the deactivation process (τ_{deact} = 25.64 ± 3.38 ms, for $I_{GP,R}$ and 2.27 ± 0.24 ms for $I_{GP,TEA}$).

A detailed comparison of the voltage-dependence and kinetics of the TEA-sensitive component showed that it has properties nearly identical to those of Kv3.1 and Kv3.2 currents in CHO cells (FIG. 8 and TABLE 1). In both cases the current starts activating between −10 and −20 mV, and the normalized conductance-voltage curves have similar slopes and midpoints of activation. When scaled to each other, the cloned and native currents have nearly superimposable activation and deactivation time courses when compared at the same voltages (FIG. 8; see also Refs. 25 and 81).

Previous electrophysiological analysis of the K^+ currents of pallidal neurons, in the same species, revealed a low voltage-activating fast inactivating current (I_A), a component with slower inactivation and slow recovery from inactivation that is blocked by micromolar concentrations of 4-AP (I_{As}), and two maintained components, one blocked (I_K) and one not blocked by 10 mM TEA.[82,83] None of these components resembles Kv3 currents, because the Kv3 channel-mediated current was buried in the I_K. These studies demonstrate that experimental conditions and methods to isolate individual components of the K^+ current tailored to search for specific current components are required before it is possible to determine whether native currents resemble those in heterologous expression systems.

The characteristics of the currents obtained from GP neurons described earlier were typical of the majority of the cells studied. However, we found that in a small group of cells (type "B" cells), 1 mM TEA blocked a fast inactivating current. Depolarizing pulses from a holding potential of −40 mV produced currents of the delayed rectifier type, similar to those seen in the cells described earlier (type-A cells), but had faster activation kinetics (rise time between 10 and 90% of ~14.0 ms for type "B" cells and ~22 ms for type "A" cells). Application of 1 mM TEA inhibited approximately 10–15% of the current. The TEA-resistant current had slower activation kinetics than the total current (10–90% rise time: 22.4 ± 2.5 ms). The TEA-sensitive component obtained by digital subtraction was composed predominantly of a current that activated rapidly, starting at voltages more positive than −10 mV, and inactivated quickly. The transient currents recorded from type "B"

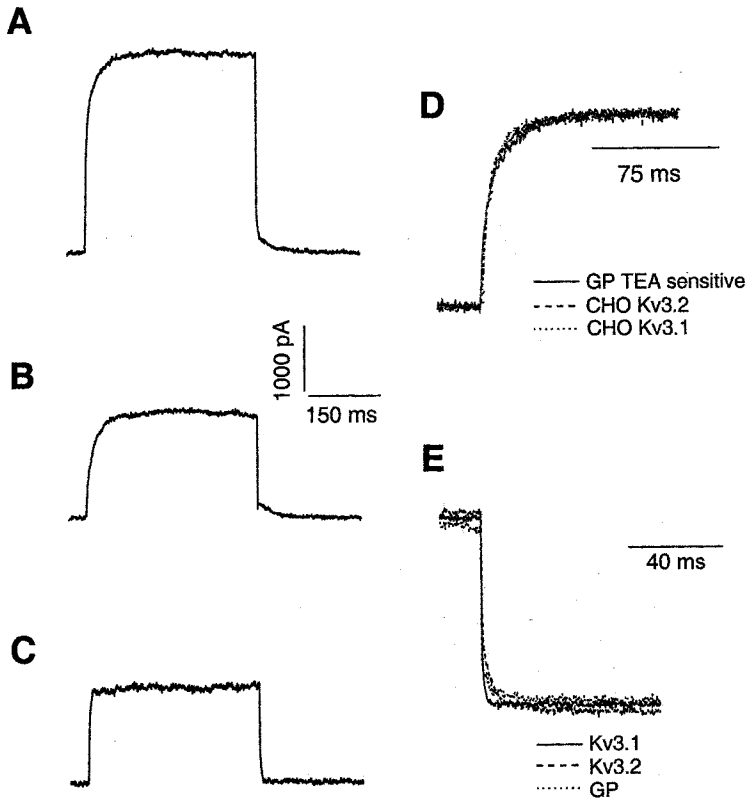

FIGURE 8. Voltage-dependent K+ currents in type "A" pallidal neurons. (**A-C**) Currents obtained from a GP neuron held at −40 mV during a depolarizing pulse to +40 mV before (**A**) and after (**B**) application of 1 mM TEA. The trace in **C** shows the TEA-sensitive component obtained by digital subtraction of the trace in **B** from the trace in **A**. (**D**) Superimposition of the first 150 ms of scaled records obtained from CHO cells transfected with Kv3.1 or Kv3.2 cDNAs and the TEA-sensitive current from a type "A" pallidal neuron. Records were obtained during voltage pulses to +30 mV applied from a holding potential of −40 mV. (**E**) Superimposition of scaled traces of tail currents obtained from the same cells as in **D** during repolarization to −40 mV following a voltage step to +40 mV.

neurons of the GP resembled closely the currents expressed by Kv3.4 proteins in voltage-dependence as well as in activation and inactivation kinetics. This result was surprising since *in situ* hybridization studies reported that signals for Kv3.4 mRNAs were "weakly above background."[21] Since we do not have antibodies against Kv3.4 proteins we used single-cell RT-PCR to investigate whether type-B cells in the GP contain Kv3.4 transcripts. These studies showed that Kv3.2 transcripts are found in most type A and some type B cells, Kv3.1 is found mainly in type A cells, and Kv3.4 only in type B cells.

As described earlier, heteromultimer formation between inactivating Kv3.4 subunits and Kv3.1 or Kv3.2 proteins results in amplification of the transient current. This phenom-

enon may account for the presence of the levels of Kv3.4-like currents seen in type "B" pallidal neurons in spite of the low-level expression of Kv3.4 transcripts. Nevertheless, relative to the other outward currents, the Kv3.4-like current in these neurons contributes a very small proportion of the total outward current. However, the current produces a large effect on the rise time of the total current, since the currents remaining after 1 mM TEA are much slower. This could be an important role for Kv3.4 currents in neurons, to accelerate the rate of rise of the repolarizing currents, without significantly increasing the steady-state levels of total outward current.

Kv3.1-like currents have also been described in central auditory-processing neurons[84] (see below), as well as in cells expressing Kv3.1 transcripts outside the nervous system. Grissmer *et al.*[57] showed that the current mediated by *l*-type channels in T lymphocytes was very similar to Kv3.1 currents in *Xenopus* oocytes when recordings in the two preparations were obtained with the same solutions.

It appears from these results that the main biophysical properties of native channels containing Kv3.1, Kv3.2, and Kv3.4 proteins, in both neurons and other cell types, are not significantly affected by factors such as associated subunits or posttranslational modifications as might be the case for other cloned subunits, at least in the cells studied until now.

Kv3.1 AND Kv3.2 CHANNELS PLAY UNIQUE ROLES IN THE GENERATION OF SUSTAINED HIGH FREQUENCY FIRING

The unusual properties of Kv3 channels, and in particular their voltage-dependence and their fast rate of deactivation, are likely to provide these channels with unique effects on neuronal excitability. Since Kv3 channels open significantly only when the membrane potential is depolarized beyond −10 mV, we expect that physiologically they will be activated mainly during action potentials. They may be activated also by receptor-mediated depolarizations that depolarize the membrane to potentials more positive than −10 mV, as might be encountered in the end bulb synapses in the ventral cochlear nucleus.[70]

It has been suggested that these channels are activated during the peak of the action potential and that, when present in sufficient amounts, they influence the rate of repolarization of the action potential and thus help dictate action potential duration.[15,34,66,67,69] Indeed, when HEK293 cells expressing Kv3.1 or Kv3.2 channels are voltage-clamped to a waveform in the shape of a brief action potential, current is not seen until after the action potential has reached its peak, achieving a maximum value during the repolarizing phase of the spike, in contrast to what is observed when cells expressing Kv1.1 are clamped to the same waveform (FIG. 9). These experiments also illustrate the effect of the fast deactivation of Kv3.1 and Kv3.2 channels. The K^+ current is quickly eliminated during the fast hyperpolarization and thus little Kv3.1/Kv3.2 currents remain during the interspike interval. The predominant somato-axonal localization of Kv3 proteins in CNS neurons (see above) is consistent with a role in the shaping and transmission of action potentials. The low levels of expression in fine dendrites suggests that these channels play little role in the local integration of postsynaptic signals at axo-dendritic synapses.

Although K^+ channels that activate at more negative voltages could also repolarize spikes and reduce their duration, high voltage-activating K^+ channels would modulate firing properties more selectively. By virtue of the fact that they are not opened until the spike has been generated, they are less likely to influence the initial threshold of an action

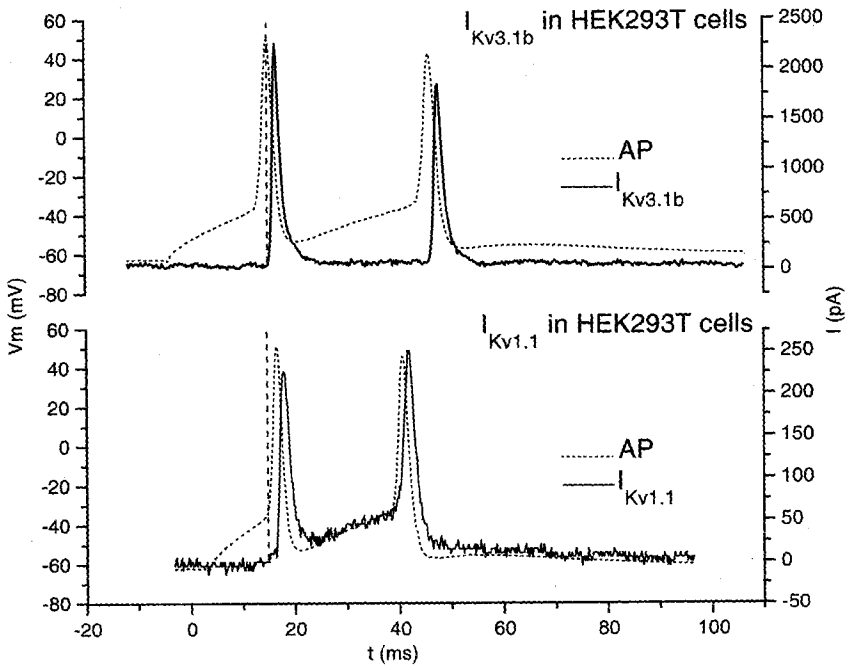

FIGURE 9. Currents evoked in cells expressing Kv3.1b or Kv1.1 when depolarized with a fast action potential. HEK293 cells were transfected with Kv3.1b cDNA **(upper traces)** or Kv1.1 cDNA **(lower traces)** and voltage-clamped to a waveform corresponding to the action potential (AP) recorded from a neocortical neuron. The currents, shown with *continuous black lines* have been superimposed on the command voltage trace. A *perpendicular broken line* has been drawn at the time that the current begins to rise (shown only during the first spike) to illustrate the temporal relationship between current activation and the action potential. The Kv1.1 current begins to rise early during the rising phase of the action potential, while the Kv3.1 current rises much later (similar results were obtained with Kv3.2). Note also that the Kv3.1 current is completely deactivated during the interspike interval, while the Kv1.1 channels close slowly and are activated by the inter-spike depolarization. After the second spike the Kv1.1 current deactivates slowly.

potential.[34,66] Given their fast deactivation, Kv3.1–Kv3.2 channels are also less likely to contribute to increase the duration of refractory periods. In neurons containing additional K^+ channels, their differential modulation by neurotransmitters and neuromodulators could independently regulate different aspects of the cell's electrical behavior.

Many of the neuronal populations expressing Kv3 gene products fire trains of action potentials at very high rates, such as neurons in the reticular thalamic nucleus (RT) and fast-spiking (FS) interneurons in the neocortex and the hippocampus.[14,21,59,66,67,68] It has been proposed that Kv3.1–Kv3.2 channels play key roles in the firing properties of these cells. An emphasis of recent investigations by us and others[68,70,84,85] has been on exploring the role of Kv3.1–Kv3.2 channels on high-frequency firing.

FS cells of the cerebral cortex are GABAergic inhibitory interneurons characterized by brief action potentials, a large and fast after-hyperpolarization (fAHP) and the ability to fire at high frequency with little accommodation. Cortical GABAergic interneurons play multiple central roles in the processing of cortical information. They are thought to be important in the synchronization of cortical circuits, in the establishment and reorganization of cortical representation maps, in the establishment of cortical columns during development, in the generation of some forms of cortical rhythms, and in the pathogenesis of seizures.[86–92]

In a recent study, we examined the effects of low TEA concentrations (<1 mM) on the electrophysiological properties of visually identified nonpyramidal cells in mouse cortical slices using whole-cell patch clamp methods.[93,94] We found that TEA had dramatic, reversible effects on the shape of the action potential and the repetitive firing characteristics of fast-spiking (FS) neurons. TEA nearly abolished the fast-afterhyperpolarization (fAHP), increased the spike duration, and decreased the maximum rate of spike repolarization (FIG. 10A; TABLE 3). Moreover, for a given current strength, TEA also produced a reduction in the steady firing rate (FIG. 10B). This effect of TEA was manifest over a large range of injected currents and reduced the maximum steady firing rate that could be achieved by direct-current injection into FS neurons (TABLE 3).

As described in the subsection in this paper entitled Pharmacological Properties (see also Coetzee *et al.* in this volume) at the concentrations of TEA used in the studies by Erisir *et al.*, the only known voltage-gated K^+ channels that are significantly blocked by this drug are, in addition to Kv3.1–Kv3.4 channels, those containing the K^+ channel proteins Kv1.1 and KCNQ2 as well as the BK (also called maxi-K) Ca^{2+}-activated K^+ channels containing proteins of the *slo* family. To test the possible involvement of these channels in the TEA-effect on FS neurons, Erisir *et al.* applied toxins specific for Kv1 and BK channels. 100 nM Dendrotoxin, which selectively blocks Kv1.1 and other Kv1 channels (see Coetzee *et al.* in this volume and Ref. 45), had few measurable effects on the shape of individual action potentials. However, and in contrast to the effects of TEA, it produced a significant *increase* in the maximum firing frequency achieved with current injection into FS neurons. Application of Charybdotoxin (100 nM) or Iberiotoxin (50 nM), which block Ca^{2+}-activated BK channels, produced minimal effects on spike shape or firing frequency.[93,94] The recently discovered KCNQ2 subunits express very slowly activating and deactivating (time constants of hundreds of milliseconds to seconds) voltage-gated K^+ channels that are unlikely to be activated during short action potentials and have not been shown to be expressed in cortical interneurons[95] (see also Coetzee *et al.* in this volume).

These results support the hypothesis that Kv3.1–Kv3.2 potassium channels are important for the elaboration of fast-spiking properties in cortical interneurons. Moreover, the fact that blockade of Kv1 channels had the opposite effect of low TEA concentrations supports the notion that the high voltage activation and rapid deactivation kinetics of Kv3.1–Kv3.2 channels are necessary for sustained high-frequency firing. This idea was further supported by results from voltage-clamp analysis of voltage-dependent K^+ currents recorded from macropatches excised from *somata* of FS cells. These currents showed two main components, the larger of which (>75% of the total) was blocked by 1 mM TEA. This component had a voltage-dependence and activation and deactivation kinetics that were similar to those of Kv3.1 and Kv3.2 currents in heterologous expression systems and the Kv3.1–Kv3.2-like current isolated from pallidal neurons described above. Thus, the native TEA-sensitive channels which were necessary for sustained high-frequency firing

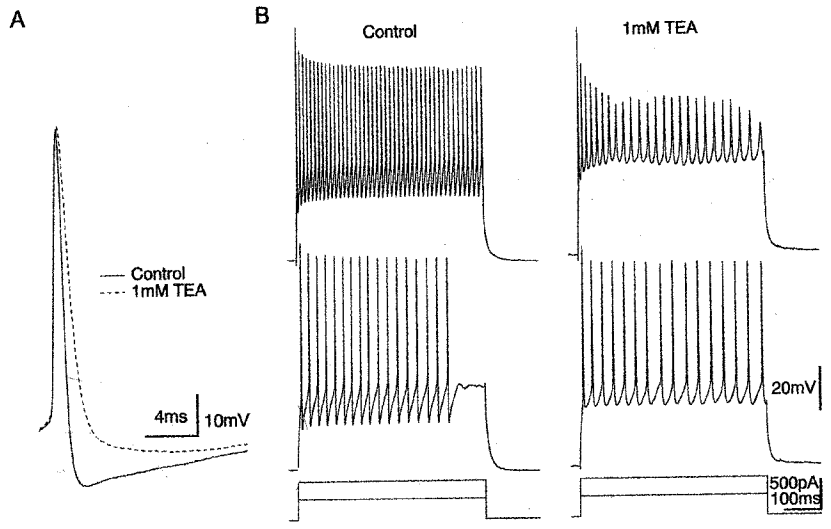

FIGURE 10. Low concentrations of TEA impair spike repolarization and slow high-frequency firing of fast-spiking (FS) layer II/III neocortical interneurons. (**A**) 1 mM TEA caused spike broadening by reducing the maximum rate of spike repolarization and suppressed the fast-AHP of single action potentials evoked by near-threshold depolarizations. (**B**) **left panel** shows repetitive firing of the same FS neuron in response to 350-pA **(bottom)** and 650pA currents under control conditions. **Right panel** shows the responses to identical currents in the presence of 1 mM TEA. TEA reduced the steady firing rate from 35 to 29 spikes/s and from 75 to 33 spikes/s for the 350- and 650pA currents, respectively.

in FS cells had similar properties to Kv3.1–Kv3.2 channels in heterologous expression systems.

Kv3 transcripts are also abundantly expressed in other sensory neurons in the brain, including in neurons of most of the midbrain and hindbrain auditory nuclei.[14,21,59,66,70] There is co-expression of Kv3.1 and Kv3.3 in many of these nuclei, including the ventral cochlear nucleus (VCN), the medial nucleus of the trapezoid body (MNTB), the lateral lemniscus nuclei and the inferior colliculus.[21] It remains to be shown whether the protein products are co-localized in the same neurons and whether they can be co-precipitated. There are also Kv3.2 mRNAs and proteins in the inferior colliculus (Ref. 21 and unpublished observations), but it has not yet been shown that Kv3.1 and Kv3.2 proteins are in the same neuronal populations or that they are present in the same channel complex. In other auditory nuclei there is actually a reciprocal expression between Kv3.1–Kv3.3 and Kv3.2 transcripts, as is seen in the thalamus. Kv3.2 is more abundantly expressed in the dorsal cochlear nucleus, while Kv3.1 and Kv3.3 are more abundant in the ventral nuclei. Similarly Kv3.2 mRNA transcripts and proteins are more abundant in the ventral lateral lemniscus nuclei and Kv3.1 and Kv3.3 in the dorsal nuclei.

These auditory neurons do not respond with high-frequency trains of action potentials when depolarized by steady current injection. However, many of these cells, includ-

TABLE 3. Effects of 1 mM TEA on the Firing Properties of Fast-Spiking Neocortical Interneurons

	FS Neurons	FS Neuron + 1 mm TEA
Spike duration (ms) (width at half-amplitude)	0.64	1.16
Maximal repolarization rate (mV/ms)	148.7	62.8
Fast after-potential (mV) (relative to threshold)	−12.5	0.8
Maximal firing frequency (Hz)	104.6	65.6

ing many of those expressing Kv3 products, are capable of entraining at very high frequencies when stimulated with high-frequency inputs (>600 Hz). The ability to follow high-frequency stimulation allows these neurons to preserve the timing information contained in auditory signals. The temporal precision of auditory signals is important for the faithful transmission and localization of sound.[84,96,97] Len Kaczmarek and coworkers have been studying the role of Kv3 channels in central auditory neurons. In the MNTB, application of low concentrations of TEA did not alter the ability of the cells to follow stimulation up to 200 Hz, but reduced their ability to follow higher frequency stimuli.[84]

Together, the pharmacological studies provide very strong circumstantial evidence for a role of Kv3.1–Kv3.2 channels in sustained high-frequency firing, but, of course, we cannot exclude the possibility that there are unknown K^+ channels that are also blocked by low TEA concentrations. However, the observations with different K^+ channel blockers and with modeling studies indicate that the relatively positive activation range and the deactivation rates of Kv3.1 and Kv3.2 channels are important for these apparent roles.[93,94]

How do the special properties Kv3.1 and Kv3.2 channels facilitate high-frequency firing? In trains of Na^+ spikes, the inter-spike interval is established in part by the amount of Na^+ channel inactivation that accumulates during the train. By increasing the rate of spike repolarization and by keeping action potentials short, Kv3.1–Kv3.2 currents would reduce the amount of Na^+ channel inactivation that occurs during the action potential. Moreover, the large, fast after-hyperpolarization produced by the Kv3.1–Kv3.2 current would function to speed up recovery from Na^+-channel inactivation and thus increase the amount of recovery that occurred following a spike. Indeed, examination of the effects of low TEA concentration on cortical interneurons revealed that 1 mM TEA produced a significant reduction in the maximum rate of rise of the second, but not the first, spike in a train. This suggested that there was significantly greater Na^+-channel inactivation at the onset of the second spike in the presence of TEA. This interpretation of the TEA results was strongly supported by results from computer simulations of a fast-spiking neuron.[94] In that model, blocking 95% of the Kv3.1–Kv3.2-like channels resulted in spike-broadening, a reduction in the after-hyperpolarization and a slowing of the frequency of repetitive firing for a given current injection as observed experimentally. Accompanying this slowdown in firing was a decrease in both the amount of recovery and speed of recovery from Na^+-channel inactivation. Thus, one function of the Kv3.1–Kv3.2 current is to reduce the impact of Na^+-channel inactivation on repetitive firing.

Another unique feature of Kv3.1–Kv3.2 currents is their rapid rates of deactivation. The importance of this for high-frequency firing was also apparent from the simulations. The large AHP produced by activation of Kv3.1–Kv3.2-channels also serves to rapidly terminate the Kv3.1–Kv3.2 current, which, because of its rapid deactivation rates, does not contribute increases in the duration of the refractory period. The situation is completely different for K^+ channels with slower deactivation kinetics. For example, a Kv1.3-like current deactivates slowly enough that its conductance decays relatively little during the interspike interval and therefore, it contributes to delaying the onset of the next spike. Hence, blocking such a current in the model produced an *increase* in spike frequency for a given current injection. These modeling studies strongly suggest that the particular activation range and fast deactivation kinetics of Kv3.1–Kv3.2 channels function specifically to enable sustained high-frequency firing.

The presence of Kv3.1–Kv3.2 channels alone is not sufficient for the generation of sustained high-frequency firing. The firing properties of the cell depend on the interplay between passive electrical properties of the cell and the various ionic conductances that are active when the cell is stimulated. Pallidal and brainstem auditory neurons may be a case in point. Two main types of neurons from the point of view of their intrinsic electrophysiological properties have been described in pallidal neurons recorded in guinea pig brain slices. Type I neurons were not spontaneously active and fired spike bursts with strong accommodation upon depolarization. Type II cells fired spontaneously at the resting level (~ −60 mV) and displayed fast repetitive firing (≤200 Hz) with some accommodation when depolarized.[99,100] Type II cells resemble the "repetitively firing cells" recorded in an *in vivo* intracellular study in rats by Kita and Kitai,[101] while type I neurons resemble the periodic burst firing cells in this study. The majority of the cells in the rat study (73%) were of the repetitive firing type and most likely correspond to the neurons we classified as type "A" in the study described earlier.

The firing frequency of the repetitive firing cells in the globus pallidus is not as high or sustained as that of fast-spiking cortical neurons. The analysis made by Erisir *et al.*[93,94] of the currents in the latter cells suggests that they have a higher proportion of Kv3.1–Kv3.2-like currents and less Ca^{2+}-activated K^+ currents than do pallidal neurons. These differences in channel composition may explain the differences in firing frequency adaptation of the two cell types. Moreover, owing to the presence of a large component of inactivating current in PV+ pallidal neurons (see above), changes in the resting potential of the cell will change the contribution of Kv3.1–Kv3.2 channels to the total current. This may, in turn, change the maximum firing frequencies of these neurons.

The central auditory neurons described earlier can follow spikes at very high frequencies, but they respond with one or few spikes to steady depolarizations, unlike fast-spiking cortical interneurons. These different firing properties of the two cell types, both of which express abundant Kv3.1–Kv3.2 channels, could be explained by the different levels of low-voltage-activating dendrotoxin-sensitive K^+ channels.[84]

Kv3 CHANNELS IN AXONS AND TERMINALS

Kv3 proteins are prominently expressed in nonmyelinated axons and in presynaptic terminals in the CNS (see above); however not much is known about their function in these neuronal compartments. For that matter, little is known about the role of any specific

K^+ channels in axons and terminals in the CNS. This is not surprising, since until recently it was very difficult to study axonal and presynaptic function in central neurons. Nevertheless, there is clearly a large diversity of K^+ channels in axons and terminals (see Coetzee *et al.* in this volume), and we can expect a richness of functions as that seen in the generation of firing properties in the somatic compartment. It is also becoming clear that, as in the soma, several types of K^+ channels may coexist in the same terminal and/or in axons. Any mechanism affecting Ca^{2+} entry into the presynaptic terminal is likely to have strong effects on neurotransmitter release. K^+ channels are likely to modulate in complex and subtle ways the invasion, magnitude, and shape, and temporal relationships of action potentials of presynaptic terminals, which in turn will regulate the magnitude and kinetics of Ca^{2+} entry. Because of our ignorance of necessary details on action potential propagation and synaptic transmission in central neurons it is more difficult to generate predictable hypotheses about the role of specific channels. Therefore the investigation of these roles becomes more urgent.

Nevertheless, that presynaptic K^+ channels affect Ca^{2+} entry and/or neurotransmitter release is well established (in the CNS as well), and two K^+ channel blockers, 4-AP and DTX, are well known to increase transmitter release in several CNS synapses.[46,102–112]

We can expect that with the development of methods to study axonal and synaptic function in the CNS and of tools to specifically control the activity of specific K^+ channels, our knowledge of this area will grow enormously. A very recent study, taking advantage of the ability to record simultaneously from two connected cells, showing that an A-type K^+ channel, probably Kv1.4, could gate action potential propagation in hippocampal axons, illustrates this point.[113]

We expect that, as in the soma, Kv3 channels and their modulation will play special roles in axons and presynaptic terminals. These roles might be related to the ability of Kv3 channels to keep action potentials short and facilitate recovery of processes that accumulate during repetitive action potentials and can limit the frequency of action potential transmission. By minimizing these changes, Kv3 channels could facilitate the reliable transmission of impulses at high frequency. In synapses, by increasing action potential repolarization and helping to generate large fast AHPs without increasing the duration of the refractory period, Kv3 channels could help increase the temporal resolving abilities of the terminal. The presence of Kv3 channels together with other K^+ channels in terminals could allow the cell to regulate independently the amount of transmitter release per spike and the frequency of release.[34,66,70] Wang and Kaczmarek[98] recently showed that high-frequency firing speeds up the recovery of synaptic depression in auditory neurons by helping replenish the pool of releasable vesicles. Kv3 channels may thus also modulate the rates of recovery of terminals that undergo synaptic depression. The availability of pharmacological tools and mouse models (see below) to study Kv3 channels will be particularly useful to investigate the roles of these channels in axonal conduction and synaptic transmission.

FUNCTIONAL ROLES OF ALTERNATIVE SPLICING

The significance of the alternative splicing of Kv3 genes has remained unknown until recently. None of the alternatively spliced transcripts yet tested in heterologous expression systems (Kv3.1a;[1] Kv3.1b;[5] Kv3.2a;[2] Kv3.2b;[35] Kv3.2d, Moreno and Rudy,

unpublished observations; Kv3.3a;[9] Kv3.3b, Vega-Saenz de Miera, unpublished observations; Kv3.4a;[4] and Kv3.4b[3]) expresses currents noticeably different from those of any other transcript from the same gene. However, a more in-depth analysis of the channels expressed by these transcripts that may reveal overlooked subtle differences is yet to be done. Since alternatively spliced C-termini have different putative-phosphorylation sequences (see TABLE 4 in Ref. 15), it was suggested that distinct alternatively spliced isoforms may respond differently to various second-messenger systems. Alternative splicing may thus allow for isoform-specific differences in the modulation of channel function by neurotransmitters and neuropeptides. We have also suggested that the divergent carboxy termini could be used in protein–protein interactions, conferring isoform-specific channel localization or mobility.

Evidence in support of these proposals is now becoming available. In a study comparing the modulation of Kv3.2a and Kv3.2b channels expressed in HEK-293T cells by PKA and PKC, we found that while both currents are similarly suppressed by PKA, only Kv3.2b channels are affected by phorbol esters activating PKC[35] (see TABLE 1). The similarity of the effects of PKA are consistent with the conclusion, mentioned earlier, that the effects of this kinase are due to phosphorylation at the single PKA consensus site, which is present in the Kv3.2 C-terminal sequence *prior* to the site of divergence of alternatively spliced isoforms. Several putative PKC phosphorylation sites are present in the Kv3.2b alternatively spliced C-terminus which are lacking in the Kv3.2a C-terminus. Phosphorylation of one or more of these sites may mediate the isoform-specific modulation by this kinase.

Data supporting the view that the alternatively spliced C-termini may participate in targeting Kv3 channels to different compartments of the neuronal membrane is also forthcoming. In a study in monolayers of polarized epithelial MDCK cells, Ponce *et al.*[114] showed that in Kv3.2a-transfected cells the Kv3.2 channels are expressed mainly in the basolateral membrane, while Kv3.2b is expressed mainly in the apical membrane. Interestingly a sequence analysis of the alternatively spliced C-termini of all four Kv3 genes showed that the sequences fall into two groups: those that resemble the C-terminus of Kv3.2a and those that resemble the C-terminus of Kv3.2b.[114]

More recently, we have been able to raise antibodies that distinguish the two Kv3.1 isoforms, and have begun a study of the cellular and subcellular distribution of the two proteins in CNS neurons. The results strongly support the notion that the divergent C-termini play a role in targeting the channels to distinct neuronal compartments. While Kv3.1b is expressed strongly in somatic, axonal, and terminal membranes (see above), Kv3.1a is expressed mainly in axons and terminals, including in many neuronal populations expressing Kv3.1b somatically, as in basket cells in the hippocampus.[64,65] We hypothesize that the Kv3.1a C-terminus (which resembles the C-terminus of Kv3.2b) contains signals for transport to axons and terminals, and that the Kv3.1b protein is carried to these compartments by forming heteromeric channels with Kv3.1a and other Kv3 proteins having the proper signals.[64,65]

CONCLUSIONS AND PERSPECTIVES

This chapter summarizes the results of a six-year effort by ourselves and others to discover the physiological roles of Kv3 proteins. Studies in heterologous expression systems,

including *Xenopus* oocytes and transfected mammalian cell lines, showed that these proteins form homomultimeric and heteromultimeric delayed-rectifier and A-type voltage-gated K^+ channels mediating currents with several unusual properties. All Kv3 currents studied thus far have, compared to other voltage-dependent K^+ currents, a relatively positive activation voltage. Significant Kv3 currents are not seen until the membrane is depolarized beyond −10 mV.

Studies on the localization of Kv3 mRNA transcripts and proteins have been key to select neurons and other cells where the properties of native channels containing Kv3 proteins could be analyzed, and to generate hypotheses as to their physiological roles. In the cells studied so far, Kv3.1, Kv3.2, and Kv3.4 channels mediate currents which resembled those in heterologous expression systems. Native Kv3.3 channels have not been pursued yet.

Kv3.1 and Kv3.2 proteins are expressed in somatic and/or axonal-terminal membranes of selected neuronal populations in the CNS. These include many GABAergic neurons that are capable of firing action potentials at very high frequencies. Kv3.1 and/or Kv3.2 channels may play interesting roles in several central midbrain and brain stem sensory processing systems, and in the thalamocortical circuit. In some neurons, Kv3.1 and Kv3.2 proteins may be part of the same heteromeric channels. A careful utilization of the limited pharmacological tools available to differentiate Kv3 currents from other K^+ currents, and in particular the use of low concentrations of the K^+ channel blocker TEA (<1 mM), in electrophysiological recordings from cortical fast-spiking interneurons, support the suggestion that Kv3.1–Kv3.2 channels play *unique* roles in maintaining sustained high-frequency firing. These roles may critically depend on two of the unusual properties of the currents mediated by these channels: (1) Their voltage-dependence and (2) their fast closing rate upon membrane repolarization. The role of Kv3.1–Kv3.2 channels in fast-spiking neurons might not be easily replaceable by other K^+ channels.

In our laboratory[115,116] and others'[117,118] mouse lines with disrupted Kv3 genes have been generated, utilizing homologous recombination in embryonic stem cells. Mice that do not produce Kv3.1, Kv3.2, and/or Kv3.3 proteins are now available. Mice lacking Kv3.1 proteins have several behavioral deficits.[117,119] Kv3.2 knockout mice are very interesting: they have abnormal sleep cycles, epileptic seizures, and abnormal EEG patterns. These defects could well be associated with disruption of thalamocortical circuits and/or cortical inhibition, systems in which Kv3.2 proteins are so prominent. Bearing in mind all the precautions necessary to interpret results from this experimental paradigm (see the Introduction to this volume), we believe that these mice are likely to become important tools, in conjunction with the other experimental tools described in this chapter, to deepen our understanding of the physiological roles of Kv3 channels. In particular, if there have not been compensatory changes, and if the primary result of the genetic disruption has not initiated a cascade of secondary changes (as appears to be the case so far, and is probably minimized by the late appearance of these channels during development), the mice will allow us to confirm the roles of Kv3.1 and Kv3.2 channels on fast spiking and will be particularly helpful to analyze roles of Kv3 channels in signal transmission through axons and terminals. Moreover, these mice might be important experimental models to investigate the roles of the signaling patterns of the affected neuronal systems on brain function.

ACKNOWLEDGMENTS

The work in the Rudy lab described here was supported by NIH Grants NS30989, NS35215 and NSF Grant IBN9630832. Work in the C. L. lab is supported by NIH Grant NS27881.

REFERENCES

1. Yokoyama, S., K. Imoto, T. Kawamura, H. Higashida, N. Iwabe, T. Miyata & S. Numa. 1989. Potassium channels from NG108-15 neuroblastoma-glioma hybrid cells. Primary structure and functional expression from cDNAs. FEBS Lett. **259:** 37
2. McCormack, T., E.C. Vega-Saenz de Miera & B. Rudy. 1990. Molecular cloning of a member of a third class of Shaker-family K^+ channel genes in mammals [published erratum appears in Proc. Natl. Acad. Sci. U.S.A. 1991 May 1:88(9):4060]. Proc. Natl. Acad. Sci. USA **87:** 5227.
3. Rudy, B., K. Sen, E. Vega-Saenz de Miera, D. Lau, T. Ried & D.C. Ward. 1991. Cloning of a human cDNA expressing a high voltage-activating, TEA-sensitive, type-A K^+ channel which maps to chromosome 1 band p21. J. Neuroscie. Res. **29:** 401.
4. Schroter, K.H., J.P. Ruppersberg, F. Wunder, J. Rettig, M. Stocker & O. Pongs. 1991. Cloning and functional expression of a TEA-sensitive A-type potassium channel from rat brain. FEBS Lett. **278:** 211.
5. Luneau, C.J., J.B. Williams, J. Marshall, E.S. Levitan, C. Oliva, J.S. Smith, J. Antanavage, K. Folander, R.B. Stein, R. Swanson, *et al.* 1991. Alternative splicing contributes to K^+ channel diversity in the mammalian central nervous system. Proc. Natl. Acad. Sci. U.S.A. **88:** 3932.
6. Luneau, C., R. Wiedmann, J.S. Smith & J.B. Williams. 1991. Shaw-like rat brain potassium channel cDNAs with divergent 3′ ends. FEBS Lett. **288:** 163.
7. Vega-Saenz de Miera, E.C., K. Sen, P. Serodio, T. McCormack & B. Rudy. 1990. Description of a new class of potassium channel genes. Soc. Neurosci. Abst. **16:** 4.
8. Vega-Saenz de Miera, E.C., N. Chiu, K. Sen, D. Lau, J.W. Lin & B. Rudy. 1991. Toward an understanding of the molecular composition of K^+ channels: Products of at least nine distinct Shaker family K^+ channel genes are expressed in a single cell. Biophys. J. **59:** 197a.
9. Vega-Saenz de Miera, E., H. Moreno, D. Fruhling, C. Kentros & B. Rudy. 1992. Cloning of ShIII (Shaw-like) cDNAs encoding a novel high-voltage-activating, TEA-sensitive, type-A K^+ channel. Proc. R. Soc. Lond. B Biol. Sci. **248:** 9.
10. Ghanshani, S., M. Pak, J.D. McPherson, M. Strong, B. Dethlefs, J.J. Wasmuth, L. Salkoff, G.A. Gutman & K.G. Chandy. 1992. Genomic organization, nucleotide sequence, and cellular distribution of a Shaw-related potassium channel gene, Kv3.3, and mapping of Kv3.3 and Kv3.4 to human chromosomes 19 and 1. Genomics **12:** 190.
11. Ried, T., B. Rudy, E. Vega-Saenz de Miera, D. Lau, D.C. Ward & K. Sen. 1993. Localization of a highly conserved human potassium channel gene (NGK2-KV4; KCNC1) to chromosome 11p15. Genomics **15:** 405.
12. Haas, M., D.C. Ward, J. Lee, A.D. Roses, V. Clarke, P, D.E., D. Lau, E. Vega-Saenz de Miera & B. Rudy. 1993. Localization of Shaw-related K^+ channel genes on mouse and human chromosomes. Mamm. Genome **4:** 711.
13. Goldman-Wohl, D.S., E. Chan, D. Baird & N. Heintz. 1994. Kv3.3b: A novel Shaw type potassium channel expressed in terminally differentiated cerebellar Purkinji cells and deep cerebellar nuclei. J. Neurosci. **14:** 511.
14. Rudy, B., C. Kentros, M. Weiser, D. Fruhling, P. Serodio, E. Vega-Saenz de Miera, M.H. Ellisman, J.A. Pollock & H. Baker. 1992. Region-specific expression of a K^+ channel gene in brain. Proc. Natl. Acad. Sci. USA **89:** 4603.
15. Vega-Saenz de Miera, M. Weiser, C. Kentros, D. Lau, H. Moreno, P. Serodio & B. Rudy. 1994. Shaw-related K^+ channels in mammals. *In* Handbook of Membrane Channels. C. Peracchia, Ed. 41. Academic Press, Inc. Orlando, FL.

16. COETZEE, W.A., Y., J. CHIU, A. CHOW, D. LAU, T. MCCORMACK, T. MORENO, M. NADAL, A. OZAITA, D. POUNTNEY, M. SAGANICH, E. VEGA-SAENZ DE MIERA & B. RUDY. 1999. Molecular diversity of K^+ channels. Ann. N.Y. Acad. Sci. This volume.
17. RASHID, A.J. & R.J. DUNN. 1998. Sequence diversity of voltage-gated potassium channels in an electric fish. Brain Res. Mol. Brain Res. **54:** 101.
18. SPITZER, N.C. & D. GURANTZ. 1996 Xenopus Kv3.3 potassium channel transcripts are developmentally upregulated in the embryonic spinal cord. Soc. Neurosci. Abst. **22:** 1753.
19. KENTROS, C., M. WEISER, E. VEGA-SAENZ DE MIERA, K. MOREL, H. BAKER & B. RUDY. 1992. Alternative splicing of the 5′ untranslated region of a gene encoding K channel components. Soc. Neurosci. Abst. **18**.
20. ERGINEL-UNALTUNA, N., W.P. YANG & M.A. BLANAR. 1998. Genomic organization and expression of KCNJ8/Kir6.1, a gene encoding a subunit of an ATP-sensitive potassium channel. Gene **211:** 71.
21. WEISER, M., E. VEGA-SAENZ DE MIERA, C. KENTROS, H. MORENO, L. FRANZEN, D. HILLMAN, H. BAKER & B. RUDY. 1994. Differential expression of Shaw-related K^+ channels in the rat central nervous system, J. Neurosci. **14:** 949.
22. HOSHI, T., W.N. ZAGOTTA & R.W. ALDRICH. 1990. Biophysical and molecular mechanisms of Shaker potassium channel inactivation [see comments]. Science **250:** 533.
23. SMITH-MAXWELL, C.J., J.L. LEDWELL & R.W. ALDRICH. 1998. Role of the S4 in cooperativity of voltage-dependent potassium channel activation. J. Gen Physiol. **111:** 399.
24. JOHNSTONE, D.B., A. WEI, A. BUTLER, L. SALKOFF & J.H. THOMAS. 1997. Behavioral defects in C. elegans egl-36 mutants result from potassium channels shifted in voltage-dependence of activation, Neuron **19:** 151.
25. HERNÁNDEZ-PINEDA, R., A. CHOW, Y. AMARILLO, H. MORENO, M. SAGANICH, E. VEGA-SAENZ DE MIERA, A. HERNÁNDEZ-CRUZ & B. RUDY. 1999. Kv3.1–Kv3.2 heteromultimeric channels underlie a high voltage-activating component of the delayed rectifier K^+ current in projecting neurons from the Globus Pallidus. J. Neurophysiol. In press.
26. GRISSMER, S., A.N. NGUYEN, J. AIYAR, D.C. HANSON, R.J. MATHER, G.A. GUTMAN, M.J. KARMILOWICZ, D.D. AUPERIN & K.G. CHANDY. 1994. Pharmacological characterization of five cloned voltage-gated K^+ channels, types Kv1.1, 1.2, 1.3, 1.5, and 3.1, stably expressed in mammalian cell lines. Mol. Pharmacol. **45:** 1227.
27. CRITZ, S.D., B.A. WIBLE, H.S. LOPEZ & A.M. BROWN. 1993. Stable expression and regulation of a rat brain K^+ channel, J. Neurochem. **60:** 1175.
28. KALMAN, K., A. NGUYEN, J. TSENG-CRANK, I.D. DUKES, G. CHANDY, C.M. HUSTAD, N.G. COPELAND, N.A. JENKINS, H. MOHRENWEISER, B. BRANDRIFF, M. CAHALAN, G.A. GUTMAN & K.G. CHANDY. 1998. Genomic organization, chromosomal localization, tissue distribution, and biophysical characterization of a novel mammalian Shaker-related voltage-gated potassium channel, Kv1.7. J. Biol. Chem. **273:** 5851.
29. HARRIS, R.E. & E.Y. ISACOFF. 1996. Hydrophobic mutations alter the movement of Mg^{2+} in the pore of voltage-gated potassium channels. Biophys. J. **71:** 209.
30. RUPPERSBERG, J.P., M. STOCKER, O. PONGS, S.H. HEINEMANN, R. FRANK & M. KOENEN. 1991. Regulation of fast inactivation of cloned mammalian IK(A) channels by cysteine oxidation. Nature **352:** 711.
31. VEGA-SAENZ DE MIERA, E. & B. RUDY. 1992. Modulation of K^+ channels by hydrogen peroxide. Biochem. Biophys. Res. Commun. **186:** 1681.
32. SERODIO, P., C. KENTROS & B. RUDY. 1994. Identification of molecular components of A-type channels activating at subthreshold potentials. J. Neurophysiol. **72:** 1516.
33. RUPPERSBERG, J.P., R. FRANK, O. PONGS & M. STOCKER. 1991. Cloned neuronal IK(A) channels reopen during recovery from inactivation [see comments]. Nature **353:** 657.
34. MORENO, H., C. KENTROS, E. BUENO, M. WEISER, A. HERNANDEZ, E. VEGA-SAENZ DE MIERA, A. PONCE, W. THORNHILL & B. RUDY. 1995. Thalamocortical projections have a K^+ channel that is phosphorylated and modulated by cAMP-dependent protein kinase. J. Neurosci. **15:** 5486.
35. MCINTOSH, P., H. MORENO, B. ROBERTSON, & B. RUDY. 1998. Isoform-specific modulation of rat Kv3 potassium channel splice variants. J. Physiol. **511P:** 147.
36. KANEMASA, T., L. GAN, T.M. PERNEY, L.Y. WANG & L.K. KACZMAREK. 1995. Electrophysiological and pharmacological characterization of a mammalian Shaw channel expressed in NIH 3T3 fibroblasts. J. Neurophysiol. **74:** 207.

37. COVARRUBIAS, M., A. WEI, L. SALKOFF & T.B. VYAS. 1994. Elimination of rapid potassium channel inactivation by phosphorylation of the inactivation gate. Neuron **13:** 1403.
38. BECK, E.J., R.G. SORENSEN, S.J. SLATER & M. COVARRUBIAS. 1998. Interactions between multiple phosphorylation sites in the inactivation particle of a K^+ channel. Insights into the molecular mechanism of protein kinase C action. J. Gen. Physiol. **112:** 71.
39. VEGA-SAENZ DE MIERA, E., H. MORENO & B. RUDY. 1994. Modulation of Kv3.3 K^+ channels by oxidation and phosphorylation, in Soc. Neurosci. Abst. **20:** 725.
40. VEGA-SAENZ DE MIERA, E., H. MORENO & B. RUDY. 1995. Phosphorylation may be required to activate Shaw related K^+ channels. Soc. Neurosci. Abst. **21:** 505.
41. MORENO, H., E. BUENO, A. HERNANDEZ CRUZ, A. PONCE & B. RUDY. 1995. Nitric oxide and cGMP modulate a presynaptic K^+ channel *in vitro*. Soc. Neurosci. Abst. **21:** 506.
42. MORENO, H., M.S. NADAL, E. VEGA-SAENZ DE MIERA & B. RUDY. 1999. Modulation of Kv3 potassium channels by a nitric oxide-activated phosphatase. J. Neurosci. Submitted for publication.
43. SHIEH, C.C. & G.E. KIRSCH. 1994. Mutational analysis of ion conduction and drug binding sites in the inner mouth of voltage-gated K^+ channels. Biophys. J. **67:** 2316.
44. KIRSCH, G.E. & J.A. DREWE. 1993. Gating-dependent mechanism of 4-aminopyridine block in two related potassium channels. J. Gen. Physiol. **102:** 797.
45. CHANDY, K.G. & G.A. GUTMAN. 1995. Voltage gated channels. *In* Handbook of Receptors and Channels: Ligand-gated and Voltage-gated Ion Channels. R.A. North, Ed.: 1–71. Boca Raton, FL.
46. BARISH, M.E., M. ICHIKAWA, T. TOMINAGA, G. MATSUMOTO & T. IIJIMA. 1996. Enhanced fast synaptic transmission and a delayed depolarization induced by transient potassium current blockade in rat hippocampal slice as studied by optical recording. J. Neurosci. **16:** 5672.
47. WU, R.L. & M.E. BARISH. 1992. Two pharmacologically and kinetically distinct transient potassium currents in cultured embryonic mouse hippocampal neurons. J. Neurosci. **12:** 2235.
48. DIOCHOT, S., H. SCHWEITZ, L. BERESS & M. LAZDUNSKI. 1998. Sea anemone peptides with a specific blocking activity against the fast inactivating potassium channel Kv3.4. J. Biol. Chem. **273:** 6744.
49. MCCORMACH, K., J.W. LIN, L.E. IVERSON & B. RUDY. 1990. Shaker K^+ channel subunits from heteromultimeric channels with novel functional properties. Biochem. Biophys. Res. Commun. **171:** 1361.
50. ISACOFF, E.Y., Y.N. JAN & L.Y. JAN. 1990. Evidence for the formation of heteromultimeric potassium channels in Xenopus oocytes [see comments]. Nature **345:** 530.
51. RUPPERSBERG, J.P., K.H. SCHROTER, B. SAKMANN, M. STOCKER, S. SEWING & O. PONGS. 1990. Heteromultimeric channels formed by rat brain potassium-channel proteins [see comments]. Nature **345:** 535.
52. MACKINNON, R. 1991. Determination of the subunit stoichiometry of a voltage-activated potassium channel. Nature **350:** 232.
53. CHRISTIE, M.J., R.A. NORTH, P.B. OSBORNE, J. DOUGLASS & J.P. ADELMAN. 1990. Heteropolymeric potassium channels expressed in Xenopus oocytes from cloned subunits. Neuron **4:** 405.
54. DIXON, J.E. & D. MCKINNON. 1994. Quantitative analysis of potassium channel mRNA expression in atrial and ventricular muscle of rats. Circ. Res. **75:** 252.
55. BRAHMAJOTHI, M.V., M.J. MORALES, R.L. RASMUSSON, D.L. CAMPBELL & H.C. STRAUSS. 1997. Heterogeneity in K^+ channel transcript expression detected in isolated ferret cardiac myocytes. Pacing Clin. Electrophysiol. **20:** 388.
56. DIXON, J.E. & D. MCKINNON. 1996. Potassium channel mRNA expression in prevertebral and paravertebral sympathetic neurons. Eur. J. Neurosci. **8:** 183.
57. GRISSMER, S., S. GHANSHANI, B. DETHLEFS, J.D. MCPHERSON, J.J. WASMUTH, G.A. GUTMAN, M.D. CAHALAN & K.G. CHANDY. 1992. The Shaw-related potassium channel gene, Kv3.1, on human chromosome 11, encodes the type 1 K^+ channel in T cells. J. Biol. Chem. **267:** 20971.
58. ROE, M.W., J.F. WORLEY, III, A.A. MITTAL, A. KUZNETSOV, S. DASGUPTA, R.J. MERTZ, S.M. WITHERSPOON, III, N. BLAIR, M.E. LANCASTER, M.S. MCINTYRE, W.R. SHEHEE, I.D. DUKES & L.H. PHILIPSON. 1996. Expression and function of pancreatic beta-cell delayed rectifier K^+ channels. Role in stimulus-secretion coupling. J. Biol. Chem. **271:** 32241.
59. PERNEY, T.M., J. MARSHALL, K.A. MARTIN, S. HOCKFIELD & L.K. KACZMAREK. 1992. Expression of the mRNAs for the Kv3.1 potassium channel gene in the adult and developing rat brain, J. Neurophysiol. **68:** 756.

60. DREWE, J.A., S. VERMA, G. FRECH & R.H. JOHO. 1992. Distinct spatial and temporal expression patterns of K^+ channel mRNAs from different subfamilies. J. Neurosci. **12:** 538.
61. NGUYEN, T.D. & G. JESERICH. 1998. Molecular structure and expression of shaker type potassium channels in glial cells of trout CNS. Neurosci. Res. **51:** 284.
62. CHOW, A., A. ERISIR, C. FARB, D.H.P. LAU & B. RUDY. 1998. Kv3.1 and Kv3.2 proteins distingish three subpopulations of GABA-ergic interneurons in the mouse cortex. Soc. Neurosci. Abst. **24:** 1579.
63. CHOW, A., C. FARB, A. ERISIR, D. LAU & B. RUDY. 1999. K^+ channel expression distinguishes between two subpopulations of parvalbumin-containing cortical interneurons. J. Neurosci. Submitted for publication.
64. OZAITA, A., E. VEGA-SAENZ DE MIERA, A. CHOW, T.R. MUTH, M.J. CAPLAN & B. RUDY. 1998. Differential targeting of Kv3.1–Kv3.2 containing potassium channels produced by alternatively-spliced C-termini. Soc. Neurosci. Abst. **24:** 1580.
65. OZAITA, A., A. CHOW, M. MARTONE, M. ELLISMAN, E. VEGA-SAENZ DE MIERA & B. RUDY. 1999. Differential subcellular localization of the two Kv3.1 K^+ channel alternatively-spliced isoforms in brain neurons. J. Neurosci. Submitted for publication.
66. WEISER, M., E. BUENO, C. SEKIRNJAK, M.E. MARTONE, H. BAKER, D. HILLMAN, S. CHEN, W. THORNHILL, M. ELLISMAN & B. RUDY. 1995. THe potassium channel subunit Kv3.1b is localized to somatic and axonal membranes of specific populations of CNS neurons. J. Neurosci. **15:** 4298.
67. SEKIRNJAK, C., M.E. MARTONE, M. WEISER, T. DEERINCK, E. BUENO, B. RUDY & M. ELLISMAN. 1997. Subcellular localization of the K^+ channel subunit Kv3.1b in selected rat CNS neurons. Brain Res. **766:** 173.
68. DU J., L. ZHANG, M. WEISER, B. RUDY & C.J. MCBAIN. 1996. Developmental expression and functional characterization of the potassium-channel subunit Kv3.1b in parvalbumin-containing interneurons of the rat hippocampus. J. Neurosci. **16:** 506.
69. LENZ, S., T.M. PERNEY, Y. QIN, E. ROBBINS & M.F. CHESSELET. 1994. GABA-ergic interneurons of the striatum express the Shaw-like potassium channel Kv3.1. Synapse **18:** 55.
70. PERNEY, T.M. & L.K. KACZMAREK. 1997. Localization of a high threshold potassium channel in the rat cochlear nucleus. J. Comp. Neurol. **386:** 178.
71. SHENG, M., Y.J. LIAO, Y.N. JAN & L.Y. JAN. 1993. Presynaptic A-current based on heteromultimeric K^+ channels detected *in vivo*. Nature **365:** 72.
72. WANG, H., D.D. KUNKEL, T.M. MARTIN, P.A. SCHWARTZKROIN & B.L. TEMPEL. 1993. Heteromultimeric K^+ channels in terminal and juxtaparanodal regions of neurons. Nature **365:** 75.
73. VEH, R. W., R. LICHTINGHAGEN, S. SEWING, F. WUNDER, I.M. GRUMBACH & O. PONGS. 1995. Immunohistochemical localization of five members of the Kv1 channel subunits: Contrasting subcellular locations and neuron-specific co-localizations in rat brain. Eur. J. Neurosci. **7:** 2189.
74. LAUBE, G., J. ROPER, J.C. PITT, S. SEWING, U. KISTNER, C.C. GARNER, O. PONGS & R.W. VEH. 1996. Ultrastructural localization of Shaker-related potassium channel subunits and synapse-associated protein 90 to septate-like junctions in rat cerebellar Pinceaux. Mol. Brain Res. **42:** 51.
75. BUENO, E., D.H.P. LAU, A. CHOW, S. CHEN, G. RAMEAU, C. SEKIRNJAK, M.E. MARTONE, M. ELLISMAN, D. HILLMAN, B. RUDY & W. THORNHILL. 1995. Developmental expression of Kv3.2, Kv3.1, and GIRK K^+ channel proteins in the mammalian CNS. Soc. Neurosci. Abst. **21:** 1329.
76. KENTROS, C. 1996. The expression of the Kv3.2 gene. Ph.D. thesis. New York University Medical School, New York.
77. VULLHORST, D., R. KLOCKE, J.W. BARTSCH & H. JOCKUSCH. 1998. Expression of the potassium channel Kv3.4 in mouse skeletal muscle parallels fiber type maturation and depends on excitation pattern. FEBS Lett. **421:** 259.
78. DELONG, M.R. 1971. Activity of pallidal neurons during movement. J. Neurophysiol. **34:** 414.
79. CHUDLER, E.H. & W.K. DONG. 1995. The role of the basal ganglia in nociception and pain. Pain **60:** 3.
80. HAUBER, W., S. LUTZ, & M. MUNKLE. 1998. The effects of globus pallidus lesions on dopamine-dependent motor behaviour in rats. Neuroscience **86:** 147.
81. HERNANDEZ-PINEDA, R., H.-C. A., H. MORENO, A. CHOW & B. RUDY. 1996. Identification of voltage-gated K^+ channels containing Kv3 subunits in neurons from the globus pallidus. Soc. Neurosci. Abst. **22:** 1754.

82. STEFANI, A., P. CALABRESI, N.B. MERCURI & G. BERNARDI. 1992. A-current in rat globus pallidus: A whole-cell voltage clamp study on acutely dissociated neurons. Neurosci. Lett. **144:** 4.
83. STEFANI, A., A. PISANI, A. BONCI, F. STRATTA & G. BERNARDI. 1995. Outward potassium currents activated by depolarization in rat globus pallidus. Synapse **20:** 131.
84. WANG, L.Y., L. GAN, I.D. FORSYTHE & L.K. KACZMAREK. 1998. Contribution of the Kv3.1 potassium channel to high-frequency firing in mouse auditory neurones. J. Physiol. (London) **509:** 183.
85. MASSENGILL, J.L., M.A. SMITH, D.I. SON & D.K. O'DOWD. 1997. Differential expression of K4-AP currents and Kv3.1 potassium channel transcripts in cortical neurons that develop distinct firing phenotypes. J. Neurosci. **17:** 3136.
86. SILLITO, A.M. 1984. Functional consideration of the operation of GABAergic inhibitory process in the visual cortex. *In* Cerebral Cortex. Vol. 2, A.P. Jones, E.G., Ed.: 107. Plenum Press. New York and London.
87. GILBERT, C.D. 1993. Circuitry, architecture, and functional dynamics of visual cortex. Cereb. Cortex **3:** 373.
88. JONES, E.G. 1993. GABAergic neurons and their role in cortical plasticity in primates. Cereb. Cortex **3:** 361.
89. STERIADE, M., A. NUNEZ & F. AMZICA. 1993. A novel slow (1 Hz) oscillation of neocortical neurons in vivo: Depolarizing and hyperpolarizing components. J. Neurosci. **13:** 3252.
90. JEFFERYS, J.G., R.D. TRAUB & M.A. WHITTINGTON. 1996. Neuronal networks for induced '40 Hz' rhythms [see comments]. Trends Neurosci. **19:** 202.
91. JACOBS, K.M. & J.P. DONOGHUE. 1991. Reshaping the cortical motor map by unmasking latent intracortical connections. Science **251:** 944.
92. STERIADE, M. 1997. Synchronized activities of coupled oscillators in the cerebral cortex and thalamus at different levels of vigilance [published erratum appears in Cereb. Cortex 1997 Dec; **7(8):** 779], Cereb. Cortex **7:** 583.
93. ERISIR, A., D. LAU, B. RUDY & C.S. LEONARD. 1998. Low TEA concentration disrupts high frequency firing of fast spiking cells in mouse somatosensory cortex. Soc. Neurosci. Abst. **24:** 632.
94. ERISIR, A., D. LAU, B. RUDY & C.S. LEONARD. 1999. Contrasting effects on high frequency firing of fast spiking cortical interneurons produced by differential K^+ channel blockade, J. Neuroscience. Submitted for publication.
95. YANG, W.P., P.C. LEVESQUE, W.A. LITTLE, M.L. CONDER, P. RAMAKRISHNAN, M.G. NEUBAUER & M.A. BLANAR. 1998. Functional expression of two KvLQT1-related potassium channels responsible for an inherited idiopathic epilepsy. J. Biol. Chem. **273:** 19419.
96. RALEIGH, R. 1907. On our perception of sound direction. Phylosophical Magazine **13:** 214–232.
97. BREW, H.M. & I.D. FORSYTHE. 1995. Two voltage-dependent K^+ conductances with complementary functions in postsynaptic integration at a central auditory synapse. J. Neurosci. **15:** 8011.
98. WANG, L.Y. & L.K. KACZMAREK. 1998. High-frequency firing helps replenish the readily releasable pool of synaptic vesicles. Nature **394:** 384.
99. NAMBU, A. & R. LLINAS. 1994. Electrophysiology of globus pallidus neurons in vitro. J. Neurophysiol. **72:** 1127.
100. NAMBU, A. & R. LLINAS. 1997. Morphology of globus pallidus neurons: its correlation with electrophysiology in guinea pig brain slices [published erratum appears in J. Comp. Neurol. 1997 Mar 31; **380(1):** 154], J. Comp. Neurol. **377:** 85.
101. KITA, H. & S.T. KITAI. 1991. Intracellular study of rat globus pallidus neurons: Membrane properties and responses to neostriatal, subthalamic and nigral stimulation. Brain Res. **564:** 296.
102. KLEIN, M., J. CAMARDO & E.R. KANDEL. 1982. Serotonin modulates a specific potassium current in the sensory neurons that show presynaptic facilitation in Aplysia. Proc. Natl. Acad. Sci. USA **79:** 5713.
103. AUGUSTINE, G.J. 1990. Regulation of transmitter release at the squid giant synapse by presynaptic delayed rectifier potassium current. J. Physiol. (London) **431:** 343.
104. JACKSON, M.B., A. KONNERTH & G.J. AUGUSTINE. 1991. Action potential broadening and frequency-dependent facilitation of calcium signals in pituitary nerve terminals. Proc. Natl. Acad. Sci. USA **88:** 380.

105. ROBERTS, W.M., R.A. JACOBS & A.J. HUDSPETH. 1990. Colocalization of ion channels involved in frequency selectivity and synaptic transmission at presynaptic active zones of hair cells. J. Neurosci. **10:** 3664.
106. ANDERSON, A.J. & A.L. HARVEY. 1988. Effects of the facilitatory compounds catechol, guanidine, noradrenaline and phencyclidine on presynaptic currents of mouse motor nerve terminals. Naunyn Schmiedebergs Arch. Pharmacol. **338:** 133.
107. VAUGHAN, C.W., S.L. INGRAM, M.A. CONNOR & M.J. CHRISTIE. 1997. How opioids inhibit GABA-mediated neurotransmission [see comments]. Nature **390:** 611.
108. COLMERS, W.F., K. LUKOWIAK & Q.J. PITTMAN. 1988. Neuropeptide Y action in the rat hippocampal slice: Site and mechanism of presynaptic inhibition. J. Neurosci. **8:** 3827.
109. SOUTHAN, A.P. & D.G. OWEN. 1997. The contrasting effects of dendrotoxins and other potassium channel blockers in the CA1 and dentate gyrus regions of rat hippocampal slices. Br. J. Pharmacol. **122:** 335.
110. HARVEY, A.L. & A.J. ANDERSON. 1985. Dendrotoxins: Snake toxins that block potassium channels and facilitate neurotransmitter release. Pharmacol. Ther. **31:** 33.
111. ROBITAILLE, R. & M.P. CHARLTON. 1992. Presynaptic calcium signals and transmitter release are modulated by calcium-activated potassium channels. J. Neurosci. **12:** 297.
112. WHEELER, D.B., A. RANDALL & R.W. TSIEN. 1996. Changes in action potential duration alter reliance of excitatory synaptic transmission on multiple types of Ca^{2+} channels in rat hippocampus. J. Neurosci. **16:** 2226.
113. DEBANNE, D., N.C. GUERINEAU, B.H. GAHWILER & S.M. THOMPSON. 1997. Action-potential propagation gated by an axonal I(A)-like K^+ conductance in hippocampus [published erratum appears in Nature 1997 Dec 4; **390:** 536]. Nature **389:** 286.
114. PONCE, A., E. VEGA-SAENZ DE MIERA, C. KENTROS, H. MORENO, B. THORNHILL & B. RUDY. 1997. K^+ channel subunit isoforms with divergent carboxy-terminal sequences carry distinct membrane targeting signals. J. Membr. Biol. **159:** 149.
115. LAU, D., M. CASTRO-ALAMANCOS, A. CHOW, A. OZAITA, E. VEGA-SAENZ DE MEIRA, S. MATHEW, J. GIBSON, B. CONNORS & B. RUDY. 1998. Targeted disruption in mouse of a voltage-gated potassium channel gene that is expressed predominantly in the thalamocortical system. J. Physiol. **511P:** 147.
116. LAU, D., M. CASTRO-ALAMANCOS, A. CHOW, A. OZAITA, E. VEGA-SAENZ DE MIERA, S. MATHEW, J. GIBSON, B.W. CONNORS & B. RUDY. 1998. Targeted disruption of a K^+ channel gene that is principally expressed in the presynaptic terminals of thalamic relay neurons in mice. Soc. Neurosci. Abst. **24:** 128.
117. HO, C.S., R.W. GRANE & R.H. JOHO. 1997. Pleiotropic effects of a disrupted K^+ channel gene: Reduced body weight, impaired motor skill and muscle contraction, but no seizures. Proc. Natl. Acad. Sci. USA **94:** 1533.
118. CHAN, E. 1997. Regulation and function of Kv3.3. Ph.D. thesis. Rockefeller University, New York.
119. JOHO, R.H., C.S. HO & G.A. MARKS. 1998. Increase in gamma oscillations and altered learning performance in a mouse deficient for the K^+ channel Kv3.1. Soc. Neurosci. **24:** 828.

Kv3.4 subunits enhance the repolarizing efficiency of Kv3.1 channels in fast-spiking neurons

Gytis Baranauskas[1,3], Tatiana Tkatch[1], Keiichi Nagata[2], Jay Z. Yeh[2] and D. James Surmeier[1]

[1] *Department of Physiology and* [2] *Departments of Molecular Pharmacology and Biological Chemistry, Feinberg School of Medicine, 303 E. Chicago Ave., Northwestern University, Chicago, Illinois 60611, USA*

[3] *Present address: Psychiatric Institute, Department of Psychiatry, University of Illinois at Chicago, Chicago, Illinois 60612, USA*

The first two authors contributed equally to this work.

Correspondence should be addressed to D.J.S. (j-surmeier@northwestern.edu)

Published online 18 February 2003; doi:10.1038/nn1019

Neurons with the capacity to discharge at high rates—'fast-spiking' (FS) neurons—are critical participants in central motor and sensory circuits. It is widely accepted that K^+ channels with Kv3.1 or Kv3.2 subunits underlie fast, delayed-rectifier (DR) currents that endow neurons with this FS ability. Expression of these subunits in heterologous systems, however, yields channels that open at more depolarized potentials than do native Kv3 family channels, suggesting that they differ. One possibility is that native channels incorporate a subunit that modifies gating. Molecular, electrophysiological and pharmacological studies reported here suggest that a splice variant of the Kv3.4 subunit coassembles with Kv3.1 subunits in rat brain FS neurons. Coassembly enhances the spike repolarizing efficiency of the channels, thereby reducing spike duration and enabling higher repetitive spike rates. These results suggest that manipulation of K3.4 subunit expression could be a useful means of controlling the dynamic range of FS neurons.

Since the time of Hodgkin and Huxley, delayed-rectifier (DR) currents have been known to be primary determinants of spike repolarization in neurons[1,2]. Recently, it has become clear that these currents are heterogeneous with properties tailored to the signaling and computational needs of particular neuronal classes. One group of neurons that has drawn a great deal of attention in this regard is the 'fast-spiking' (FS) class. These neurons can discharge at high rates for long periods with little spike frequency adaptation or attenuation in spike height. This property of FS neurons is attributable in large measure to their expression of fast DR channels—channels that activate and deactivate very quickly[3].

At present, only Kv3-family potassium channels produce currents similar to those seen in neurons that spike at high rates[3,4]. There are four members of this family; two of them, Kv3.1 and Kv3.2, produce currents in heterologous expression systems resembling neuronal fast DR currents. Both channels activate only at depolarized membrane potentials and have rapid activation and deactivation kinetics. Both are very sensitive to tetraethylammonium (TEA) and 4-aminopyridine, as are fast DR currents in neurons[5,6]. The discovery that Kv3.1 and/or Kv3.2 genes are expressed in FS neurons prompted early suggestions that Kv3 channels are responsible for fast DR currents[7–9]. Subsequent studies, ranging from modeling to electrophysiological analysis of knockout animals, unambiguously support the conclusion that FS neurons depend on K^+ channels containing Kv3.1 or Kv3.2 subunits.

However, there is a major problem with this story. In FS neurons, the fast DR currents begin to activate near –30 mV with half-activation voltages between –18 and –7 mV[10,11]. In heterologous expression systems, Kv3.1/3.2 channel activation voltage dependence is much more depolarized with half-activation voltages well above 0 mV[12]. This is a critical difference. With the voltage dependence and activation kinetics seen in heterologous systems, only a small fraction of Kv3.1/2 channels will open during a spike, making them very inefficient mediators of fast repolarization. Theoretical studies suggest there are two ways to deal with the problem. One strategy is to increase Kv3 current density to levels not seen in neurons[13]. The other strategy is to shift the voltage dependence of the Kv3 current toward more negative potentials, increasing the efficiency of the channels in spike repolarization, as seen in neurons[3].

If Kv3 channels are responsible for DR currents in FS neurons, then how can the differences in gating between native and heterologous channels be explained? One possibility is that native channels are heteromeric and contain subunits not found in heterologous systems. Four members of the Kv3 class—Kv3.1, 3.2, 3.3 and 3.4—are known to coassemble. The experiments reported here argue that the incorporation of a splice variant of the Kv3.4 subunit transforms Kv3.1 channels, giving them gating properties very similar to those found in FS neurons. Furthermore, molecular, biochemical and pharmacological data suggest that this splice variant coassembles with Kv3.1 subunits in FS neurons, increasing their efficiency in promoting spike repolarization and repetitive firing.

Results

Kv3.1 homomeric channels differ from FS channels

We studied three types of neuron, identified by single-cell RT-PCR (scRT-PCR), in which Kv3 channel currents are thought to be key

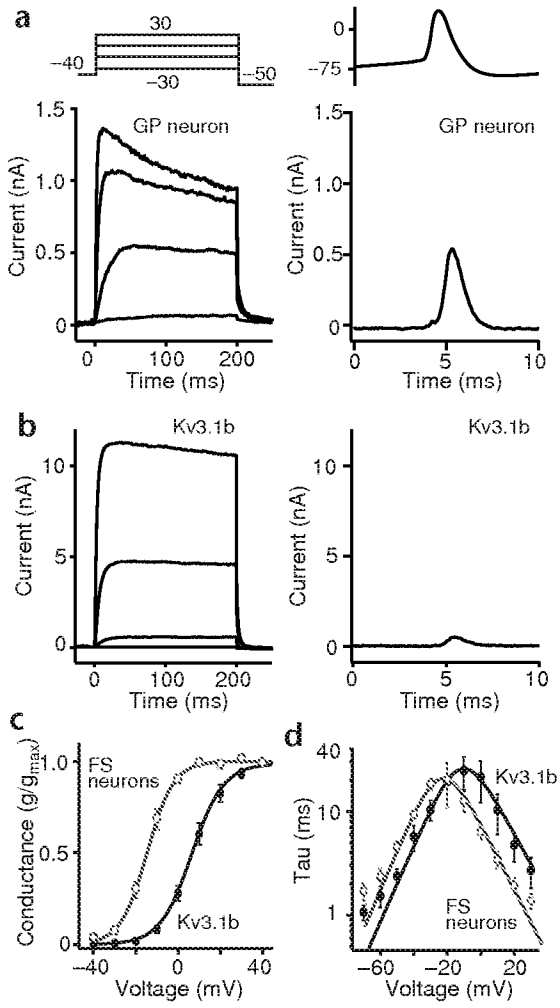

Fig. 1. In contrast to currents in FS neurons, Kv3.1b channel currents are inefficiently activated by spike waveforms. (**a**) Fast DR currents in a GP neuron evoked by voltage steps (left) or a spike waveform (right). Currents shown were obtained from control currents by subtracting the currents not blocked by 150 μM TEA. (**b**) Currents in HEK293 cells transfected with Kv3.1b cDNA. Currents were leak subtracted. (**c**) Activation voltage dependence of the currents obtained in transfected HEK293 cells (open circles, $n = 8$) and of the TEA-sensitive current in neurons (filled circles, GP and hippocampal interneurons, pooled data, $n = 8$). Data were fit with first-order Boltzmann function; fitted parameters for Kv3.1b currents were: $V_h = 7$ mV, $V_c = 7.5$ mV; for neurons the parameters were: $V_h = -15$ mV, $V_c = 6.3$ mV. (**d**) Time constants of activation and deactivation plotted as a function of voltage. Data were fit with a two-state Markov model.

regulators of repetitive activity: (i) parvalbumin-expressing, GABAergic, globus pallidus (GP) neurons, (ii) parvalbumin-expressing, GABAergic CA1 hippocampal interneurons and (iii) glutamatergic subthalamic nucleus (STN) neurons[10,11,14]. All three types of neuron are capable of sustained high-frequency (>100 Hz) discharge without significant accommodation and will be referred to as fast-spiking (FS). A key feature of Kv3 channel currents in these neurons is their activation during the upstroke of the spike, leading to rapid repolarization of the membrane potential and brief spikes. The ability to be activated efficiently during the upstroke of the spike depends on the voltage at which channels begins to open and the rate at which they enter the open state. In FS neurons, TEA-sensitive Kv3 channels begin to activate just above spike threshold (around −30 mV) (**Fig. 1a** (left) and **c**). A spike waveform obtained from an FS neuron at the same temperature does an excellent job of activating these channels and evoking current (**Fig. 1a**, right). To quantify the relative repolarizing efficiency of native channels, the amplitude of the current evoked by the spike waveform was divided by the amplitude of the current evoked by a long step to the voltage reached by the peak of the action potential (+30 mV). On average, the repolarizing efficiency of fast, Kv3 DR channels in FS neurons was 0.42 ± 0.03 ($n = 6$).

In contrast, homomeric Kv3.1b channels expressed in HEK293 cells yielded K^+ currents that activated at relatively depolarized membrane potentials (**Fig. 1b**). The same action potential waveform evoked little Kv3.1b current (**Fig. 1b**, right). On average, the efficiency of Kv3.1b current was 0.09 ± 0.02 ($n = 4$)—one-fourth that of Kv3 channel currents in FS neurons.

There were two obvious reasons for the greater efficiency of the neuronal channels. First, as mentioned, the Kv3 channels in FS neurons activated at significantly more negative membrane potentials than did homomeric Kv3.1b channels. The steady-state half-activation voltage of Kv3 channels in FS neurons was around −15 mV, whereas it was near +7 mV for Kv3.1b channels—a 22-mV difference (**Fig. 1c**). Second, the negative shift in the voltage dependence of activation was paralleled by a shift in activation kinetics. At depolarized membrane potentials, the relationship between membrane voltage and activation time constant in FS neurons was shifted by about the same amount (18 mV) as the steady-state activation curves (**Fig. 1d**). This led to a significant acceleration in the opening of neuronal Kv3 channels during the upstroke of the spike (between −20 and 30 mV).

FS neurons coexpress Kv3.1 and Kv3.4a subunits

In agreement with *in situ* hybridization work[8], scRT-PCR studies by our group had shown that GABAergic GP neurons expressed Kv3.1 mRNA and TEA-sensitive, fast DR channels[11]. As a first step toward understanding the origin of the biophysical difference between these channels and Kv3.1 homomeric channels, scRT-PCR profiling of these neurons was expanded to include the other members of the Kv3 family: Kv3.3 and Kv3.4. Kv3.3 mRNA was rarely detected in GP neurons. But, as shown for the cell in **Fig. 2a**, GABAergic GP neurons consistently expressed both Kv3.1 and Kv3.4 mRNAs. Kv3.4 mRNA was detected in 96% (45/47) of our GP sample. In fact, GP neurons coexpressed two of the three known Kv3.4 splice variants. These splice variants appeared as a small ('c' variant, 460 bp) and a large ('a' variant, 522 bp) amplicon in the scRT-PCR profiles (**Fig. 2a**). Sequencing verified their identity. Both Kv3.4 mRNAs were relatively abundant in these neurons and could be reliably detected with as little as 10% of the total cellular cDNA. To determine if this expression pattern was peculiar to GP FS neurons, other cell types were profiled (**Fig. 2b**). To our surprise, Kv3.4 mRNA was reliably detected in all the FS neurons examined; STN neurons (100%, 13/13), hippocampal parvalbumin GABAergic interneurons (100%, 8/8) and inferior collicular neurons (100%, 7/7) all expressed Kv3.4 mRNA. Moreover, in all of these cell types, Kv3.4 was abundant with detection requiring as little as 10% of the total cellular cDNA. In contrast, Kv3.4 mRNA was not detected in neurons that did not show FS behavior. scRT-PCR profiling of striatal cholinergic interneurons ($n = 27$), of striatal medium spiny neurons ($n = 8$), of basal forebrain cholinergic neurons ($n = 37$) and of pyramidal neurons (from

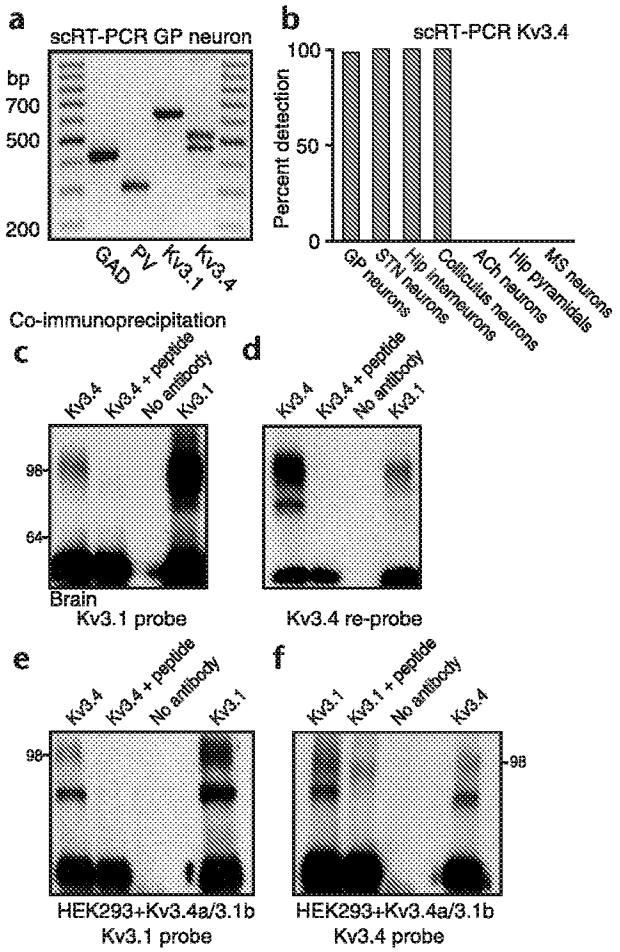

Fig. 2. FS neurons coexpress Kv3.1 and Kv3.4a mRNA and these subunits coassemble. (**a**) A representative gel from a parvalbumin-positive GP neuron that had detectable levels of GAD67, parvalbumin, and Kv3.4a and Kv3.4c mRNAs. Two Kv3.4 splice variants (Kv3.4a and Kv3.4c) are represented by two bands in the gel. The upper band of 522 base pairs corresponds to Kv3.4a and the lower band of 460 base pairs correspond to Kv3.4c. The identity of PCR products was verified by sequencing. (**b**) Bar graph summarizing the detection of Kv3.4 mRNA in various neuronal populations. GP, globus pallidus; STN, subthalamic nucleus; Hip, hippocampus; ACh, cholinergic; MS, medium spiny. (**c**) Detection of Kv3.1b protein in anti-Kv3.4 immunoprecipitates of detergent lysate of adult rat brain membranes (left panel). Membranes (0.2 mg) were precipitated with Kv3.4 antibody (left lane), Kv3.4 antibody pre-incubated with immunogenic Kv3.4 peptide (second lane), in the absence of any antibody (third lane) and with Kv3.1 antibody (right lane). Resulting blot was probed with Kv3.1b antibodies. (**d**) The blot was stripped and reprobed with Kv3.4 antibody. (**e**) Detection of Kv3.1b protein in anti-Kv3.4 immunoprecipitates of membrane extracts from HEK293 cells transfected with Kv3.1b and Kv3.4a cDNAs. Membranes were precipitated with Kv3.4 antibody (left lane), Kv3.4 antibody pre-incubated with immunogenic Kv3.4 peptide (second lane), in the absence of any antibody (third lane) and with Kv3.1 antibody (right lane). Resulting blot was probed with Kv3.1b antibodies. (**f**) Detection of Kv3.4 protein in anti-Kv3.1b immunoprecipitates of membrane extracts from HEK293 cells transfected with Kv3.1b and Kv3.4a cDNAs. Membranes were precipitated with Kv3.1b antibody (left lane), Kv3.1b antibody pre-incubated with immunogenic peptide (second lane), in the absence of any antibody (third lane) and with Kv3.4 antibody (right lane). Resulting blot was probed with Kv3.4 antibodies.

hippocampus; $n = 10$) did not detect Kv3.4 mRNA, even with up to 50% of the total cellular cDNA as a template.

The coexpression of Kv3.4 and Kv3.1 mRNAs in FS neurons raises the possibility that they form heteromers, resulting in channels with altered properties. To determine whether these subunits coassembled, we attempted to immunoprecipitate Kv3.1 protein with an antibody to the Kv3.4 subunit. Kv3.1b protein was detected in brain membranes precipitated with Kv3.4 antibody (Fig. 2c, left lane) but was absent when Kv3.4 antibody was pretreated with Kv3.4 peptide or if the antibody was omitted (Fig. 2c, middle lanes). Kv3.1b protein was not detected in brain membranes precipitated with Kv4.2 antibody (data not shown). Stripping and re-probing the same western blot with Kv3.4 antibody confirmed the association of Kv3.1b and Kv3.4 protein in a significant fraction of channels, as Kv3.1b precipitates were labeled by Kv3.4 antibody (Fig. 2d, right lane). Kv3.4 and Kv3.1 subunits also coassembled when expressed in HEK293 cells. Membrane protein precipitated with Kv3.4 antibodies from HEK293 cells co-transfected with Kv3.1b and Kv3.4a cDNA was recognized by the Kv3.1 probe (Fig. 2e). Conversely, Kv3.1 precipitates from these co-transfected cells were recognized by the Kv3.4 antibody (Fig. 2f). The antibodies did not cross-react, as transfection of HEK293 with a single subunit resulted in protein that was only recognized by the appropriate antibody (data not shown). Taken together, these results show that FS neurons coexpress Kv3.1 and Kv3.4 mRNA, and that these channel subunits coassemble.

Kv3.4a shifts the voltage dependence of Kv3 channels

If the key features of Kv3 channels in FS neurons depend solely upon coassembly of Kv3.4 and Kv3.1 subunits, then expression of just these subunits in a heterologous system should yield K^+ currents like those found in FS neurons. To test this hypothesis, Kv3.1 and Kv3.4 subunits were cloned and expressed in HEK293 cells. Expression of Kv3.4a subunits in HEK293 cells yielded currents that were activated rapidly and then inactivated (Fig. 3a), as described previously for Kv3.4 channels[3,15,16]. At 10 mV, the Kv3.4a currents decayed mono-exponentially with a time constant of 20 ± 5 ms ($n = 4$). However, unlike previous descriptions, Kv3.4a channels activated at relatively hyperpolarized membrane potentials, having a steady-state half-activation voltage (–15 mV) near that found for Kv3 currents in FS neurons (Fig. 3b). This relatively hyperpolarized activation voltage dependence was isoform-specific, as the activation profile of Kv3.4c channels resembled that previously found for Kv3.4b channels (data not shown)[3]. Homomeric Kv3.4a channels also had faster activation kinetics than did Kv3 channels in FS neurons (Fig. 3a).

Coexpression of Kv3.4a and Kv3.1b cDNA in HEK293 cells produced K^+ currents with properties resembling those of Kv3 channels in FS neurons. The K^+ currents in co-transfected HEK293 cells activated rapidly at relatively negative membrane potentials and were efficiently activated by a spike waveform (Fig. 4a). These currents also were blocked at micromolar concentrations of TEA, as are Kv3 channel currents in neurons (data not shown). Importantly, as predicted by the co-immunoprecipitation data, the biophysical features of currents in co-transfected cells could not be attributed to a sum of homomeric Kv3.1b and Kv3.4a channel currents. With strong depolarization, currents activated rapidly and then inactivated ($n = 9$). In most cells (67%), inactivation had a fast component in addition to a ubiquitous slow component. In these cells, the fast inactivation time constant was 38 ± 9 ms (52 ± 4% of total peak current at +10 mV)—twice that seen with 3.4a homomeric channels at the

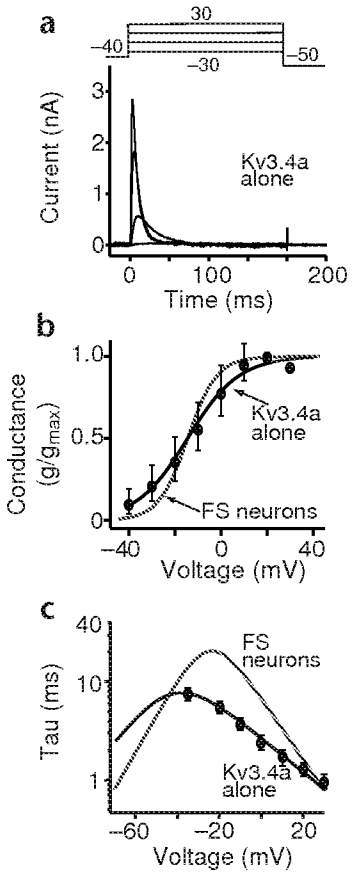

Fig. 3. Kv3.4a channels activate at more negative membrane potentials than do Kv3.1b channels. (**a**) Current recorded in a HEK293 cell after Kv3.4a DNA transfection. Voltage protocol is shown at the top. (**b**) Summary of voltage dependence of Kv3.4a current (open circles, $n = 4$). Boltzmann fit parameters were $V_h = -15$ mV, $V_c = 11$ mV. A Boltzmann fit of fast DR currents (**Fig. 1c**) is shown in red. (**c**) Activation time constants are plotted as a function of voltage (open circles) and fit as in **Fig. 1**. For comparison, the fit of the FS neuronal data is shown in red.

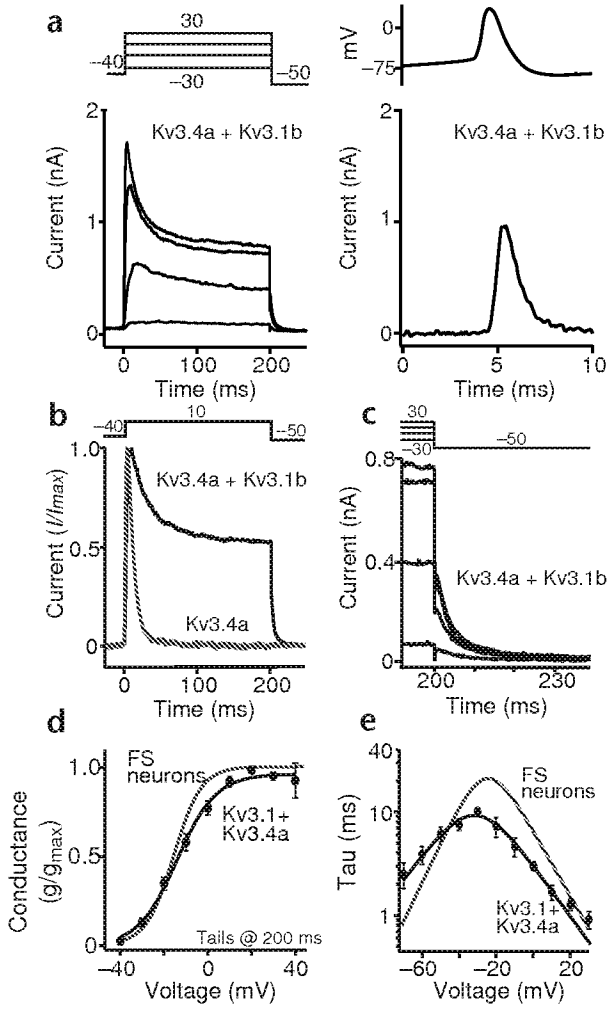

Fig. 4. Kv3.4a + Kv3.1b heteromeric channels produce currents with properties resembling those seen in neurons. (**a**) Currents evoked in HEK293 cells co-transfected with Kv3.4a and Kv3.1b cDNAs. Currents were evoked by voltage steps (left) or a spike waveform (right). Currents were leak subtracted. In most cells (6/9), current inactivation could be fit with fast and slow exponentials; the amplitude of the fast component never exceeded 50% of the total current. (**b**) Overlay of currents evoked in HEK293 cells expressing Kv3.1b and Kv3.4a subunits (black) with those from HEK293 cells expressing only Kv3.4a subunits (green). Currents were normalized by the peak current in each to facilitate comparison of time courses. (**c**) Tail currents from (**a**) on an expanded time scale. Note that tail currents are clearly present with a test step to −30 mV. (**d**) Activation voltage dependence of the Kv3.4a/3.1b heteromeric channels determined from the tail currents at the end of a 200-ms test step ($n = 9$). Means are shown as a function of the preceding step voltage; data were then fitted with a first-order Boltzmann function. Fitted parameters were $V_h = -14$ mV, $V_c = 10.3$ mV. The Boltzmann fit from the neuronal data is shown in red. (**e**) Activation (above −25 mV) and deactivation (below −25 mV) time constants are plotted as a function of voltage; data were fit as above. The fit to the neuronal data is shown in red.

same membrane potential. Although dissimilar to that of homomeric channel currents, this time constant is very close to that seen in FS GP neurons at similar potentials (38 ± 8 ms; 38 ± 3% of total current at +30 mV, $n = 5$). To see if this resemblance extended to activation voltage dependence, two types of measurement were taken. First, peak currents were measured, converted to conductance and plotted as a function of step voltage. Second, tail currents were measured at the end of the 200-ms voltage step (**Fig. 4c**). At this time point, homomeric K3.4a channels have completely inactivated and do not contribute any detectable tail current (**Fig. 4b**). If the currents in these cells were simply a sum of currents arising from Kv3.4a and Kv3.1b homomers, then the peak and tail conductance plots should differ markedly (compare **Figs. 1c** and **3b**). Yet, both measures of voltage dependence yielded very similar relative conductance plots, demonstrating that channels with novel properties were created by coexpression of these subunits. Moreover, these new channels had an activation voltage dependence that was indistinguishable from that of native Kv3 channels (**Fig. 4d**).

Another important feature of heteromeric channels was that they activated rapidly and deactivated at nearly the same rate as Kv3.1b homomeric channel currents (**Fig. 4e**). The combination of a relatively low threshold of activation and rapid kinetics led to very efficient activation by the action potential waveform (**Fig. 4a**, right). On average, the repolarizing efficiency of the heteromeric Kv3.4a/Kv3.1b channels was 0.43 ± 0.04 ($n = 7$), compared to 0.42 for Kv3 channels in FS neurons and 0.09 for Kv3.1b channels.

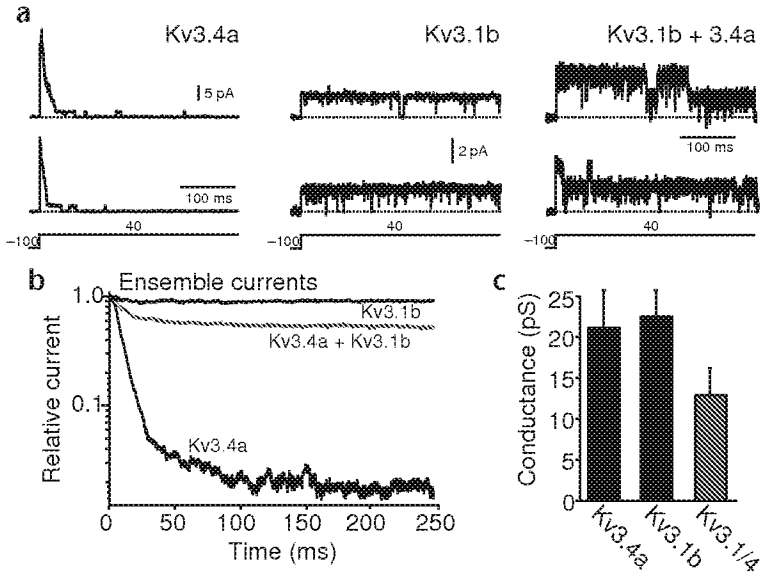

Fig. 5. Single-channel recordings show that coexpression of Kv3.1b and Kv3.4a subunits results in the formation of a channel with distinctive properties. (**a**) Single-channel activity evoked in cell-attached patches by a voltage step from −100 mV to +40 mV. Left, currents of Kv3.4a channels; more than ten Kv3.4a channels transiently opened and then decayed to a low open probability with a mean open time of 8.05 ± 0.5 ms. Center, currents of Kv3.1b channels; the prolonged burst of openings of one channel was interrupted by brief closures. Right, currents produced by two channels in a cell coexpressing Kv3.1b and Kv3.4a subunits showed short (t = 16 ms) and long (t = 250 ms) bursts of openings. (**b**) Ensemble averages of Kv3.1b, Kv3.4a and Kv3.1b+Kv3.4a channels reveal decay kinetics resembling those of whole-cell currents. Currents are plotted on a semi-logarithmic scale to better illustrate decay kinetics. The Kv3.4a channel current decayed with a time constant of 8.2 ms; Kv3.1b + Kv3.4a channel currents decayed bi-exponentially with time constants of 14 ms (33%) and 273 ms; the Kv3.1b channel currents showed little decay. (**c**) Slope conductance was calculated from the currents measured between 0 and 40 mV were 22.5 ± 0.5 pS for the Kv3.1b channels (n = 5); 21.0 ± 0.3 pS for Kv3.4a channels (n = 5); 12.8 ± 0.3 pS for Kv3.1b + Kv3.4a channels (n = 5). The conductance of the heteromeric channels was significantly different than the other two conductances (P < 0.05, Kruskal-Wallis).

To provide additional evidence that heteromeric channels were formed by coexpression of Kv3.1b and Kv3.4a subunits, we made single-channel recordings. In response to membrane depolarization, homomeric Kv3.4a channels showed short openings with a mean open time of 8.05 ± 0.50 ms (**Fig. 5a**, left panel, n = 5). The slope conductance for these channels was 21.0 ± 3.5 pS (n = 5, **Fig. 5c**). In contrast, homomeric Kv3.1b channels had long opening bursts interrupted by very brief closures (**Fig. 5a**, center panel, n = 9). The slope conductance of these channels was 22.5 ± 5.0 pS (n = 5, **Fig. 5c**). Channels in cells coexpressing Kv3.1b and Kv3.4a subunits had short and long bursts of openings with the mean burst durations of 16.2 ± 4.03 ms (33 ± 10% of all bursts) and 250 ± 50 ms, respectively (**Fig. 5a**, right panel, n = 11). In spite of the similarity in the amplitude at +40 mV, the slope conductance of Kv3.4a/Kv3.1b channels was smaller than that of Kv3.1b channels (12.8 ± 3.3 pS; n = 5). Ensemble averages were compiled from 30 successive sweeps to compare the kinetic features of single channels with those of whole-cell currents. There was a very clear correlation in the kinetics of current decay in the ensemble averages (**Fig. 5b**) and those found in whole cell recordings (compare **Figs. 1, 3** and **4**). The decay time constant of Kv3.4a channel currents was similar to the single-channel open time, whereas the decay of Kv3.1b and Kv3.4a/Kv3.1b currents was strongly correlated with burst duration (see **Fig. 5** legend). These data corroborate the inference that coexpression of Kv3.1b and Kv3.4a subunits leads to the formation of a heteromeric channel with distinctive properties.

The data presented thus far show (i) that several types of FS neuron coexpress Kv3.4a and Kv3.1 mRNA, (ii) that these two subunits coassemble in rat brain and HEK293 cells and (iii) that Kv3.4a and Kv3.1b heteromeric channels are formed in HEK293 cells and these channels capture the key features of native Kv3 channels in FS neurons. As these findings suggest, but do not directly show, that Kv3.1 channels incorporate Kv3.4 subunits in FS neurons, we took a pharmacological approach to confirm this.

The Kv3.4 toxin, BDS-I, blocks Kv3 currents in FS neurons

At low micromolar concentrations, the sea anemone toxin BDS-I blocks homomeric Kv3.4 channels with only minor effects on Kv3.1 channel currents[17]. In FS neurons, BDS-I slowed the rising phase of DR currents evoked by depolarization and reduced their amplitude, arguing that Kv3.4a subunits contributed to channels underlying these currents (**Fig. 6a**). To kinetically identify these channels, currents evoked in the presence of BDS-I were subtracted from control currents. If BDS-I simply eliminated currents through channels containing Kv3.4 subunits, the subtracted traces should resemble either homomeric Kv3.4 or heteromeric Kv3.4/Kv3.1 channel currents. The subtracted currents did not resemble currents arising from either channel type (compare **Figs. 3, 4** and **6b**). With modest depolarization (−10 mV), the subtracted (difference) currents appeared to be slowly inactivating, whereas with stronger depolarization (+20 mV), the subtracted currents quickly decayed. Similar results were seen in every GP neuron tested (n = 6). To gain a better idea of how BDS-I was acting, it was applied to homomeric Kv3.4a channels expressed in HEK293 cells. In this case, the toxin slowed the rising phase of the currents but led to larger currents later in the step (n = 5) (**Fig. 6c**). This 'cross-over' blocking pattern is reminiscent of the voltage-dependent block of Kv4 A-type channels by 4-aminopyridine[18,19] where initially blocked channels unblock with sustained depolarization. As predicted

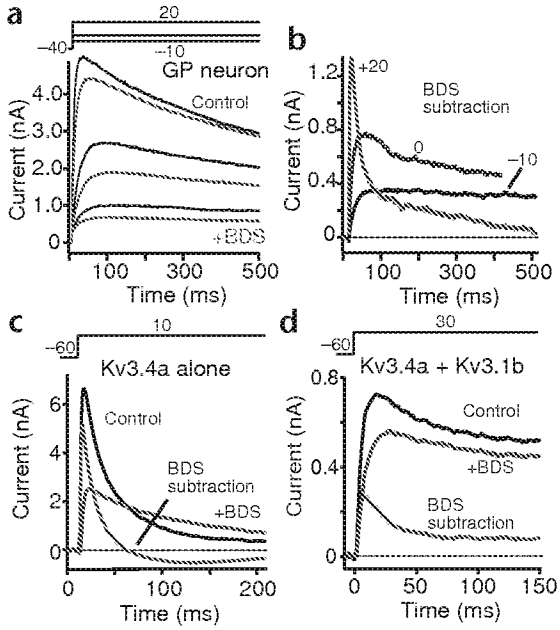

Fig. 6. BDS-I produces a voltage-dependent block of currents in FS neurons and HEK293 cells. (**a**) Currents evoked in a STN neuron in the presence (red) and absence (black) of BDS-I toxin (2 μM, BDS) by voltage clamp steps shown at the top. (**b**) Currents at three different voltages were computed by subtraction of those currents evoked in the presence of BDS-I from control currents. Note the differences in apparent inactivation kinetics. (**c**) Currents evoked in a HEK293 cell expressing Kv3.4a channels by stepping to +10 mV. Black, control currents; red, in the presence of BDS-I; green, the subtraction current. (**d**) Currents evoked in a HEK293 cell expressing Kv3.4a/Kv3.1b channels by stepping to +30 mV. Same color coding.

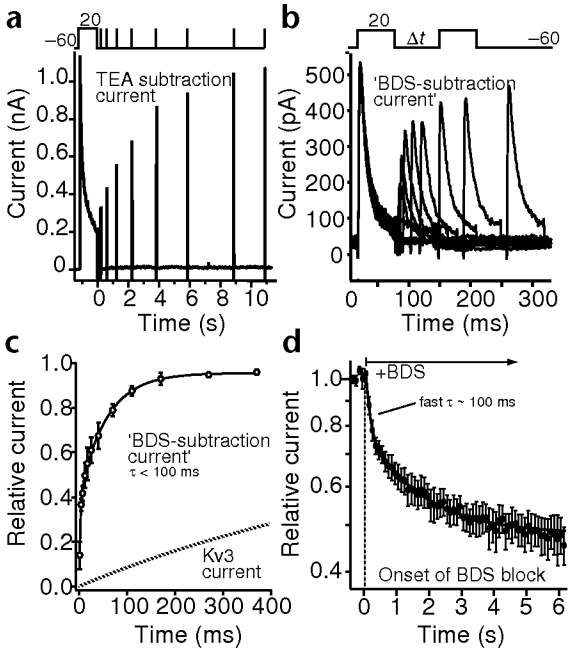

Fig. 7. The recovery of BDS-I sensitive current does not match that of Kv3 family channels. (**a**) Inactivation of TEA-sensitive Kv3 channels recovers slowly, over seconds at −60 mV. Voltage protocol used to inactivate and then de-inactivation currents in a GP neuron is shown at the top; initial step to +20 mV is 1 s, subsequent test steps are 2.1 ms. Currents were obtained by subtraction as above. (**b**) In GP neurons, application of BDS-I (2 μM) leads to subtraction currents that rapidly decay and then recover quickly, over milliseconds. Currents evoked by the protocol at the top in the presence of BDS-I were subtracted from currents evoked in its absence. (**c**) The relative amplitude of the BDS-I subtracted currents is shown as a function of time at −60 mV before the test step (see **b**). Data from three neurons was pooled and plotted as means (± s.d.) and fitted with a bi-exponential function having time constants of 3 (41% of total) and 56 ms. There was an additional very slow component of the recovery that was not accurately estimated from the fits and was attributable to inactivation of Kv3 currents during the initial conditioning step. This component was similar to that of the recovery of the TEA-sensitive Kv3 current in (**a**); the fit to this data is shown in (**c**) and labeled 'Kv3 current'. (**d**) Onset of the BDS-I block (2 μM) was determined by measuring the amplitude of currents evoked by a brief (2.1 ms) test pulse to +20 mV from a holding potential of −60 mV. Test steps were repeated every 100 ms. Data from five neurons are shown (mean ± s.d.). Current decay was fit with a bi-exponential function having time constants of 110 ms (20% of total decay) and 1.7 s. The relative amplitude of the slow component was decreased by increasing the duration between test pulses to 400 ms.

by this model, the BDS-I block of Kv3.4a/Kv3.1b heteromeric channels in HEK293 cells was strong at the beginning of a depolarizing step and then waned with maintained depolarization ($n = 4$) (Fig. 6d).

This interpretation also is consistent with the apparent inactivation recovery kinetics of the BDS-I sensitive current in GP neurons. In both heterologous and native expression systems, Kv3 channels take seconds to recover from inactivation produced by strong depolarization[15,16]. Here, as in heterologous systems, de-inactivation of TEA-sensitive, Kv3 currents at −60 mV was slow, taking seconds (Fig. 7a). In contrast, the major component of the BDS-I difference currents recovered nearly two orders of magnitude faster, taking less than a second at −60 mV ($n = 4$, Fig. 7b and c). If these currents were attributable to rapidly inactivating, homomeric, Kv3.4a channels, the recovery should have been slow. Rather, the rapid decay of currents during the conditioning step is attributable to the unbinding of BDS-I from channels containing Kv3.4 subunits; with repolarization, these channels re-block, leading to a progressive increase in the difference currents and a spurious recovery when the subtraction is performed. The speed of re-block is similar to that seen initially when BDS-I is applied using a rapid perfusion system (Fig. 7d). The slower component of this block is attributable to unblocking during test pulse, as its magnitude was diminished by decreasing the rate at which the test pulse was delivered. What do these results tell us about the subunit composition of Kv3 channels in GP neurons? Although the voltage dependence of the BDS-I block precludes an accurate determination of the kinetic signature of native channels containing Kv3.4 subunits, it is clear that these channels do not inactivate rapidly, as do Kv3.4 homomeric channels. Here, BDS-I subtraction yielded slowly decaying currents with moderate depolarizations (compare Figs. 3 and 6b), consistent with the proposition that Kv3.1 subunits in FS neurons form heteromers with Kv3.4 subunits.

Because it takes more than 5 ms at +20 mV for substantial unblocking and because re-blocking is fast at potentials below spike threshold (around −60 mV), BDS-I should function as an effective blocker of channels containing Kv3.4 subunits during repetitive spiking. Indeed, BDS-I substantially broadened spikes in FS neurons (Fig. 8a), much as sub-millimolar concentrations of TEA have been shown to in previous studies[13]. On average,

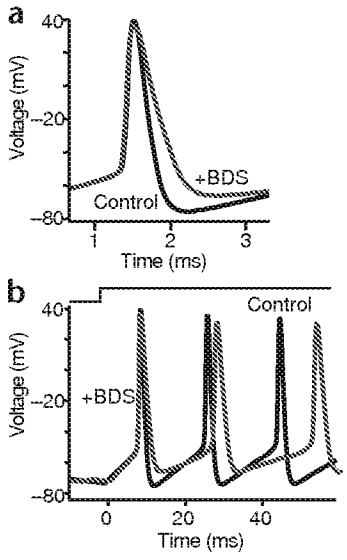

Fig. 8. BDS-I toxin broadens spikes and reduces spike frequency in FS neurons even in the presence of 2 mM Ca^{2+}. (**a**) Spike evoked in a GP neuron in the presence and absence of BDS-I (2 μM) (external solution contained 2 mM Ca^{2+}). (**b**) Repetitive firing in FS neurons evoked by intrasomatic current injection was slowed by BDS-I (2 μM). Note the spike broadening in this GP neuron. Similar results were seen in three other FS neurons tested.

the duration of spikes in FS neurons increased 53 ± 13% in the presence of BDS-I (2 μM) and extracellular Ca^{2+} (2 mM; to allow activation of Ca^{2+} activated K^+ channels) (n = 4). BDS-I produced no obvious change in the rate of rise in the spike and didn't significantly alter the inactivation kinetics of Na^+ currents in FS neurons (n = 3, data not shown, see ref. 17). In addition, BDS-I slowed the rate of repetitive spiking evoked by sustained current injection in FS neurons (**Fig. 8b**), in much the same way as selective block of Kv3 channels by TEA in cortical interneurons[13]. Similar results were seen in three neurons examined with extracellular Ca^{2+} and in eight of nine FS neurons recorded in the absence of extracellular Ca^{2+}. Together, the BDS-I data show that a functionally critical subset of Kv3 channels in FS neurons, if not all, contain Kv3.4 subunits.

Discussion

Previous studies have shown that the FS phenotype depends on the expression of a fast DR current[3]. These currents activate rapidly during the upstroke of the spike, resulting in rapid repolarization of the membrane. The narrow spikes characteristic of FS neurons minimize Na^+ channel inactivation, keeping the somatic and initial segment membrane responsive. Upon repolarization, these channels deactivate quickly, removing any impediment to subsequent depolarizing influences. Together, these features enable neurons to sustain spiking at high frequencies.

A broad array of experimental data support the proposition that the fast DR channel underlying FS behavior incorporates Kv3.1 and/or Kv3.2 subunits[3]. But the view that these channels are Kv3.1/Kv3.2 homomers or heteromers of just these subunits is difficult to support. Although their gating kinetics are rapid, both Kv3.1 and Kv3.2 channels activate at significantly more depolarized potentials (~20 mV) than do native, fast DR channels. This difference is critical. With the properties seen in heterologous systems, only a small fraction of Kv3.1/2 channels will open during spike, making them very inefficient mediators of fast repolarization.

Our results show that the repolarizing efficiency of Kv3 channels is increased by the incorporation of another subunit into the channel complex, the Kv3.4a subunit. Several lines of evidence support this conclusion. First, single-cell RT-PCR profiling found coexpression of Kv3.4a and Kv3.1 mRNA in FS neurons from the GP, STN, inferior colliculus and hippocampus. On the other hand, Kv3.4 mRNA was not found in regular spiking neurons from the hippocampus, striatum or basal forebrain. Second, co-immunoprecipitation experiments showed that Kv3.4 and Kv3.1 subunits coassemble in brain membranes and HEK293 cells that coexpress Kv3.4a and Kv3.1b subunits. Coexpression of these subunits resulted in HEK293 cells that yielded distinctive single-channel currents, and their macroscopic currents resembled those of Kv3 channels in FS neurons. Third, BDS-I, a Kv3.4-selective toxin, efficiently blocked TEA-sensitive, Kv3 channel currents in FS neurons. Together, these three observations show that Kv3 channels in many FS neurons contain Kv3.4 subunits.

Not only do Kv3.4a and Kv3.1 subunits coassemble, but their association is sufficient to produce channels that strongly resemble Kv3 channels in neurons. Coexpression of Kv3.4a and Kv3.1b transcripts in HEK293 cells yielded currents with a sensitivity to BDS-I and TEA like that of native Kv3 channels. Moreover, these heterologously expressed, heteromeric channels had activation properties that were nearly identical to those of native channels and were efficiently activated by a spike waveform, in contrast to Kv3.1b channels. Kv3.1b/Kv3.4a channels also had a rapidly inactivating component (~40 ms) at depolarized potentials, much like native Kv3 channels and unlike Kv3.1b channels. Inclusion of the Kv3.4a splice variant was essential to mimic native channels, as heteromers containing Kv3.4b or Kv3.4c subunits activated at potentials similar to those of Kv3.1 homomeric channels[3] (unpub. observ.). On the face of it, this seems at odds with previous studies of Kv3.4a channels expressed in *Xenopus* oocytes where they activated at more depolarized membrane potentials[16]. However, the half-activation voltage of Kv3.4a channels in these studies was 10–20 mV more negative than that of Kv3.1/3.2 channels in the same preparation (as found here), suggesting that post-translational processing in mammalian cells shifts the voltage dependence of all Kv3 channels.

The small deviations in the inactivation and activation kinetics of the Kv3.4a/Kv3.1b channels in HEK293 cells from those in FS neurons may be attributable to differences in subunit stoichiometry. Both biophysical parameters were biased toward those of Kv3.4a channels in our studies, indicating that this subunit may have been expressed at relatively high levels. The differences also may be due to inclusion of Kv3.4c subunits in channels from FS neurons. The mRNA for this splice variant was found in all tested FS neurons, along with that of Kv3.4a. By varying the mix of Kv3.4a, Kv3.4c and Kv3.1 (or Kv3.2) subunits, it may be possible to 'tune' the properties of fast DR channels to the particular needs of a neuronal class. This strategy—forming heteromeric channels to tune gating properties—is apparently common in the construction of K^+ channels in excitable cells[20–23]. This finding also suggests that alterations in subunit composition could be used to alter the functional properties of neurons in disease states. For example, in Parkinson's disease (PD) the FS neurons of the STN and GP discharge in high-frequency bursts[24,25]. This pattern of discharge is thought to be critical to the emergence of PD motor symptoms and serves as a rationale for deep-brain stimulation and lesioning[26]. The suppression of Kv3.4a expression in STN

neurons could prove to be an effective therapeutic alternative in that it should selectively eliminate high-frequency bursts without otherwise disrupting neuronal function.

Although the inclusion of Kv3.4a subunits in Kv3.1 channels increases their efficiency in spike repolarization in some FS neurons, other mechanisms could serve a similar end. It is clear from our immunoprecipitation experiments that much of the Kv3.1b protein in the brain is not associated with Kv3.4 protein. Moreover, in some brain regions, there are FS neurons but Kv3.4 mRNA appears to be absent. One such area is the medial nucleus of the trapezoid body (MNTB). In FS MNTB neurons, the voltage dependence of Kv3 channels is shifted toward more negative membrane potentials by dephosphorylation of the channel or a closely related protein[27]. Kv3.1 channels expressed in CHO cells are constitutively phosphorylated by casein kinase II and affected by dephosphorylation in much the same way[27]. Kinetically slower, Kv2.1 DR channels also are phosphorylated early in their biosynthesis with a similar consequence for gating[28]. Could differential phosphorylation provide an alternative mechanism for regulating the gating of Kv3 channels? Perhaps, but phosphorylated MNTB Kv3 channels activate in a voltage range that is similar to that of the neuronal Kv3 channels studied here, which is significantly more negative than that of heterologously expressed Kv3.1 channels[27]. Another possibility is that an as-yet-unidentified accessory subunit is capable of modifying Kv3 channel gating in FS MNTB neurons, in much the same way as incorporation of the Kv3.4a subunit does in the neurons studies here[29].

A cardinal feature of voltage-gated K^+ channels is that the pore-forming region can be heteromeric, being composed of four independent subunits. The ability of Kv3.4a subunits to modify the gating of Kv3.1b channels illustrates how this capacity can be used to 'tune' properties to particular functional needs. By varying the stoichiometry of Kv3.4a and Kv3.4c subunits in the channel complex, a range of gating behaviors may be possible, effectively controlling the neuronal dynamic range. Manipulation of Kv3.4a expression could prove to be a useful and powerful means of controlling this FS range in disease states such as Parkinson's disease, where symptoms have been linked to episodic, high-frequency discharge.

Methods

Tissue preparation. Neurons from the GP, STN, inferior colliculus and CA1 of hippocampus from young adult rats were acutely dissociated, using procedures similar to those we have described previously[30] and approved by the Northwestern University Animal Care and Use Committee. Hippocampal interneurons and GP were identified as CaMKII-negative, GAD67- and parvalbumin-positive neurons by single-cell RT-PCR detection of corresponding mRNAs following physiology experiments (see below).

Electrophysiology. Whole-cell recordings were done by standard techniques[30,31]. The internal solution consisted of 30–90 mM K_2SO_4, 0–60 mM *N*-methyl-D-glucamine, 2 mM $MgCl_2$, 40 mM HEPES, 5 mM EGTA, 12 mM phosphocreatine, 2 mM Na_2ATP, 0.2 mM Na_3GTP and 0.1 mM leupeptin, pH 7.2 with H_2SO_4 (osmolarity 260–270 mOsm/l). The external solution consisted of 140 mM sodium isethionate, 2 mM KCl, 4 mM $MgCl_2$, 10 mM HEPES, 12 mM glucose and 0.001 mM TTX, pH 7.35 with NaOH (osmolarity 295–305 mOsm/l). The internal solution for current clamp recordings consisted of 110 mM potassium methylsulphate, 2 mM $MgCl_2$, 40 mM HEPES, 5 mM EGTA, 12 mM phosphocreatine, 2 mM Na_2ATP, 0.2 mM Na_3GTP and 0.1 mM leupeptin, pH 7.2 with H_2SO_4 (osmolarity 260–270 mOsm/l). In the case of current-clamp recordings, TTX was omitted from external solution. For the recordings in the presence of Ca^{2+} ions, EGTA was omitted from internal solution and 4 mM of $MgCl_2$ was substituted by 2 mM of $CaCl_2$ and 2 mM of $MgCl_2$. All drugs were obtained from Sigma (St. Louis, Missouri) except BDS-I, which was from Alomone Labs (Jerusalem, Israel). Solutions were applied by a gravity-fed sewer pipe system. Recordings were obtained with Axon Instruments 200 patch-clamp amplifier and controlled and monitored with a PC running pClamp 7.0 software (Axon Instruments, Union City, California). Electrode resistance was typically 1.5–2.2 MΩ in the bath. After seal rupture, series resistance (2–10 MΩ) was compensated (75–90%) and periodically monitored. For application of action potential waveforms, the cells were selected for relaxation times <0.3 ms. Potentials were not corrected for the liquid junction potential, which was estimated to be 1–2 mV. All averaged data is presented as mean ± standard error of the mean (s.e.m.). All data fits were obtained using Igor Pro software (WaveMetrics, Lake Oswego, Oregon) by least-square method. Activation data were fit with a Boltzmann equation of the form: $1/(1 + \exp((V_h - V)/V_c))$, where V stands for membrane potential. In the case of Kv3.4a current, an estimate of peak current was obtained by single exponential fit of decay phase extrapolated to the start of test pulse. In all other instances, the voltage dependence of the currents was obtained from the amplitude of tail currents measured following 200 ms long voltage steps.

Single-channel recordings were made from HEK293 cells using the cell-attached variation of the patch clamp technique. HEK293 cells were transfected with Kv3.1, Kv3.4 or both Kv3.1 and Kv3.4 cDNA. The patch pipettes were pulled from 0.8 mm (i.d.) borosilicate glass capillary tubes with filament (G150F-4, Warner Instrument Corp., Hamden, Connecticut) to the final resistance of 15 MΩ when filled with extracellular recording solution. The electrodes were coated with a semiconductor protective coating material R-6101 (Dow Corning Corporation, Midland, Michigan) and fire-polished. The signals were recorded using an Axopatch 200 amplifier and stored in a microcomputer via analog-to-digital converter. From a holding potential of –100 mV, patches were depolarized to potentials between 0 and +40 mV (700 ms). The resting membrane potential measured at the end of experiments was typically –40 mV. The temporal properties of single-channel events were analyzed with pClamp8 software. The slope conductance was calculate from the single-channel currents measured between 0 and 40 mV. Closed times <5 ms were considered to be part of a burst; the mean closed time within unambiguous bursts was 1.5 ms. Using this criterion, the probability that a gap or closing within a burst will be misidentified as a between-burst closing is less than 5%.

Single-cell RT-PCR (scRT-PCR). Two types of scRT-PCR profiling were performed. To maximize mRNA yields, some neurons were aspirated without recording. Isolated neurons were patched in the cell-attached mode and lifted into a stream of control solution. Neurons were then aspirated into an electrode containing sterile water. In other experiments, neurons were briefly subjected to whole-cell voltage-clamp recordings before aspiration. In these cases, the electrode recording solution was made nominally RNase-free. RT procedure was performed using Superscript First-Strand Synthesis System (Invitrogen, Carlsbad, California). Primers for PCR were as previously described[19,32,33].

Heterologous expression. Kv3.4a and Kv3.4c cDNA was sub-cloned into pcDNA3 (Invitrogen). Kv3.1b cDNA clone was a gift from B. Rudy. HEK293 cells (gift from R. Miller) were transfected using Effectene Transfection Reagent (QIAGEN, Valencia, California). Cells were used for whole-cell recordings or harvested for membrane extraction 36–60 h after transfection. In the case of co-transfection with Kv3.4a and Kv3.1b cDNA, single cell RT-PCR was used to confirm the presence of both mRNAs in the recorded cell. The presence of both inactivating and non-inactivating components of potassium current was an additional criterion for cell selection.

Immunoprecipitation. The crude membranes were solubilized in lysis buffer (1% Triton X-100, 150 mM NaCl, 1 mM EDTA, 10 mM Tris-HCl, pH 8.0) containing a protease inhibitor mixture[34]. Samples were incubated for 1 h at 4 °C on a rotator, followed by addition of anti-Kv3.1b or anti-Kv3.4 antibodies (Alomone Labs) and further incubation for 1 h. Then protein A–sepharose was added. After 45 min incubation, protein A–sepharose was pelleted by centrifugation at 10,000*g* for 30 s, and

resulting pellets were washed six times with lysis buffer. The final pellets were re-suspended in reducing SDS sample buffer.

SDS-polyacrylamide gels and immunoblotting. Products of immunoprecipitation reactions were size-fractionated on a 10% SDS-polyacrylamide gel. After electrophoretic transfer to nitrocellulose, the resulting blots were blocked in Blotto, incubated in Anti-Kv3.1b or Anti-Kv3.4 antibodies for 1 h, and washed four times in TBS. Blots were then incubated in HRP-conjugated secondary antibody (PerkinElmer, Boston, Massachusetts) and washed four times in TBS, followed by Chemiluminescence Reagent Plus (PerkinElmer).

Acknowledgments

This work was supported by the National Institute of Neurological Disorders and Stroke (NS26473, NS34696 to D.J.S. and a National Parkinson Foundation (NPF) grant to T.T.

Competing interests statement

The authors declare that they have no competing financial interests.

RECEIVED 3 DECEMBER 2002; ACCEPTED 10 JANUARY 2003

1. Hodgkin, A.L. & Huxley, A.F. Currents carried by sodium and potassium ions through the membrane of the giant axon of *Loligo*. *J. Physiol.* **116**, 449–472 (1952).
2. Hodgkin, A.L. & Huxley, A.F. The components of membrane conductance in the giant axon of *Loligo*. *J. Physiol.* **116**, 473–496 (1952).
3. Rudy, B. & McBain, C.J. Kv3 channels: voltage-gated channels designed for high-frequency repetitive firing. *Trends Neurosci.* **24**, 517–526 (2001).
4. Coetzee, W.A. *et al.* Molecular diversity of K^+ channels. *Ann. NY Acad. Sci.* **868**, 233–285 (1999).
5. Brew, H.M. & Forsythe, I.D. Two voltage-dependent K+ conductances with complementary functions in postsynaptic integration at a central auditory synapse. *J. Neurosci.* **15**, 8011–8022 (1995).
6. Du, J., Zhang, L., Weiser, M., Rudy, B. & McBain, C.J. Developmental expression and functional characterization of the potassium-channel subunit Kv3.1b in parvalbumin-containing interneurons of the rat hippocampus. *J. Neurosci.* **16**, 506–518 (1996).
7. Lenz, S., Perney, T.M., Qin, Y., Robbins, E. & Chesselet, M.F. GABAergic interneurons of the striatum express the Shaw-like potassium channel Kv3.1. *Synapse* **18**, 55–66 (1994).
8. Weiser, M. *et al.* Differential expression of Shaw-related K^+ channels in the rat central nervous system. *J. Neurosci.* **14**, 949–972 (1994).
9. Weiser, M. *et al.* The potassium channel subunit KV3.1b is localized to somatic and axonal membranes of specific populations of CNS neurons. *J. Neurosci.* **15**, 4298–4314 (1995).
10. Martina, M., Schultz, J.H., Ehmke, H., Monyer, H. & Jonas, P. Functional and molecular differences between voltage-gated K^+ channels of fast-spiking interneurons and pyramidal neurons of rat hippocampus. *J. Neurosci.* **18**, 8111–8125 (1998).
11. Baranauskas, G., Tkatch, T. & Surmeier, D.J. Delayed-rectifier currents in rat globus pallidus neurons are attributable to Kv2.1 and Kv3.1/3.2 K^+ channels. *J. Neurosci.* **19**, 6394–6404 (1999).
12. Vega-Saenz de Miera, E. *et al.* Shaw-related K^+ channels in mammals. *Handbook of Membrane Channels* C. Peracchia 41–78 (Academic, New York, 1994).
13. Erisir, A., Lau, D., Rudy, B. & Leonard, C.S. Function of specific K^+ channels in sustained high-frequency firing of fast-spiking neocortical interneurons. *J. Neurophysiol.* **82**, 2476–2489 (1999).
14. Wigmore, M.A. & Lacey, M.G. A Kv3-like persistent, outwardly rectifying, Cs^+-permeable, K^+ current in rat subthalamic nucleus neurons. *J. Physiol.* **527**, 493–506 (2000).
15. Schroter, K.H. *et al.* Cloning and functional expression of a TEA-sensitive A-type potassium channel from rat brain. *FEBS Lett.* **278**, 211–216 (1991).
16. Rettig, J. *et al.* Characterization of a Shaw-related potassium channel family in rat brain. *EMBO J.* **11**, 2473–2486 (1992).
17. Diochot, S., Schweitz, H., Beress, L. & Lazdunski, M. Sea anemone peptides with a specific blocking activity against the fast inactivating potassium channel Kv3.4. *J. Biol. Chem.* **273**, 6744–6749 (1998).
18. Thompson, S. Aminopyridine block of transient potassium current. *J. Gen. Physiol.* **80**, 1–18 (1982).
19. Song, W.J. *et al.* Somatodendritic depolarization-activated potassium currents in rat neostriatal cholinergic interneurons are predominantly of the A-type and attributable to coexpression of Kv4.2 and Kv4.1 subunits. *J. Neurosci.* **18**, 3124–3137 (1998).
20. Kofuji, P., Davidson, N. & Lester, H.A. Evidence that neuronal G-protein-gated inwardly rectifying K^+ channels are activated by G beta gamma subunits and function as heteromultimers. *Proc. Natl. Acad. Sci. USA* **92**, 6542–6546 (1995).
21. Sheng, M., Liao, Y.J., Jan, Y.N. & Jan, L.Y. Presynaptic A-current based on heteromultimeric K^+ channels detected *in vivo*. *Nature* **365**, 72–75 (1993).
22. Wang, H.S. *et al.* KCNQ2 and KCNQ3 potassium channel subunits: molecular correlates of the M-channel {see comments}. *Science* **282**, 1890–1893 (1998).
23. Abbott, G.W. *et al.* MiRP2 forms potassium channels in skeletal muscle with Kv3.4 and is associated with periodic paralysis. *Cell* **104**, 217–231 (2001).
24. Raz, A., Vaadia, E. & Bergman, H. Firing patterns and correlations of spontaneous discharge of pallidal neurons in the normal and the tremulous 1-methyl-4-phenyl-1,2,3,6-tetrahydropyridine vervet model of parkinsonism. *J. Neurosci.* **20**, 8559–8571 (2000).
25. Bergman, H., Wichmann, T., Karmon, B. & DeLong, M.R. The primate subthalamic nucleus. II. Neuronal activity in the MPTP model of parkinsonism. *J. Neurophysiol.* **72**, 507–520 (1994).
26. DeLong, M.R. & Wichmann, T. Deep brain stimulation for Parkinson's disease. *Ann. Neurol.* **49**, 142–143 (2001).
27. Macica, C.M. & Kaczmarek, L.K. Casein kinase 2 determines the voltage dependence of the Kv3.1 channel in auditory neurons and transfected cells. *J. Neurosci.* **21**, 1160–1168 (2001).
28. Murakoshi, H., Shi, G., Scannevin, R.H. & Trimmer, J.S. Phosphorylation of the Kv2.1 K^+ channel alters voltage-dependent activation. *Mol. Pharmacol.* **52**, 821–828 (1997).
29. Rettig, J. *et al.* Inactivation properties of voltage-gated K^+ channels altered by presence of beta-subunit. *Nature* **369**, 289–294 (1994).
30. Surmeier, D.J., Bargas, J., Hemmings, H.C., Jr., Nairn, A.C. & Greengard, P. Modulation of calcium currents by a D1 dopaminergic protein kinase/phosphatase cascade in rat neostriatal neurons. *Neuron* **14**, 385–397 (1995).
31. Hamill, O.P., Marty, A., Neher, E., Sakmann, B. & Sigworth, F.J. Improved patch-clamp techniques for high-resolution current recording from cells and cell-free membrane patches. *Pflugers Arch.* **391**, 85–100 (1981).
32. Yan, Z. & Surmeier, D.J. Muscarinic (m2/m4) receptors reduce N- and P-type Ca^{2+} currents in rat neostriatal cholinergic interneurons through a fast, membrane-delimited, G-protein pathway. *J. Neurosci.* **16**, 2592–2604 (1996).
33. Tkatch, T., Baranauskas, G. & Surmeier, D.J. Basal forebrain neurons adjacent to the globus pallidus co-express GABAergic and cholinergic marker mRNAs. *Neuroreport* **9**, 1935–1939 (1998).
34. Rhodes, K.J. *et al.* Association and colocalization of the Kvbeta1 and Kvbeta2 beta-subunits with Kv1 alpha-subunits in mammalian brain K^+ channel complexes. *J. Neurosci.* **17**, 8246–8258 (1997).